Oxo-molybdenum(VI) complexes containing chiral ligands: catalytic applications in selective epoxidations

José Ángel Brito Castro

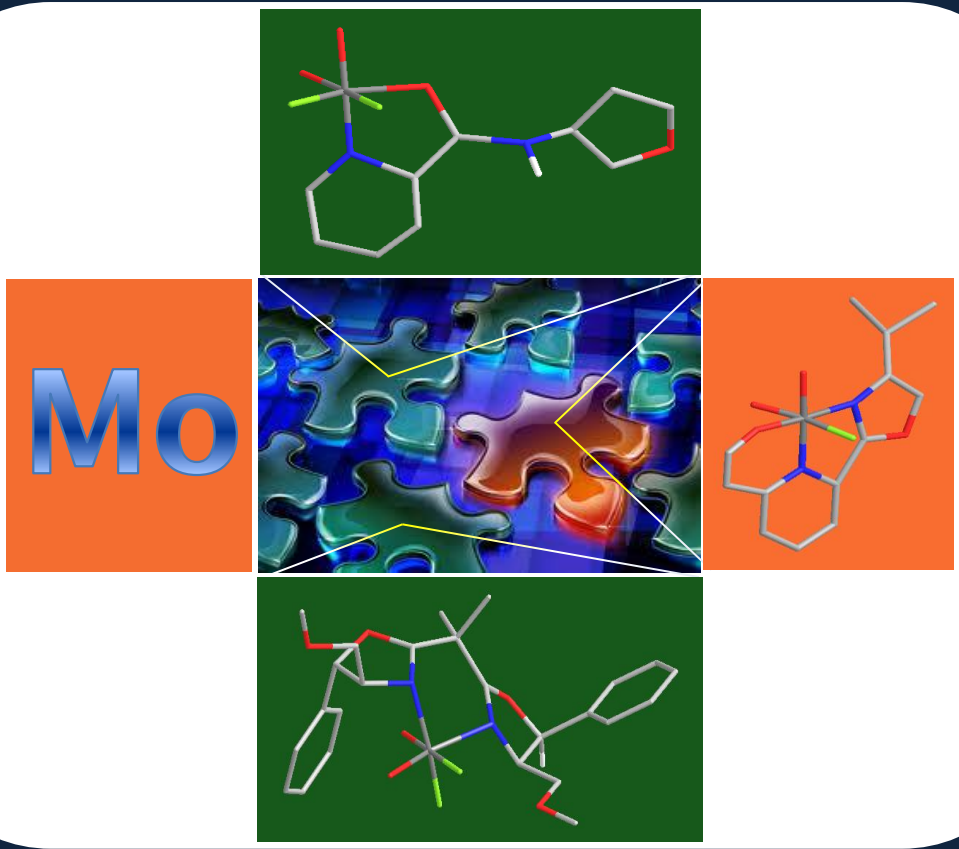

Dissertation presented to obtain the Ph.D degree in Chemistry

Instituto de Tecnologia Química e Biológica | Universidade Nova de Lisboa

Oeiras,
September, 2011

INSTITUTO
DE TECNOLOGIA
QUÍMICA E BIOLÓGICA
/UNL

Knowledge Creation

Oxo-molybdenum(VI) complexes containing chiral ligands: catalytic applications in selective epoxidations

José Ángel Brito Castro

Dissertation presented to obtain the Ph.D degree in Chemistry

Instituto de Tecnologia Química e Biológica | Universidade Nova de Lisboa

Oeiras, September, 2011

INSTITUTO
DE TECNOLOGIA
QUÍMICA E BIOLÓGICA
/UNL

Knowledge Creation

Supervisors:

Dr. Beatriz Royo

Prof. Montserrat Gómez

Examiners:

Prof. Ana Margarida Martins

Dr. Hélène Olivier-Bourbigou

Prof. Ernesto de Jesús Alcañis

Apoio financeiro da FCT e do FSE no âmbito do
Quadro Comunitário de apoio, BD nº SFRH / BD / 30917 / 2006

FCT
Fundação para a Ciência e a Tecnologia
MINISTÉRIO DA EDUCAÇÃO E CIÊNCIA

UNIÃO EUROPEIA
Fundo Social Europeu

Oeiras, September, 2011

I don't believe you have to be better than everybody else. I believe you have to be better than you ever thought you could be.

Ken Venturi

I would like to express my gratitude to all the people who directly or indirectly has supported and contributed to this work.

I would like to express my deeply gratitude to my supervisor, Dr. Beatriz Royo, for the opportunity to join her group in the homogeneous catalysis laboratory. I am also thankful for all the support, teaching, guidance and critical discussions.

I would like to express my gratitude to my co-supervisor Professor Montserrat Gómez. I am very grateful for the opportunity to visit the SYMAC group in Paul Sabatier University in Toulouse, France, in three opportunities. I owe a great debt of gratitude for all their precious support, guidance and patience and for teaching me to constantly be on a pursuit of excellence, for the special interest regarding to my work and for being a genuine example of professionalism and dedication.

I want to thank all the academic, administrative and technician service from ITQB-UNL for all their collaboration.

I want to thank all my laboratory colleagues from ITQB-UNL.

I want to thank ALFAMA for all the collaboration.

I want to acknowledge Dr. Isabelle Favier for her friendship since we met in Barcelona. I am very glad how you have improved your Spanish. For all your teaching regarding the history of France, especially Toulouse city and all these tips about French food and over all from Nice. I want also to acknowledge her for all the cooperation in the catalytic field of allylic substitution.

Dr. Emmanuelle Teuma is acknowledged for all the cooperation and her friendship during my stay in Toulouse, France.

Dr. David Madec is acknowledged for the tips concerning to organic reactions and for the Toblerone coffee breaks that include French tips.

I want to thank the rest of members of the SYMAC group and LHFA from Paul Sabatier University in Toulouse, France.

Dr. Fernando Fernández and Dr. Arnald Grabulosa are acknowledged for all these years of friendship and manly for all the unforgettable dinners and horror movie sections in Barcelona.

I want to thank Pedro Mateus and Carla Gamelas for the collaboration concerning to the Portuguese summary revision.

I would like to thank Luciana Miranda for her friendship and all these very good moments in which she attempted to teach me how to dance forró and samba and all the tips about Brazilian culture (Canta Canta, Minha Gente, Deixa a tristeza pra lá Canta forte, canta alto, Que a vida vai melhorar).

Thanks a lot to this very special person who has been there for me, for all her patience, support, for helping me so many times and mainly for loving me.

I would like to thank my parents, brothers and family in general for the unconditional love, understanding, support and for finding always the way to encourage me to continue.

Thank everybody.

José Ángel Brito Castro

SUMMARY

This thesis describes the synthesis and characterization of novel *cis*-dioxomolybdenum(VI) complexes containing chiral oxazoline-based ligands and their application in olefins epoxidation.

An overview concerning the applications of molybdenum complexes in asymmetric catalysis is presented in Chapter 1. It highlights the attractive catalytic applications of molybdenum in enantioselective processes. Although molybdenum plays several roles in biological transformations, it has been little applied in organometallic catalysis in relation to other transition metals. The versatility of molybdenum in terms of oxidation states and coordination geometries triggers its ability to catalyze different kind of processes with carbon-carbon bond formation, olefin metathesis or alkene epoxidation being among the most relevant transformations.

The significance of olefin epoxidation reactions was first recognized with the development of homogeneous catalysis based on oxomolybdenum(VI) complexes in the Halcon and Arco processes. Since then, many contributions have been reported concerning achiral molybdenum(VI) compounds. However, only some chiral molybdenum systems have been efficiently applied in the epoxidation of prochiral olefins, including heterogeneous supported catalysts. The different ligands used in selective epoxidation processes, most of them containing *N*,*O*-heterodonor ligands, appear in this chapter which underlines the most significant results for each case.

Following a critical glance at our previous results using different chiral ligands, one of the objectives of this thesis has been the preparation of new *cis*-dioxomolybdenum (VI) complexes coordinated to non-labile chiral oxazoline ligands containing *N*- and/or *O*-donor centers in order to obtain robust oxo-molybdenum(VI) catalysts. Chapter 3 describes this work and presents the synthesis of a new 2,6-difunctionalized oxazolinyl-pyridine ligand, obtained in a three-step sequence and the synthesis of a pyridine-amide ligand. Four new monometallic dioxomolybdenum(VI) complexes have been synthesized: i) one bearing a *N*,*N*',*O*-tridentate oxazolinyl-pyridyl-phenolate ligand, which shows an unusual arrangement

with the chloride ligand *trans* to one oxo group; ii) one containing a neutral *N,O*-bidentate pyridine-amide ligand; iii) a dixomolybdenum(VI) complex containing a C_2 symmetrical bis(oxazoline) ligand; and iv) one complex bearing a monoanionic *N,N*-bidentate bis(oxazoline) ligand. All these complexes have been fully characterized by NMR (^{1}H, ^{13}C and ^{95}Mo) and IR spectroscopy, mass spectrometry, elemental analysis and three of them were also characterized by X-ray diffraction.

Chapter 4 focuses on the use of ^{95}Mo NMR spectroscopy as a tool for obtaining structural information on the molybdenum species in solution, in particular those species involved in catalysis. The relationship between the electronic density on the metal tuned by the electron-donor ability of the coordinated ligands and the ^{95}Mo chemical shift has been analyzed for mono- and bimetallic oxomolybdenum(VI) complexes, showing hexa- or hepta-coordination around the metal center. The different origins of the signal broadening (associated either with the symmetry of the metallic polyhedron or with the presence of isomers or ligand de-coordination) have been also considered to rationalize the obtained data. This chapter provides evidence of the convenience of the ^{95}Mo NMR for obtaining structural information about catalytic intermediates, which is key for mechanistic studies in solution.

Chapter 5 describes the application of the new molybdenum complexes in epoxidation of cyclooctene, (*R*)-limonene and *trans*-β-methylstyrene in organic medium as well in imidazolium- and pyrrolidinium-based ionic liquids. The new molybdenum complexes were found to be efficient catalysts affording high activities and good chemoselectivity. These monometallic complexes were used as catalytic precursors for epoxidation of alkenes (cyclooctene, (*R*)-limonene, and *trans*-β-methylstyrene) in an organic medium as well in imidazolium- and pyrrolidinium-based ionic liquids, exhibiting a high chemoselectivity towards the epoxide formation, mainly for cyclooctene and (*R*)-limonene epoxidation, without formation of the corresponding diols. In [BMP][NTf_2] (BMP = butyl methyl pyrrolidinium; NTf_2 = bis(trifluoromethanesulfonyl)amide), the epoxidation reaction of (*R*)-limonene was diastereoselective when a bimetallic molybdenum precursor was used as catalyst affording exclusively *trans*-(*R*)-limonene-1,2-epoxide, while monometallic catalytic

systems led to a mixture of *trans- and cis*-(*R*)-limonene-1,2-epoxide. ^{95}Mo NMR studies helped to explain the catalytic behavior of the bimetallic and monometallic species in an ionic liquid medium and to understand the difference in selectivity observed.

Chapter 5 also describes preliminary catalytic studies of allylic substitution reactions catalyzed by palladium systems containing chiral oxazoline-based ligands in pyrrolidinium-based ionic liquids.

The conclusions and perspectives of this work appear in chapter 6.

RESUMO

Esta tese descreve a síntese e caracterização de novos complexos *cis*-dioxomolibdénio(VI) contendo ligandos quirais derivados do fragmento oxazolina, e sua aplicação em epoxidação de olefinas.

No primeiro capítulo apresenta-se uma revisão das aplicações de complexos de molibdénio em catálise assimétrica. Neste capítulo destacam-se as aplicações catalíticas de complexos de molibdénio mais atractivas em processos enantiosselectivos. Embora o molibdénio desempeña um papel fundamental em importantes transformações biológicas, tem sido pouco aplicado em catálise homogénea em relação a outros metais de transição. A versatilidade do molibdénio em ternos de estados de oxidação e geometrias de coordenação representa um factor fundamental na sua capacidade de catalisar diferentes tipos de processos, tais como a formação de ligações carbono-carbono, metátese de olefinas ou epoxidação de olefinas.

A importância das reacções de epoxidação de olefinas foi inicialmentee reconhecida com o desenvolvimento de catalisadores homogéneos baseados em complexos oxomolibdénio(VI) nos processos de Halcon e Arco. Desde então, muitas contribuições foram publicadas, relacionadas com a aplicação de compostos de molibdénio(VI) aquirais. Ainda assim, só alguns sistemas quirais de molibdénio foram eficientemente aplicados na epoxidação de olefinas proquirais, incluindo catalisadores heterogéneos suportados. Neste capítulo destacam-se os diferentes ligandos, na sua maioria contendo ligandos *N*,*O*-hetero-doadores, usados em processos de epoxidação selectiva.

Após um exame crítico dos nossos resultados prévios nos quais foram utilizados diferentes ligandos quirais, um dos objectivos desta tese foi a preparação de novo complexos *cis*-dioxomolibdénio(VI) com ligandos quirais oxazolina contendo centros doadores de *N*- e/ou *O*-, com a finalidade de obter catalisadores robustos de oxomolibdénio(VI). O Capítulo 3 descreve este trabalho e apresenta a síntese de um novo ligando 2,6-difuncionalizado oxazolinil-piridina, obtido numa sequência de três

passos. Descreve-se também a síntese de um ligando piridina-amida. Quatro complexos novos monometálicos dioxomolibdénio(VI) foram sintetizados: i) um contendo um ligando *N*,*N*',*O*-tridentado oxazolinil-piridil-fenolato, que mostra um arranjo pouco usual com o ligando cloro *trans* a um grupo oxo. ii) um contendo um ligando neutro *N*,*O*-bidentatado piridina-amida; iii) um dixomolibdénio(VI) contendo um ligando bis(oxazolina) com simetria C_2; e iv) um complexo contendo um ligando monoaniónico bis(oxazolina) *N*,*N*-bidentado. Todos estes complexos foram completamente caracterizados por RMN (^{1}H, ^{13}C e ^{95}Mo) e espectroscopia de infravermelho, espectrometria de massa, análise elementar e três deles foram caracterizados por difracção de raios-X.

O Capítulo 4 centra-se no uso de espectroscopia de ressonância magnética nuclear de ^{95}Mo como ferramenta para obter informação estrutural das espécies de molibdénio em solução, em particular das espécies envolvidas na catálise. A relação entre a densidade electrónica do metal, ajustada pela capacidade electro-doadora do ligando coordenado e o deslocamento químico das sinais de ^{95}Mo foi analisada para complexos oxomolibdénio(VI) mono- e bimetálicos. As origens dos diferentes sinais alargados (associado com a não simetria do poliedro metálico, com a presença de isómeros ou parcial descoordenação do ligando) foram também consideradas para compreender os dados obtidos. Este capítulo proporciona evidência da utilidade da ressonância magnética nuclear de ^{95}Mo para obter informação estrutural sobre intermediários catalíticos, que é fundamental para estudos mecanísticos em solução.

Capítulo 5 descreve a aplicação do novos complexos de molibdénio em epoxidação de cicloocteno, (*R*)-limoneno e *trans*-β-metilestireno em méio orgânico bem como em líquidos iónicos baseados em imidazolio e pirrolidínio. Os novos complexos de molibdénio são catalisadores eficientes que proporcionam altas actividades e boas selectividades. Estes complexos monometálicos foram utilizados como precursores catalíticos em epoxidaçao de olefinas (cicloocteno, (*R*)-limoneno, e *trans*-β-metilestireno) em meio orgânico e também em líquidos iónicos nomeadamente em imidazolio e pirrolidinio, exibindo uma alta selectividade química na formação do

correspondente epóxido, em particular na epoxidaçao de cicloocteno e (*R*)-limoneno, sem formação dos correspondentes dióis. Em [BMP][NTf_2] (BMP = butil metil pirrolidínio; NTf_2 = bis(trifluorometanosulfonil)amida) a reacção de epoxidação de (*R*)-limoneno é diastereosselectiva na presença do composto bimetálico de proporcionando exclusivamente *trans*-(*R*)-limoneno 1,2-epóxido, No entanto os sistemas catalíticos monometálicos proporcionaram uma mistura de *trans*- é *cis*-(*R*)-limoneno 1,2-epóxido.

Estudos de espectroscopia de ressonância magnética nuclear do ^{95}Mo contribuem para a explicação do diferente comportamento catalítico mostrado por espécies bimetálicas e monometálicas em líquido iónico e para entender a diferença de selectividade observada neste meio.

No Capítulo 5 descrevem-se ainda estudos preliminares das reacções catalíticas de substituição alílica catalisadas por paládio, em sistemas que contêm ligandos quirais derivados de oxazolinas, na presença de líquidos iónicos.

As conclusões e as perspectivas deste trabalho surgem no Capítulo 6.

INDEX

Chapter 1 THE APPLICATIONS OF CHIRAL MOLYBDENUM COMPLEXES IN ASYMMETRIC CATALYSIS

This chapter has originated the following publication:

José Ángel Brito, Beatriz Royo, Montserrat Gómez

Catal. Sci. Technol., 2011, **1**, 1109-1118

Summary

The aim of this chapter is to highlight the attractive applications of molybdenum in asymmetric catalysis. Even if molybdenum is involved in several biological roles mainly in metalloproteins, it has been less employed in homogeneous catalysis in comparison with other transition metals. This introduction focuses on molybdenum complexes linked to chiral ligands applied in enantioselective processes. The versatility of molybdenum in terms of oxidation states and coordination geometries triggers its capability to catalyze different kind of processes such as carbon-carbon bond formation, olefin metathesis or alkene epoxidation among the most relevant transformations.

1.1. General introduction

The synthesis of stereochemically pure compounds represents one of the key objectives for several domains of chemistry including the production of drugs, biological active compounds, agricultural chemicals and materials. The development of organometallic enantioselective catalysis has been one of the most important hits of the last century, allowing the transformation of prochiral and racemic substrates into enantioenriched products. This successful research led to the Royal Swedish Academy of Sciences to award in 2001 to W. S. Knowles, R. Noyori and K. B. Sharpless, pioneering chemists in the field of asymmetric catalysis, with the Nobel Prize in Chemistry. At present, one of the challenges from an industrial and environmental point of view is to design processes highly active, inducing full control in chemo-, regio- and stereo-selectivity, decreasing the by-products and allowing the recycling of catalyst. The use of cheap and less toxic catalysts in relation to late transition metals signifies an attractive way for homogeneous catalysis. Although molybdenum plays several roles in biological transformations, it has been little applied in organometallic catalysis in relation to other transition metals. Molybdenum complexes have attracted much attention because of their applications in organic syntheses, such as olefin metathesis, allylic substitution and olefin epoxidation of alkenes.

1.2. Asymmetric allylic alkylation

Transition-metal-catalyzed enantioselective allylic substitutions stand for a powerful synthetic tool to form carbon-carbon and carbon-heteroatom bonds.[1] In particular, asymmetric allylic alkylations are catalyzed by a large variety of metal complexes,[2] being catalysts based on palladium most widely used in organic synthesis.[3] A large variety of chiral ligands has been applied in enantioselective allylation reactions using different kind of substrates, nucleophiles and reaction conditions, leading to high yields and excellent asymmetric inductions. However, when unsymmetrical substrates mainly aryl-substituted allyl systems are involved, palladium catalysts direct the nucleophilic attack to the less substituted allylic terminal carbon atom, giving the achiral regioisomer.[4] In contrast, metals such as iridium,[5] tungsten[6] or molybdenum[7] generally favor the nucleophilic attack at the more substituted terminus (Scheme 1.1). In this context, molybdenum represents an attractive alternative due to the relative low cost of its organometallic precursors (mainly $[Mo(CO)_6]$, $[Mo(CO)_3(EtCN)_3]$ and $[Mo(CO)_3(C_7H_8)]$) and the robustness of the corresponding complexes under catalytic reactions.[7]

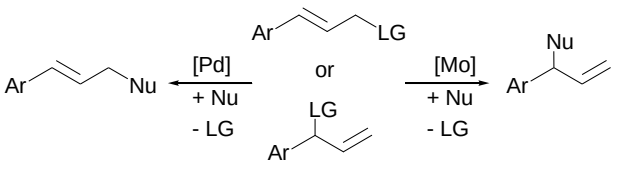

Scheme 1.1. Allylic substitution catalyzed by Pd or Mo systems using unsymmetrical substrates (LG = leaving group).

The first highly regio- and enantio-selective catalytic asymmetric Mo-catalyzed allylic alkylation was reported by Trost and co-workers in 1998, achieving the best results with a C_2-symmetric bis(pyridyl-amide) ligand (**I**, $R_1 = R_2 = H$ in Figure 1.1),[8] which still remains the most efficient system for synthetic purposes;[9] some time before Faller and Murray independently reported stoichiometric alkylations using π-allylmolybdenum complexes.[10] Since then, works concerning both the design of new ligands and comprehension of the mechanism have been carried out.

In Figure 1.1, the most effective chiral ligands used in Mo-catalyzed allylic alkylation reactions are collected.[11] In order to compare the regio- and the enantio-selectivity induced by these catalytic systems, cinammyl carbonate using dimethylmalonate (as neutral nucleophile in the presence of a base or as the corresponding sodium salt, $NaCH(COOMe)_2$) is taken into account as a benchmark reaction. First Trost[8] and later Moberg[12] used bis(pyridyl-amide) ligands containing a *trans*-1,2-diaminocyclohexyl scaffold (type **I** ligands, Figure 1.1), giving excellent regio- (up to 49:1 for branched:linear regioisomer ratio) and enantio-selectivity (up to 99% of ee) (entries 1-4, Table 1.1); working under microwave heating, a cheaper and more stable molybdenum precursor, $[Mo(CO)_6]$, could be used instead of $[Mo(CO)_3(EtCN)_3]$ (entries 2-4 and 10, Table 1.1).[12]

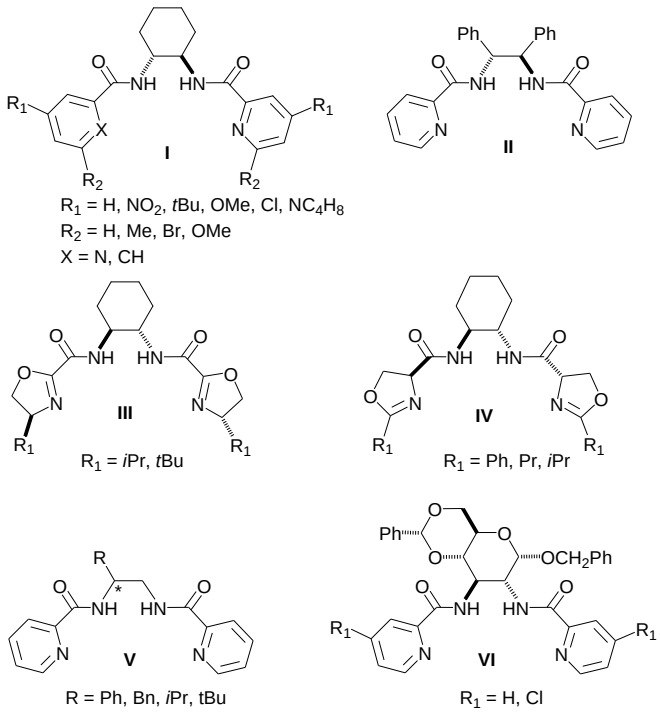

Figure 1.1. Efficient representative chiral ligands applied in Mo-catalyzed allylic alkylation.

When *trans*-1,2-diamino-1,2-diphenylethyl is present in the ligand structure instead of the analogous cyclohexyl backbone (ligand **II**, Figure 1.1), the regioselectivity decreases maintaining high asymmetric induction (entry 5, Table 1.1).[13] Based on

these highly successful pyridyl-amides, Pfaltz developed new C_2-symmetrical bis(oxazolinyl-amide) ligands (types **III**[14] and **IV**,[15] Figure 1.1). These Mo catalytic systems induced excellent enantioselectivity, but in both cases, the regioselectivity decreased (entries 6 and 7, Table 1.1). Kočovský and Lloyd-Jones designed C_1-symmetrical ligands of type **V** (Figure 1.1) in order to study the effect of the chiral environment on the selectivity of the reaction.[16] The high selectivity obtained (entry 8, Table 1.1) evidenced that one stereocenter on the ligand is enough to render efficient Mo catalytic systems. This result is in agreement with those obtained by Trost using ligands containing only one pyridyl group (entry 9, Table 1.1 and ligand **VII**, Figure 1.2)[13]. More recently, Moberg and co-workers have synthesized new bis(pyridyl-amide) ligands containing a carbohydrate-based backbone instead of chiral 1,2-diamino scaffolds (type **VI** ligands, Figure 1.1)[17]. The ligand coming from α-D-glucose gave the same regio- and enantio-selectivity than the ligand designed by Trost, which represents one of the highest selective Mo system currently reported (entry 10 *vs* 1, Table 1.1).

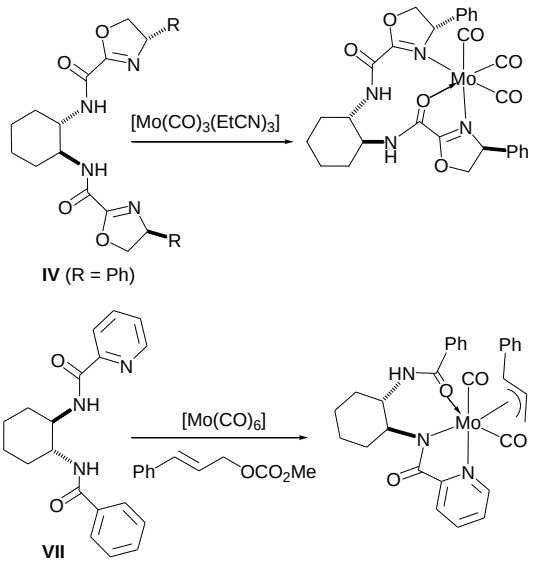

Figure 1.2. Three-coordination of bis(oxazoline) (top) and bis(amide) (down) ligands involved in carbonyl molybdenum complexes (refs. 15 and 18, respectively).

Concerning the coordination chemistry, Pfaltz and and co-workers proved that the potential tetra-coordinated bis(oxazolinyl-amide) (type **IV** ligand, Figure 1.1) behaves as a tri-coordinated framework when reacts with carbonyl molybdenum precursors,

giving [Mo(CO)$_3$(κ^3-*N*,*N*',O-**IV**)] (for **IV**, R = Ph) (Figure 1.2).[15] Analogously, Trost *et al.* isolated the π-allyl Mo(II) complex containing mono-deprotonated pyridyl-bisamide ligand (type **I**) starting from [Mo(CO)$_6$] in the presence of cinnamyl carbonate (Figure 1.2).[18] This coordination mode agrees with the stereochemical requirements observed in the catalytic allylic alkylation (see above, entry 9 vs 1 in Table 1.1). From a mechanistic point of view, metal-catalyzed asymmetric allylic alkylations using soft nucleophiles mainly carry on in two steps: oxidative addition of the allylic substrate leading to a metal-allyl intermediate followed by nucleophilic attack to give the substitution product. Both steps can proceed with either retention or inversion of configuration. For Pd catalytic systems, the overall stereochemistry is retention with the two steps undergoing inversion.[19] For Mo, the overall reaction also takes place with retention, [8] but as proved by Kočovský and Lloyd-Jones the mechanism in this case proceeds by a retention-retention step-way.[16a,20]

Table 1.1. Mo-catalyzed allylic alkylation of cinnamyl carbonate using dimethylmalonate as nucleophile.

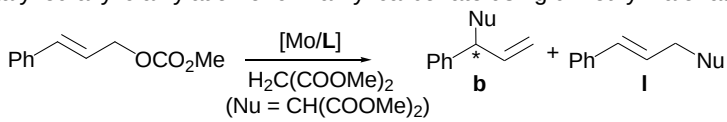

Entry [Ref]	**L**[a]	Mo precursor (mol%)	R_1, R_2	**b**:**l** (ee,%)
1[8]	**I** (X=N)	[Mo(CO)$_3$(EtCN)$_3$] (15)	H, H	49:1 (99)
2[12]	**I** (X=N)	[Mo(CO)$_6$] (4)[b]	OMe, H	41:1 (>99)
3[12]	**I** (X=N)	[Mo(CO)$_6$] (4)[b]	Cl, H	74:1 (96)
4[12]	**I** (X=N)	[Mo(CO)$_6$] (4)[b]	NC_4H_8, H	88:1 (96)
5[13]	**II**	[Mo(CO)$_3$(EtCN)$_3$] (10)	-	19:1 (99)
6[14]	**III**	[Mo(CO)$_3$(EtCN)$_3$] (10)	*i*Pr, -	14:1 (99)
7[15]	**IV**	[Mo(CO)$_3$(EtCN)$_3$] (10)	Pr, -	6:1 (98)
8[16]	**V**	[Mo(CO)$_3$(EtCN)$_3$] (10)	(*S*)-*i*Pr, -	38:1 (97)
9[13]	**I** (X=CH)	[Mo(CO)$_3$(C_7H_8)] (10)	H, -	60:1 (99)
10[17]	**VI**	[Mo(CO)$_6$] (10)[b]	H, -	49:1 (99)

[a] See Fig. 1.1. [b] Microwave heating.

1.3. Asymmetric alkene metathesis

Olefin metathesis has been established as an indispensable method in organic synthesis for the preparation of a myriad of compounds. Nowadays, Ru- and Mo-catalyzed olefin metathesis is routinely used to prepare an array of complex molecules, including small, medium and large rings.[21]

During the last decade, research efforts have focused on the development of efficient catalytic enantioselective olefin metathesis reactions. Schrock, Hoveyda and co-workers have developed a series of optically pure chiral Mo-based arylimido alkylidene complexes that efficiently promote asymmetric ring-closing as well as ring opening metathesis reactions (ARCM and AROM, respectively). The majority of these catalysts are four or five-coordinated species bearing an imido functionality and a chiral diolate.[22] Representative chiral molybdenum alkylidene complexes are summarized in Figure 1.3.

The first example of catalytic enantioselective metathesis was described by using the chiral biphen-Mo containing the 6,6´-dimethyl-3,3´-5,5´-tetra-tert-butyl-1,1´-biphenyl-2,2´-diol unit (type **1** complexes in Figure 1.3).[23] Type **1** complexes were proved to be highly effective catalysts in ARCM of 1,6-dienes affording five-membered carbo- and hetero-cycles in high optical purity. However, lower asymmetric induction was obtained in the reactions involving 1,7-dienes. Soon after, a new class of binol-based chiral Mo catalysts, complexes **2** in Figure 1.3, were disclosed by the same authors. These new complexes were particularly effective in the enantioselective synthesis of chiral cyclohexenes, dihydropyranes and 1,7-dienes giving high enantiomeric excesses.[24]

Since then, an impressive number of molybdenum-based alkylidene complexes bearing functionalized chiral binol ligands have been designed and applied in both ARCM and AROM transformations by Schrock, Hoveyda and co-workers. It has been proved that smooth modification of the chiral alkoxide leads to substantial improvement of selectivity. As an example, type **3** complexes (Figure 1.3) share structural features with both biphen-**1** and binol-**2** based systems representing an

hybrid between both **1** and **2** catalysts, and provides a unique selectivity profile, not observed using these latter systems.[25] From a practical point of view, catalysts **3** offer an important advantage because they can be prepared from commercially available starting materials and used *in situ*, without isolation, to attain enantioselective olefin metathesis.

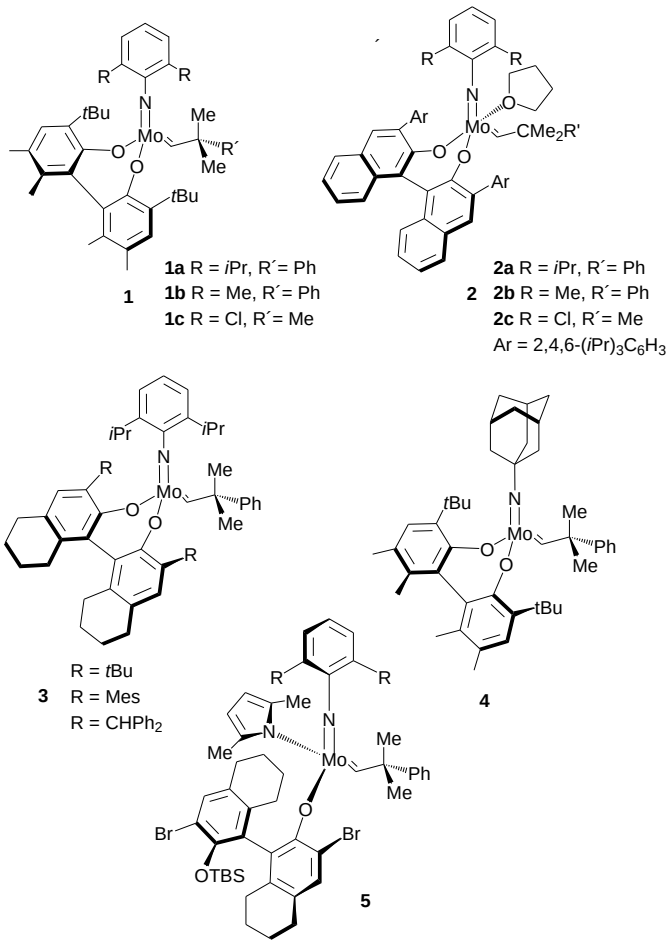

Figure 1.3. Representative chiral alkylidene molybdenum complexes. OTBS = OSi(*t*Bu)Me_2.

The applicability of molybdenum-based catalysts in both ARCM and AROM reactions to obtain optically pure products, unavailable by other methods, is now well demonstrated.[26] Substantial variations in reactivity and selectivity arises from subtle changes in catalyst structures. Structural modifications of diolate ligands have proved to control both the selectivity and reactivity of olefin metathesis reactions.

Selected examples illustrating the importance of catalyst modularity and substrate specificity in asymmetric catalysis are depicted in Schemes 1.2 and 1.3. The binol-based catalyst **2a** promotes the RCM of dienes **S-I** and **S-II** with outstanding levels of selectivity in contrast to complex **2b** that is not an efficient catalyst for the kinetic resolution of **S-I** and **S-II** (Scheme 1.2).

The ARCM processes presented in Scheme 1.3 involve the catalytic desymmetrization of 1,6- and 1,7-dienes. Catalyst **2a** is unable to initiate RCM of substrate **S-III**, being complex **1b** the best choice for this transformation. In contrast, **2a** readily promotes the conversion of silyl ether **S-IV** to the six-membered ring allyl silane **P-IV** giving 99% ee with a 98% yield in 3h. Biphen-based **2a** complex is significantly less effective affording lower levels of enantioselection and low yield of product.[24]

Structural changes of the catalysts have also been introduced taking into account the substituents on the imido ligand. Mo-biphen complexes bearing an alkylimido group (complex **4**, Figure 1.3) instead of arylimido displayed reactivity and enantioselectivity levels that are not accessible by the complexes previously described.[27]

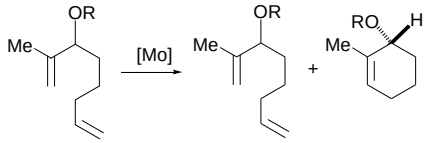

S-I, R = TES
S-II, R = TBS

P-Ia
P-IIa

P-Ib
P-IIb

(*S*)-**S-I,** k_{rel} = 24, [Mo] = **2a**
(S)-**S-I**, k_{rel} = 5, [Mo] = **2b**
(*S*)-**S-II,** k_{rel} = 25, [Mo] = **2a**
(*S*)-**S-II,** k_{rel} = 5, [Mo] = **2b**

Scheme 1.2. Mo-catalyzed kinetic resolution of 1,7-dienes. For the corresponding complexes, see Figure 1.3 TES = $SiEt_3$; TBS = Si(*t*Bu)Me_2.

One illustrative example is the better performance of the alkylimido **4** in the asymmetric ring-opening/cross metathesis with triene **S-V** compared to the arylimido **1a**. As showed in Scheme 1.4, the reaction promoted by arylimido **1a** gives significant amount of **P-Vb** (an achiral by-product) and low enantioselectivities.

However, under identical reaction conditions, catalyst **4** yields the desired product **P-Va** with high conversion and selectivity (96% ee, 82% isolated yield).[27b]

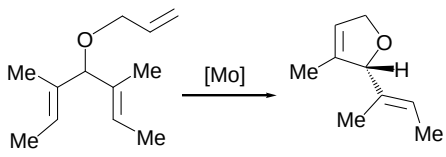

S-III **P-III**

[Mo] = **1a** 99% ee; 83% yield
[Mo] = **2a** 0% ee; 5% yield

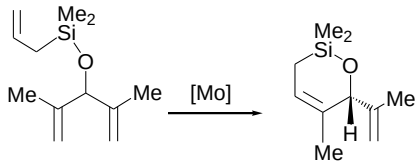

S-IV **P-IV**

[Mo] = **1a** 65% ee; 17% yield
[Mo] = **2a** 99% ee; 98% yield

Scheme 1.3. Mo-catalyzed asymmetric desymmetrization of trienes. For the corresponding complexes, see Figure 1.3.

Catalytic AROM transformations have been developed as tandem processes involving the catalytic enantioselective C-C bond cleavage (ring-opening) followed by an intramolecular ring closing metathesis (RCM) or intermolecular cross-metathesis (CM).[28] As an example, Scheme 1.5 illustrates the tandem Mo-catalyzed AROM/CM reaction of a norbornyl ether with styrene to afford the corresponding cyclopentyl derivatives in high levels of selectivity and efficiency.[29]

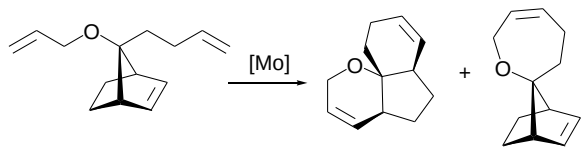

S-V **P-Va** **P-Vb**

[Mo] = **4** 96% ee; 82% yield for compound **P-Va**
[Mo] = **1a** 18% ee; 45% yield for compound **P-Va**

Scheme 1.4. Mo-catalyzed asymmetric ring-opening/cross metathesis. For the corresponding complexes, see Figure 1.3.

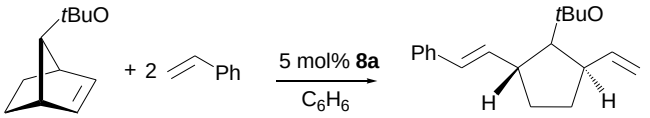

98% ee
92% yield

Scheme 1.5. Mo-catalyzed tandem AROM/CM reactions. For the corresponding complexes, see Figure 1.3.

Recently, monoalkoxide pyrrolide (MAP) molybdenum species of the general formula [Mo(NR)(CHR´)(OR´´)(Pyr)] where Pyr is a pyrrolide or substituted pyrrolide ligand and OR´´ is an aryloxide, have attracted much interest in the field of enantioselective catalysis[30].

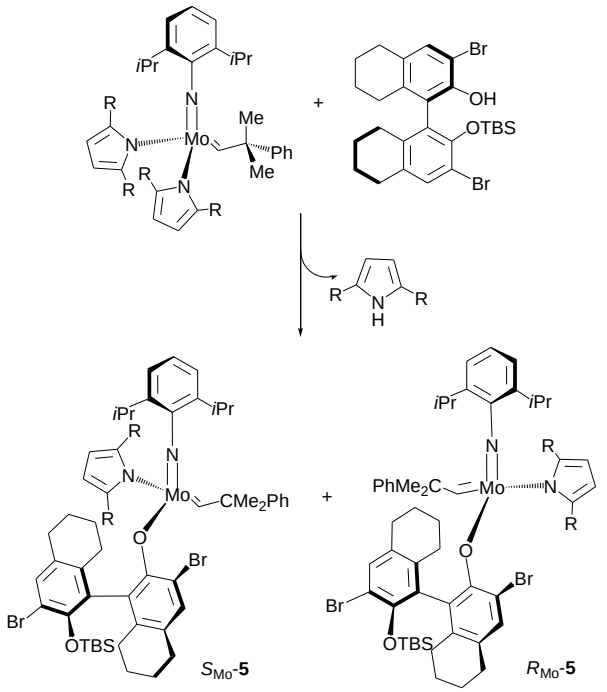

5a R = H; d.r. = 20:1
5b R = Me; d.r. = 7:1

Scheme 1.6. Diastereoselective synthesis of stereogenic-at-Mo complexes. OTBS =OSi(*t*Bu)Me_2; d.r. = diastereomeric ratio.

These new types of catalysts have a stereogenic metal center, as a consequence of the four different ligands being covalently attached to molybdenum in a tetrahedral

environment. The molybdenum-based complexes were stereoselectively prepared by a ligand exchange process involving an enantiomerically pure aryloxide (Scheme 1.6).[31] The reactivity of MAP towards olefins is often much greater than that of bisalkoxides. Theoretical studies have predicted that high-oxidation-state complexes containing two electronically distinct ligands should be particularly effective promoters of alkene metathesis.[32]

The stereogenic-at-Mo complex **5b** reported by Schrock and Hoveyda represents a rare case of the successful use of a monodentate O-based chiral ligand in enantioselective catalysis. They demonstrated the applicability of the new catalysts in the enantioselective synthesis of an Aspidosperma alkaloid, (+)-quebrachamine, through an alkane metathesis reaction that cannot be promoted by any of the previously reported chiral catalysts (Scheme 1.7).[31]

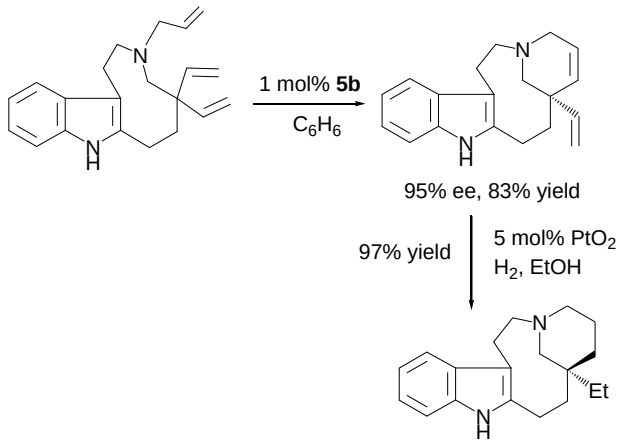

Scheme 1.7. Enantioselective synthesis of (+)-quebrachamine through an enantioselective RCM of a triene promoted by the stereogenic-at-Mo complex **5b** (results from ref [31a,b]).

The proposed mechanism of metal-catalyzed olefin metathesis promoted by stereogenic-at-metal complexes implies that the configuration at the metal center is inverted in each olefin metathesis step. As illustrated in Scheme 1.8, the olefin attacks the metal in MAP species *trans* to the pyrrolide ligand to form an intermediate metallacyclobutane that contains the pyrrolide and two carbon atoms of the resulting metallacycle in equatorial positions. The olefin then leaves *trans* to the

pyrrolide to form the new alkylidene with the opposite configuration at metal. Therefore, the reactant olefin enters *trans* to the pyrrolide and the product olefin leaves *trans* to the pyrrolide, via a trigonal bipyramidal intermediate with axial imido and aryloxide ligands, inverting the configuration at the metal in each metathesis step.[33] This pathway mechanism is consistent with theoretical calculations performed by Eisenstein and co-workers.[31]

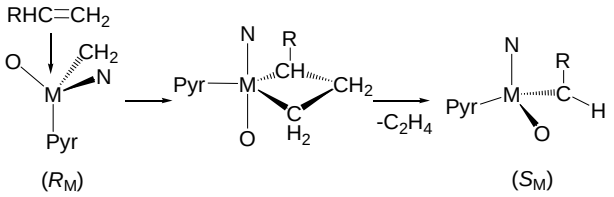

Scheme 1.8. Proposed mechanism of metal-catalyzed olefin metathesis promoted by stereogenic-at-metal complexes.

1.4. Asymmetric alkene epoxidation

The significance of olefin epoxidation reactions began with the development of homogeneous catalysts based on oxomolybdenum(VI) complexes in the Halcon and Arco Processes.[34] Since then many contributions have been reported, concerning non-chiral molybdenum(VI) complexes.[35] However only some chiral molybdenum systems have been efficiently applied in the epoxidation of prochiral olefins, also including heterogeneous supported catalysts.[36] The different ligands used in selective epoxidation processes, most of them containing *N*,*O*-heterodonor groups, will be next presented, underlining the most relevant results.

1.4.1. Chiral amides (*O*,*O*'-donor ligands)

Since 1970s, several chiral ligands have been applied trying to find an efficient chiral version of olefin epoxidation. In 1979 Schurig *et al*.[37] reported the preparation of an optically active oxodiperoxo containing the (*S*)-*N,N*-dimethyl-lactamide **VIII**, (Figure 1.4) which was applied as catalyst in the epoxidation of different olefins (propene, 1-butene, 3-methyl-1-butene); however the enantiomeric excess (ee) obtained was low (34%).

Later on, Shuring tested molybdenum complexes containing different hydroxyamide ligands, namely (*S*)-*N*,*N*,-dimethyl lactamide = **VIII**, (*S*)-piperidine lactamide = **IX**, (*S*)-*N*,*N*,-dimethyl-3-phenyl lactamide = **X**, (*S*)-2-hydroxy-3-methylbutanoic acid piperidineamide = **XI**, (*2S,3S*)-2-hydroxy-3-methylpentanoic acid piperidineamide = **XII**, (*S*)-3-hydroxybutanoic acid piperidineamide = **XIII**, (*S*)-*N*-benzoylprolinol = **XIV**, and (*S*)-*N*-acetylprolinol = **XV**).[38] In the epoxidation of *trans*-but-2-ene with the complex derived from (*S*)-piperidinelactamide an ee value of 49% was obtained; the ee value remained constant during the reaction time (from 10 min to 10 h). The substitution of acyclic dimethylamine for cyclic piperidine in the amide function did not alter the enantiomeric composition of the oxirane formed. However, an increase of the steric hindrance of the ligand (**XIII**, **XII** and **X** *vs*. **VIII**) resulted in a decrease of enantioselectivity.

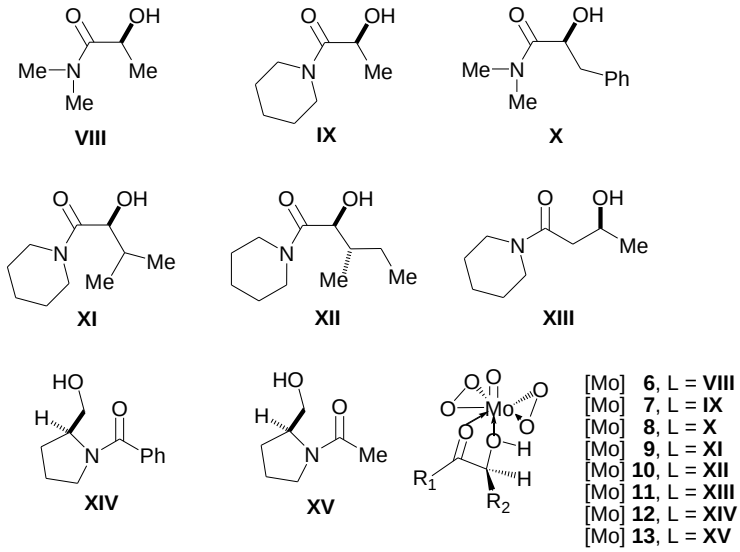

Figure 1.4. Amide ligands coordinated to an oxodiperoxo Mo(VI) unit.

The degree of substitution in the metal center shows an inverse dependency of the ee % obtained. It was also found that the type of chelate ring, with the metal affect the enantioselectivity of the oxirane formed Thus, the asymmetric induction decreases in the order: (α(**VIII**, **IX**) > β (**XIII**) > γ (**XIV**, **XV**), as well as the addition of optically pure 1,2-alkanediol by kinetic resolution of the oxiranes.

Yoon and co-workers described in 2000,[39] the use of chiral oxodiperoxo Mo(VI)-complexes, bearing (*R*)-piperidinylphenylacetamide (**XVI**) and (*R*)-piperidinylmandelamide (**XVII**), **14** and **15** in Figure 1.5, in the olefin epoxidation of *cis* and *trans*-β-methylstyrene using CCl_4 as solvent at room temperature (Scheme 1.9.)

Some of the catalysts tested were chemoselective in the epoxidation of *cis*-β-methylstyrene; accordingly, the product corresponding to the olefin isomerization was not observed. *Trans*-β-methylstyrene, was more enantioselectively epoxidized than *cis*-β-methylstyrene. Thus the *trans*-β-methyl styrene oxide was obtained in 40% of ee using the Mo catalyst **14** and in 80% of ee for molybdenum complex **15**. However, the highest asymmetric induction obtained in the epoxidation of the *cis*-β-methyl styrene olefin was only of 40% of ee for the Mo/**15** catalytic system.

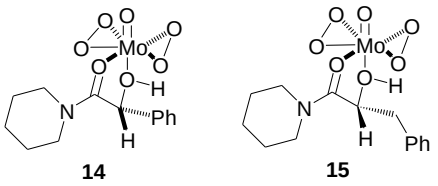

Figure 1.5. Oxodiperoxo Mo(VI) complexes containing amide ligand.

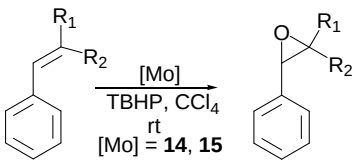

Scheme 1.9. Olefin catalytic epoxidation using oxodiperoxo Mo(VI) complexes **14** and **15**.

1.4.2. Chiral pyridyl alcohols (*N*,*O*-donor ligands)

Since 1999, the interest in the synthesis of molybdenum complexes containing pyridyl alkoxide ligands has grown up, and the reason can be probably found in: i) their straightforward synthesis, by simple reaction of 2-lithiopyridine derivatives and

the corresponding ketones, and ii) their robustness under catalytic conditions. Figure 1.6 collects the different pyridinamino alkoxide employed in asymmetric olefin epoxidations. Some of the more important results are summarized in Table 1.2.

The ee depends on the nature of the chiral ligand employed and much less on the number of equivalents of ligand around the metal (entry 4 in Table 1.2, (ligand = **XXIII**, [Mo] = **21a**, **21b**, see Figure 1.6)). The presence of bulky norbornadiene ligand gave in some cases high optical inductions (entry 2 in Table 1.2 (L = **XIX**, [Mo] = **17**)). Apparently, olefin stereoisomers react at the same rate with the same molybdenum complex (entry 3 in Table 1.2 (L = **XXII**, [Mo] = **20**)). In order to justify the low asymmetric inductions, it has been argued that the increase of the polarity of the solvent, due to the concomitant formation of *tert*-butanol which is formed as reduction product of *tert*-butylhydroperoxide (TBHP), influences negatively in the enantiomeric excess.[40]

Table 1.2. Molybdenum complexes containing pyridyl alkoxide ligands applied in olefin epoxidation using TBHP as oxidant[a].

Entry	Olefin	Ligand	Conversion (%)	ee (%)[b]
1[42]	1-hexene	**XVIII**	20	25
2[40]	*trans*-β-methyl styrene	**XIX**	76	26
		XX	71	15
		XXI	81	4
3[43]	Styrene	**XXII**	29	-
	(1*S*)-(α)-apinene		57.7	
	(1*R*)-(α)-apinene		54.6	
4[44]	*trans*-β-methyl styrene	**XXIII**	51(69)[c]	23(18)[c]
5[45]	*trans*-β-methyl styrene	**XXIV**	65 (58)[d]	0 (0)[d]
		XXV	52 (47)[d]	7 (23)[d]
		XXVI	56 (52)[d]	5 (6)[d]

[a] Molybdenum complex containing two coordinated chiral pyridinamino alcohol ligands; [b] Enantiomeric excesses (e.e.); [c] In brackets conversion or ee, for molybdenum complex containing only one chiral coordinated ligand; [d] In brackets, convertion or ee using CHP (cumyl hydroperoxide) instead of TBHP as oxidant.

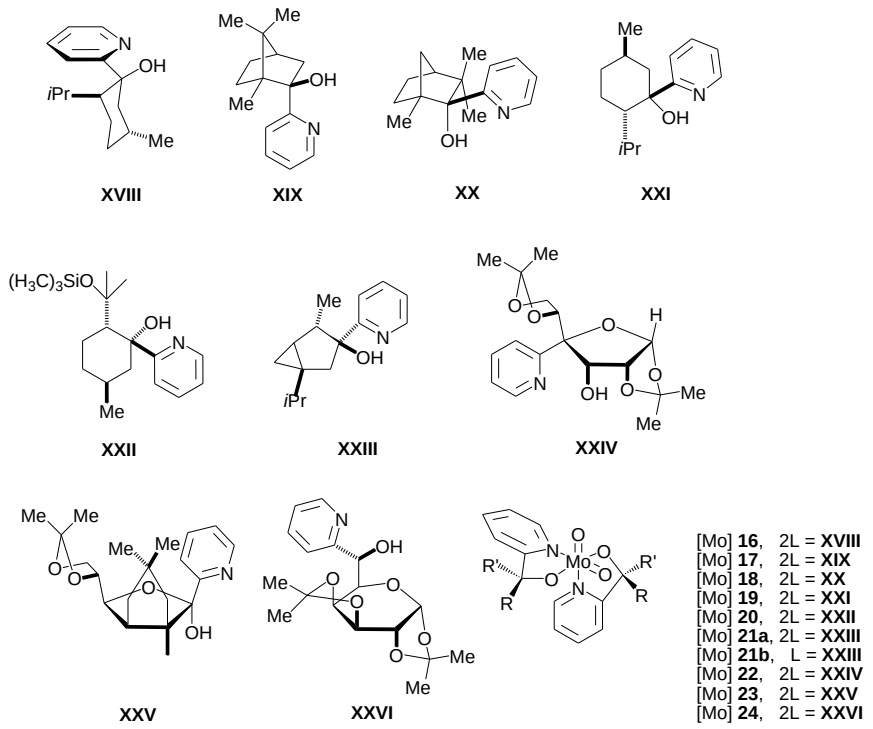

Figure 1.6. Relevant pyridyl alkoxide ligands applied in olefin epoxidation reactions.

However, pyridiyl alcohols coming from camphor and fenchone (**XIX**, **XX** in Figure 1.6) led to full conversion and noticeable enantioselectivity (up to 80% ee) for the epoxidation of *cis*-1-propenylphosphonic acid (CPPA, Table 1.3). The corresponding epoxide exhibits an antibiotic activity (Scheme 1.10).[41]

Table 1.3. Results of Mo-catalyzed epoxidation of CPPA.

Entry	Oxidant	Olefin/time	T (º C)	Ligand[a]	Mo[a]	Conversion (%)	ee (%)[b]
1	(H_2O_2 30%)	CPPA/ 24 h	0	**XIX**	**17**	28	75
			50			58	62
2	(H_2O_2 30%)	CPPA/ 24 h	0	**XX**	**18**	100	67
			50			100	80

[a] See Figure 1.6. [b] Enantiomeric excess.

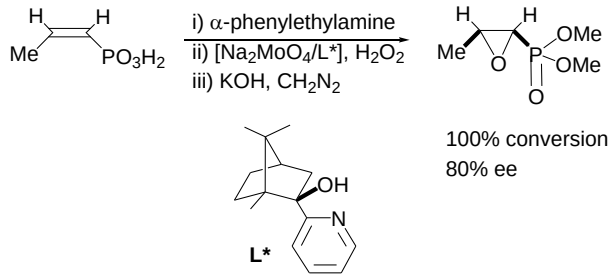

Scheme 1.10. Synthesis of fosfomycin by Mo-catalyzed epoxidation.

1.4.3. Chiral amino alcohols (*N*,*O*-donor ligands)

Direct application of natural amino acids (**XXVII**, **XXVIII** in Figure 1.7) resulted in low ee values (less than 10%), and only a small amount of epoxide was detected in the presence of aqueous TBHP in CH_2Cl_2 at 25 ºC.[46] However, amino alcohols **XXIX**-**XXXIII** (Figure 1.7) led to the formation of the epoxide in higher yields and enantiomeric excesses around 50% and 20%, under similar reaction conditions. Modification of prolinol (**XXIX**) to diphenyl-2-pyrrolidine methanol (**XXXI**) increased the enantioselectivity from 23% to 46%, pointing to a major role of the phenyl substitutents in controlling the asymmetric induction during the catalytic process. Meanwhile, changing the oxidant to cumene hydroperoxide (CHP) did not improve the result. However, the use of anhydrous TBHP instead of aqueous oxidant (57% yield and 46% ee) increased the efficiency of the catalytic reaction (67% yield and 69% ee).

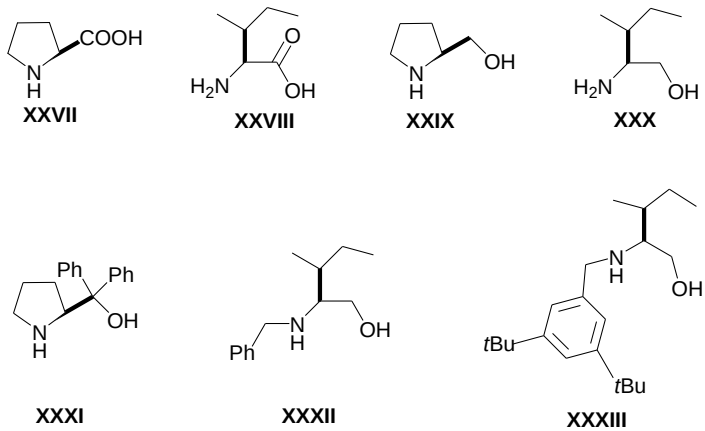

Figure 1.7. Chiral amino alcohols applied in styrene derivatives epoxidation catalyzed by molybdenum.

The molar ratio of molybdenum to ligand had also strong effects on the catalytic behavior. When the Mo:L ratio increased from 1:1.1 to 1:2.2, the enantioselectivity decreased from 69% to 25% respectively. Solvents such as toluene, THF and CH_3CN were tested giving lower yields and ee. Styrenes containing electron-withdrawing substituents were epoxidized giving better results than those bearing electron-donating groups. Therefore when the substrate changed from 4-methylstyrene to 4-chloro-styrene, ee increased from 70% to 81%. The best result in terms of enantioselectivity (up to 84%) was obtained in the catalytic epoxidation of 4-fluoro-styrene (Scheme 1.11).

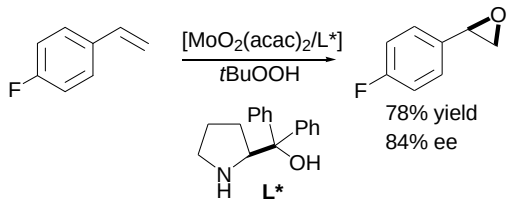

Scheme 1.11. Dioxo-molybdenum(VI) catalytic system containing a chiral amino alcohol applied in 4-fluoro-styrene epoxidation.

1.4.4. Chiral phosphinoylalcohols (*P*,*O*-donor ligands)

Chiral phosphinoylalcohols (Figure 1.8) were used under stoechiometric conditions for non-functionalized alkenes by Stirling and co-workers.[47] As expected from the coordination mode of this type of ligands (Figure 1.9), the enantioselectivity was low (10% ee) in the epoxidation of several olefins (3,3-dimethylbut-1-ene, pent-1-ene, hept-1-ene, (*E*)-pent-2-ene, (*Z*)-pent-2-ene) using TBHP as oxidant, except in the case of the binaphthyl derivatives (**XXXVIII**, **XXXIX**, Figure 1.8), obtaining 39% of enantiomeric excess. The optical yield of the epoxides did not appear to be affected by the solvent, giving similar results when the reaction was performed in dichloromethane or nitromethane.

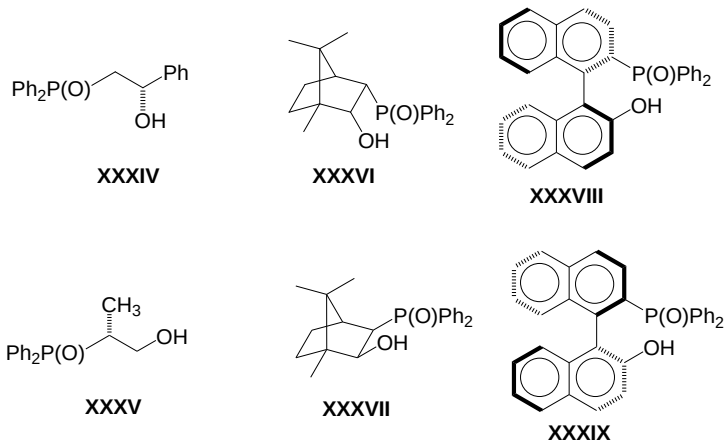

Figure 1.8. Chiral phosphinoylalcohols applied in Mo-catalyzed olefin epoxidation.

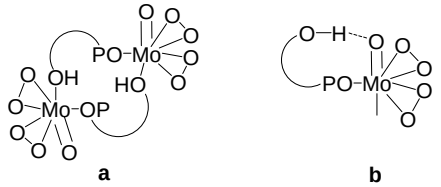

Figure 1.9. Plausible structures of molybdenum complexes containing phosphinoylalcohol under catalytic conditions.

1.4.5. Chiral *N*,*O*,*O*'-donor ligands from carbohydrates

The first carbohydrate-based ligands were coordinated to the MoO_2^{2+} moiety by Rao and co-workers[48] in 2001 (Figure 1.10), affording compounds of the general formula [MoO_2L] (L = tridentate *N*,*O*,*O*'-donor ligand bearing a carbohydrate backbone). These were applied in olefin epoxidations by Kühn *et al*. using TBHP as oxidant.[49] For the epoxidation of *cis*- and *trans*-β-methylstyrene, the general observation is that the catalytic activity as well as the asymmetric induction for the *cis* substrates were higher than those for the analogous *trans* alkene. The effect of different parameters such as temperature, solvent and the amount of catalyst was studied, observing as expected, that low temperatures are beneficial for the increase of ee. Higher amounts of catalyst also improved both ee and yield. Accordingly, the highest ee was *ca*. 30% using complex **27** (Figure 1.10) as catalytic precursor at 0 ºC.

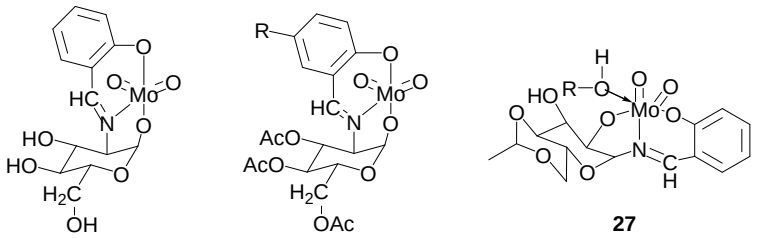

Figure 1.10. Dioxo-molybdenum(VI) complexes containing chiral *N*,*O*,*O*'-tridentate carbohydrate-based ligands.

The low asymmetric induction observed for these catalytic systems can be related to the ease exchange between the chiral ligand and oxidant (TBHP); as consequence of this exchange, the chiral center of the ligand is placed too far away from the oxygen transfer site avoiding the chirality transfer towards the epoxide.

1.4.6. Chiral diols and other related derivatives (*O*,*O*'-, *N*,*S*- and *O*,*S*-donor ligands)

Kühn and co-workers synthesize complexes of the type $[MoO_2(THF)_2L]$ (L = *cis*-*p*-methane-3,8-diol, **28**), $[MoO_2Cl_2L]$ (L = the oxime, **29**), and $[MoO_2Cl(THF)L]$ (L = 8-phenylthioneo, **30**) and they were applied in olefin epoxidations (Figure 1.11).[50] Conversions of 63–82% were obtained with the substrate *cis*-β-methylstyrene, using TBHP as oxidant and toluene as solvent at 55 ºC (Scheme 1.12). The observed ee's were low, getting 24%, corresponding to the catalytic system **28**. The reaction proceeded with retention of configuration of the epoxide and high chemoselectivity towards the formation of epoxide. *cis*-β-Methylstyrene oxide was obtained in 20-24% ee (*R*,*R* isomer) from the initial stage of the reaction to the end (up to 24 h). After a fast conversion within the first hours of the reaction (72% conversion after 4 h), the epoxidation rate slowed down and conversion reached 86% after 24 h. Complex **30**, containing an *O*,*S*-bidentate ligand corresponding to an alcoholate and phenylthio donor centers, did not give significant enantiomeric excess in the epoxidation of *cis*-β-methylstyrene.

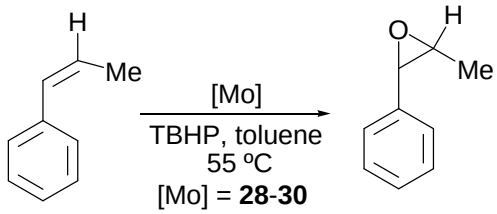

Scheme 1.12. Epoxidation of *cis*-β-methylstyrene catalyzed by **28**-**30.**

Sulfur ligands do not seem to be appropriate for this kind of oxidative chemistry since the S atom will be likely oxidized to sulfoxide or sulfone functions. The optical induction of complexes **29** and **30** was insignificant (less than 3%). This fact can be due to the oxidation of the sulfide or thioether function to sulfoxide which is more labile, losing the bidentate coordination to the metal and in consequence the asymmetric induction.

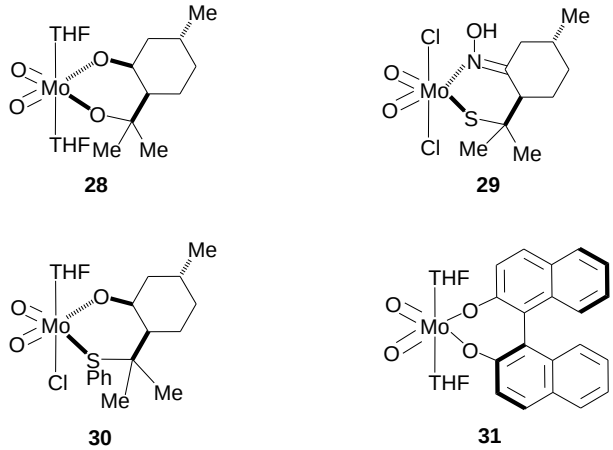

Figure 1.11. Mo complexes coordinated to chiral diols and other related derivatives applied in catalytic olefin epoxidations.

In 2008, Royo *et al*. reported a molybdenum complex containing a chiral binol ligand (**31** in Figure 1.11).[51] The catalytic performance of **31** was investigated in the oxidation of *trans*-β-methylstyrene and limonene using TBHP as oxidant in chloroform at 25 ºC. The reaction proceeded with very low rate for the epoxidation of *trans*-β-methylstyrene, affording only a 7% conversion and negligible enantiomeric excess of the corresponding epoxide (< 5% ee). Better conversion was reached when limonene was tested as a substrate under similar catalytic conditions (36%

conversion). The reaction was chemoselective, exclusively yielding 1,2-epoxy-limonene, but unfortunately it was not diastereoselective, obtaining the *cis*/trans epoxide stereoisomers in a 1/1 ratio, without asymmetric induction.

1.4.7. Chiral diazabutenes (*N*,*N*-donor ligands)

Gonçalves and co-workers prepared chiral 1,4-diazabutenes molybdenum complexes (**32**, **33** and **34**, Figure 1.12).[52] These complexes were evaluated as catalysts for the asymmetric epoxidation of *cis*- and *trans*-β-methylstyrene in toluene using TBHP as oxidant at either room temperature or 55 ºC.

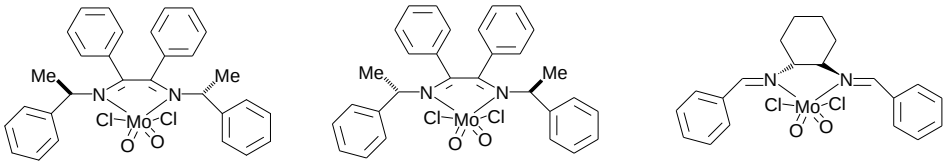

Figure 1.12. Dioxo-molybdenum complexes containing *N*,*N*-donor ligands applied in olefin epoxidations.

For the three complexes studied, the reactions proceeded with high retention of olefin configuration and high selectivity to the epoxide, but only for *cis*-β-methylstyrene significant enantiomeric excesses were obtained. During the first few hours of reaction at 55 ºC, the epoxide yields for *cis*- and *trans*-methylstyrene followed the trend **32** ~ **33** > **34** and **32** ~ **33** >> **34**, respectively. Enantioselectivity decreased with the conversion increased. In the presence of **34** at 55 ºC, (*1S*,*2R*)-*cis*-β-methylstyrene oxide was formed in 65% ee at 12% conversion (4 h), decreasing to 22% ee at 45% conversion (24 h). The enantioselectivity improved at room temperature in detriment of the catalytic activity. Thus, in the presence of **34** at rt, the (*1S*,*2R*)-epoxide was formed in 85% ee at 7% conversion of *cis*-β-methylstyrene (4 h), decreasing to 77% ee at 24% conversion (24 h). The behavior of complex **34** (higher enantioselectivity at lower conversion) is not surprising when the molecular structure is considered. Hence, on the one hand, the chiral ligand remains chelated to the Mo(VI) center during the reaction, but on the other hand it is the most sterically hampered for the approach of the substrate.

1.4.8. Chiral pyrazoles (*N*,*N*'-donor ligands)

In 2006, Carreiro *et al*. reported the synthesis of the first chiral 2-(1-pyrazole)pyridineoxodiperoxomolybdenum(VI) complex (**35** in Chart 1.1), applied to stoichiometric and catalytic olefin epoxidations using TBHP as oxidant in toluene at 100 ºC.[53] The complex **35** was tested in a series of catalytic asymmetric epoxidation reactions using styrene and related substrates. The enantioselectivities obtained for these processes were low in all cases (up to only 6% ee for the epoxidation of 4-methylstyrene).

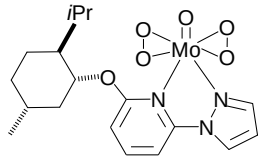

35

Chart 1.1. Oxobis(peroxo)molybdenum complex containing a chiral pyrazole.

Conversions were generally moderate, but in the case of the styrene epoxidation high conversion could be obtained (86% after 17h of reaction). In all cases, epoxide decomposition products were observed, the most detectable and notable being benzaldehyde and 4-methyl-benzaldehyde, demonstrating the lability of both the epoxides and their concomitant hydrolysis products under these reaction conditions. In the epoxidation reaction of cyclohexene in the absence of oxidant (since cyclohexene epoxide is less acid sensitive than styrene), the formation of cyclohexene oxide and cyclohexenediol were observed. This experiment helped to the authors to conclude that perhaps Mimoun and Sharpless step-ways could be competing mechanisms in the olefin epoxidation in the presence of this catalyst. The epoxidation of different olefins (styrene, 4-methylstyrene, 1-methylcyclohexene) was carried out at 100 ºC with TBHP, using the chiral Mo(VI) species generated *in situ* from MoO_3 and the corresponding pyridine or pyrazole (Figure 1.13) ligand as catalytic precursor.[54]

High conversions (around 80%) were obtained with these systems, but unfortunately no enantioselectivity was induced. Different reasons were suggested to explain this

behavior: (i) perhaps more than one chiral or achiral Mo(VI) peroxo catalytic active species are formed in solution; (ii) the labile nature of the peroxo appendage, particularly at high temperature, can lead to the generation of a number of competing diastereomeric transition states; (iii) fast exchanged of ligands or part of them from the coordination sphere of the Mo(VI) peroxo complex; and (iv) no chiral complex is formed under catalytic conditions.

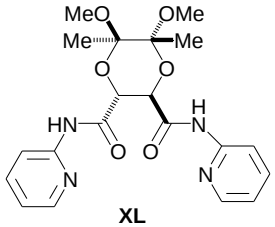

XL

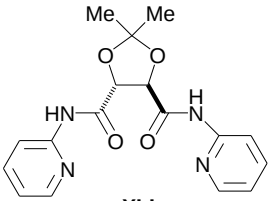

XLI

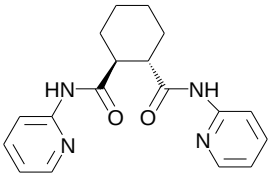

XLII

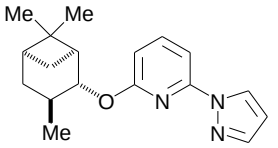

XLIII

Figure 1.13. Different *N*,*N*'-chiral ligands applied in olefin epoxidations in the presence of MoO_3.

1.4.9. Chiral bishydroxamic acid ligands (*O*,*O*-donor ligands)

In 2006, Yamamoto and co-workers published enantioselective olefin epoxidations using chiral bishydroxamic acid ligands (Figure 1.14) in the presence of $[MoO_2(acac)_2]$ as catalytic precursor (where acac = acetylacetonate anion).[55] In Table 1.5 some of the most relevant results in the epoxidation of 1,2-dihydronaphthalene are summarized. The activity and selectivity of the system clearly depend on the oxidant and the nature of the ligand (entries 1-4, Table 1.5). The bulky oxidant THP improved the ee but decreased the catalytic activity (entry 4, Table 1.5).

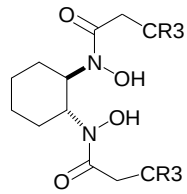

XLIV R = phenyl
XLV R = 4-*i*propylphenyl
XLVI R = 4-*t*butylphenyl

Figure 1.14. Chiral bishydroxamic acids applied in olefin epoxidations.

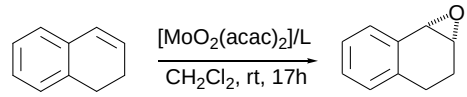

Scheme 1.13. Catalytic epoxidation of 1,2-dihydronaphthalene in the presence of chiral bishydroxamic (see Figure 1.14).

Table 1.5. Effect of the oxidant and ligand in the Mo-catalyzed 1,2-dihydronaphthalene epoxidation.[a]

Entry	Oxidant[b]	Ligand[c]	Conversion (%)	ee (%)
1	TBHP	**XLIV**	15	42
2	CHP	**XLIV**	72	66
3	THP	**XLIV**	27	96
4	CHP	**XLV**	92	80
5	CHP	**XLVI**	82	87

[a] Reactions were carried out in CH_2Cl_2 at room temperature. [b] TBHP = *t*butyl-hydroperoxide; CHP = Cumene hydroperoxide; THP = Tritylhydroperoxide. [C] see Figure 1.14.

1.4.10. Chiral Oxazolines (*N*,*N*-, *N*,*O*- and *N*,*N*,*O*,*O*,-donor ligands)

Ligands that have in particular called the attention in olefin epoxidations are oxazolines due to the robustness of this heterocycle under different reaction conditions.[56] In 2000, Yoon and co-workers reported the effect of some oxazolines (**XLVII**-**XLIX**, Figure 1.15) in the epoxidation of styrene derivatives using $[MoO_2(acac)_2]$ and TBHP in CCl_4 at 70 ºC.[57] The highest enantiomeric excess obtained for the epoxidation of styrene derivatives was less than 10%.

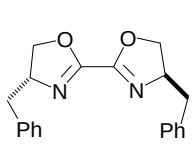

XLVII

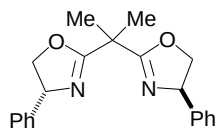

XLVIII

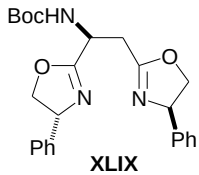

XLIX

Figure 1.15. Some bis(oxazolines) used in olefin epoxidations.

Different groups have been interested in the application of oxazoline ligands in olefin epoxidations (Figure 1.16). Some of the most relevant results are collected in Table 1.6. In general, low asymmetric induction has been found. Only in one case was obtained high diastereoselectivity for the (*R*)-limonene epoxidation using the bimetallic complex **43** (entry 3, Table 1.6). However, the mono-metallic molybdenum oxoperoxocomplex **41** containing the same chiral ligand was completely inactive.

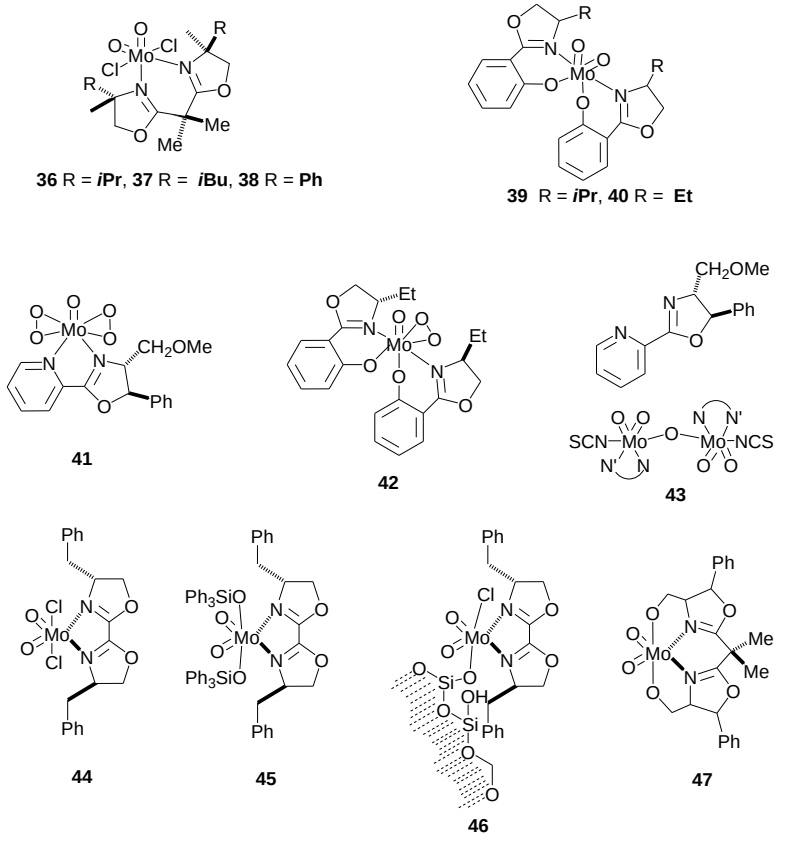

Figure 1.16. Dioxo and oxoperoxomolybdenum complexes containing oxazoline ligands.

The remarkable higher activity obtained with complex **43** compared with complex **41**, with both systems containing the same non labile bidentate ligand, is due probably to the facile formation of a vacant site in complex **43** by isothiocyanate dissociation. Thus, metallic species with unsaturated coordination environments favor either the olefin or the oxidant approach to the metal.

Based on the high activity showed by complex **42** in olefin epoxidations, a ^{1}H NMR study was carried out by Gómez and co-workers, in order to explain the high activity and low selectivity of this catalytic system (Scheme 1.14).[58] The complex can easily form a vacant site due to the hemilabile nature of the oxazolinylphenolate ligand, followed by coordination of TBHP leading to the formation of a transition state, in which the olefin approaches towards the *tert*-butyl peroxide fragment, producing the epoxide and elimination of *tert*-butanol. This mechanism could explain the low selectivity due to the decoordination of the bidentate ligand by the nitrogen donor center, placing the chiral fragment far away from the coordination sphere.

Following the mechanism study concerning olefin epoxidations, the same group published a ^{95}Mo NMR study using the bimetallic molybdenum complex **43** (Figure 1.17) to try to understand the stereoselectivity obtained with this catalyst in the (*R*)-limonene epoxidation.[59] After addition of one equivalent of olefin to a solution of the complex in $CDCl_3$, a new signal appeared at down field (δ -77 ppm) in relation to the neat complex (δ -93 ppm), increasing in intensity with time. The new signal was attributed to a bimetallic Mo species containing two different molybdenum atoms, one coordinated to the olefin (δ -77 ppm), and the other coordinated to the isothiocyanate group (δ -93 ppm); the deshilding observed is due to an electronic density increase at the molybdenum atom probably as consequence of the olefin coordination from the metal center.[60] The olefin coordination to the metal could explain the stereoselectivity observed in the (*R*)-limonene epoxidation.

Table 1.6. Olefin epoxidations catalyzed by molybdenum complexes containing oxazoline ligands using TBHP as oxidant.

Entry [Ref.]	Conditions	Olefin/time	Mo	Conv (%)[a]	ee (%)[c]	Selec (%)[d]
1[44]	50 ºC, toluene	*trans*-β-methyl styrene 18 h	**36**	59	-	
			37	72	-	
			38	86	-	
2[61]	35 ºC, toluene	Styrene/ 18 h	**39**	29	-	44
			40	25	-	35
3[58]	25 ºC, toluene	*(R)*-Limonene/ 22 h	**41**	79(60/40)[b]	-	78
			42	22(50/50)[b]	-	100
			43	50(80/20)[b]	-	78
4[62]	55 ºC, toluene	*trans*-β-methyl styrene/ 18 h	**44**	23	< 1	94
			45	76	< 1	65
			46	23	13	100
5[63]	55 ºC, toluene	*trans*-β-methyl styrene/ 24 h	**47**	44	0	94
	55 ºC, toluene	*(R)*-Limonene/ 24 h		87(22/4)	-	68

[a] Conversion (%). [b] In brackets, *trans*/*cis* ratio. [c] Enantiomeric excess. [d] Selectivity towards epoxide.

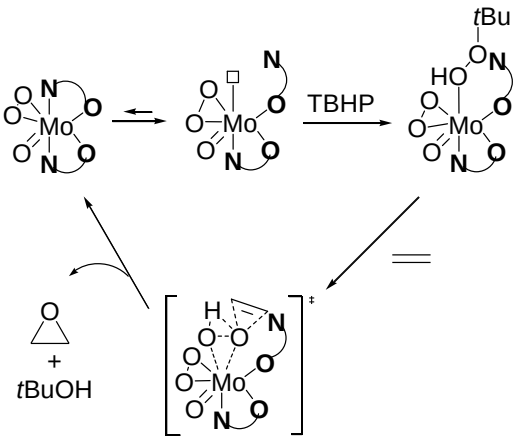

Scheme 1.14. Proposed mechanism for olefin epoxidations catalyzed by seven-coordinated molybdenum species containing hemilabile ligands.

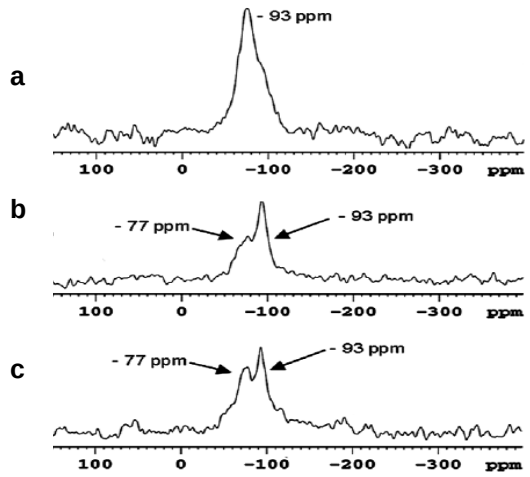

Figure 1.17. ^{95}Mo NMR spectra ($CDCl_3$, 26.08 MHz): (a) complex **43**; (b) **43** + (*R*)-limonene, after 15 min of the olefin addition; (c) **43** + (*R*)-limonene after 48 h of the olefin addition.

1.4.11. Chiral cyclopentadienyl molybdenum complexes

Since 2006, some groups have become interested in the application of cyclopentadienyl molybdenum complexes containing chiral ligands in olefin epoxidations (Figure 1.18). The most significant results are summarized in Table 1.7. From low to moderated selectivity was achieved, depending on the type of catalytic system. The highest enantiomeric excess obtained in the *trans*-β-methylstyrene epoxidation was 25% for the heterogeneous systems **49** and **50** (entry 1, Table 1.7), where complexes where supported on mesoporous MCM-41 and MCM-48 materials. Recently Royo and co-workers prepared the molybdenum complex **55** containing a cyclopentadienyl tethered to an oxazoline fragment. The lack of asymmetric induction displayed by this system in the epoxidation of *trans*-β-methylstyrene, was explained by its instability under the reaction conditions (entry 4, Table 1.7).[64] Decomposition of the catalyst by losing the cyclopentadienyl fragment was demonstrated by ESI-MS studies, corroborating the observations made by Colbran.[65] Moreover, the involvement of radicals in the epoxidation reaction was proved by spin trap experiments.[64]

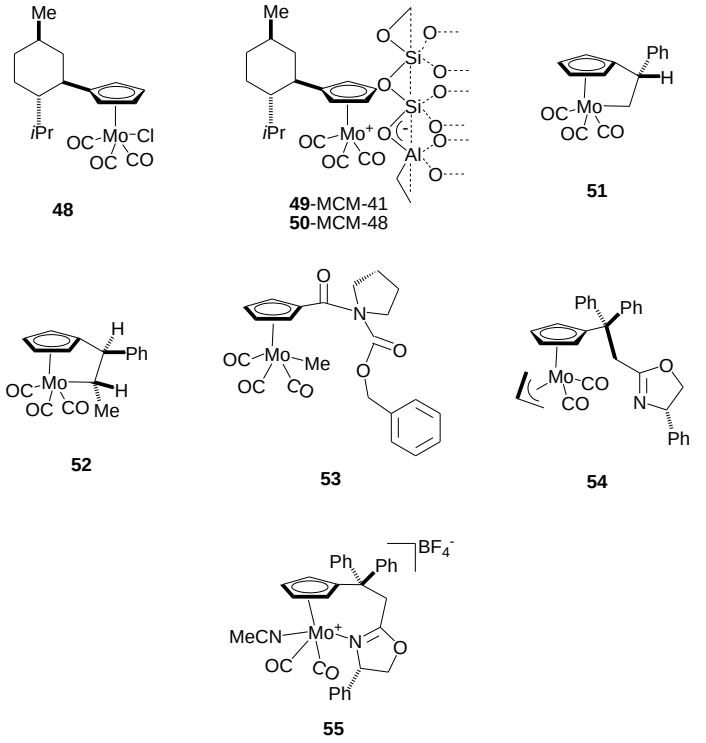

Figure 1.18. Chiral cyclopentadienyl molybdenum complexes applied in olefin epoxidations.

Table 1.7. Cyclopentadienyl molybdenum complexes applied in olefin epoxidations using TBHP as oxidant.

Entry [Ref]	Conditions	Olefin/time	Complex	Conv (%)[a]	ee (%)[c]	Selec (%)[e]
1[66]	55 ºC, $CHCl_3$	*trans*-β-methyl styrene/ 24 h	**48**	84(68)[b]	19(<5)[b,d]	100(<5)[b,d]
			49	55(75)[b]	26(-)[b,d]	100(55)[b,d]
			50	56(99)[b]	25(-)[b,d]	100(41)[b,d]
2[67]	55 ºC, toluene	*trans*-β-methyl styrene/ 4 h	**51**	66	< 15	-
			52	50	20	-
3[68]	$CHCl_3$	*trans*-β-methyl styrene/ 4 h	**53**	77	< 5	99
4[64]	55 ºC, toluene	(*R*)-Limonene/ 1 h	**54**	100(50/50)[f]	-	78
			55	100(60/40)[f]	-	100
	25 ºC, toluene	*trans*-β-methyl styrene/ 16 h	**54**	58	< 5	100
			55	14	< 5	100

[a] Conversions. [b] In brackets the result from styrene epoxidation. [c] Enantiomeric excess. [d] Styrene suffers a ring opening reaction being converted into phenylethane-1,2-diol. [e] Selectivity to epoxide; [f] In brackets *trans*/*cis* ratio.

1.5. References

1 (a) B. M. Trost, C. Lee, in: I. Ojima, *Catalytic Asymmetric Synthesis*, 2nd edition, Wiley-VCH, New-York, 2000, 593-650; (b) A. Pfaltz, M. Lautens, in: E. N. Jacobsen, A. Pfaltz, A. Yamamoto, *Comprehensive Asymmetric Catalysis*, Eds., Springer, Berlin, 1999, 833-884.

2 Z. Lu, S. Ma, *Angew. Chem. Int. Ed.,* 2008, **47**, 258-297 and references therein

3 (a) B. M. Trost, T. Zhang, J. D. Sieber, *Chem. Sci.*, 2010, **1**, 427-440; (b) B. M. Trost, *J. Org. Chem*., 2004, **69**, 5813-5837; (c) B. M. Trost, M. L. Crawley, *Chem. Rev.,* 2003, **103**, 2921-2944.

4 Few reports are described where Pd directs towards the branched regioisomer. See representative examples in: (a) S.-L. You, X.-Z. Zhu, Y.-M. Luo, X.-L. Hou, L.-X. Dai, *J. Am. Chem. Soc*., 2001, **123**, 7471-7472; (b) R. Prétôt, A. Pfaltz, *Angew. Chem. Int. Ed*., 1998, **37**, 323-325.

5 Selected references: (a) J. P. Janssen, G. Helchem, *Tetrahedron Lett.*, 1997, 38, 8025-8026; (b) B. Bartels, C. Garcia-Yebra, F. Rominger, G. Helmchen, *Eur. J. Inorg. Chem.*, 2002, 2569-2586; (c) G. Helmchen, A. Dahnz, P. Dübon, M. Schelwies, R. Weihofen, *Chem. Commun.*, 2007, 675-691; (d) S. Zheng, N. Gao, W. Liu, D. Liu, X. Zhao, T. Cohen, *Org. Lett.*, 2010, **12**, 4454-4457.

6 G. C. Lloyd-Jones, A. Pfaltz, *Angew Chem. Int. Ed.,* 1995, **34**, 462-464.

7 For a review, see: O. Belda, C. Moberg, *Acc. Chem. Res.*, 2004, **37**, 159-167.

8 (a) B. M. Trost, I. Hachiya, *J. Am. Chem. Soc.*, 1998, **120**, 1104-1105; (b) B. M. Trost, S. Hildbrand, K. Dogra, *J. Am. Chem. Soc.*, 1999, **121**, 10416-10417.

9 M. Trost, Y. Zhang, *Chem. Eur. J.,* 2011, **17**, 2916-2922.

10 (a) R. D. Adams, D. F. Chodosh, J. W. Faller, A. M. Rosan, *J. Am. Chem. Soc.*, 1979, **101**, 2570-2578; (b) J. A. McCleverty, A. J. Murray, *J. Organomet. Chem.,* 1978, **149**, C29-C36.

11 Ligands such as chiral bipyridines which gave low selectivity will not be discussed in this context, see for example: A. V. Malkov, I. R. Baxendale, M. Bella, V.

Langer, J. Fawcett, D. R. Russell, D. J. Mansfield, M. Valko, P. Kočovský, *Organometallics*, 2001, **20**, 673-690.

12 (a) O. Belda, C. Moberg, *Synthesis*, 2002, 1601-1606; (b) O. Belda, N.-F. Kaiser, U. Bremberg, M. Larhed, A. Hallberg, C. Moberg, *J. Org. Chem.*, 2000, **65**, 5868-5870.

13 B. M. Trost, K. Dogra, I. Hachiya, T. Emura, D. L. Hughes, S. Krska, R. A. Reamer, M. Palucki, N. Yasuda, P. J. Reider, *Angew Chem. Int. Ed.,* 2002, **41**, 1929-1931.

14 F. Glorius, A. Pfaltz, *Org. Lett.,* 1999, **1**, 141-144.

15 F. Glorius, M. Neuburger, A. Pfaltz, *Helv. Chim. Acta*, 2001, **84**, 3178-3196.

16 (a) A. V. Malkov, P. Spoor, V. Vinader, P. Kočovský, *Tetrahedron Lett.*, 2001, **42**, 509-512; (b) A. V. Malkov, L. Gouriou, G. C. Lloyd-Jones, I. Starý, V. Langer, P. Spoor, V. Vinader, P. Kočovský, *Chem. Eur. J.*, 2006, **12**, 6910-6929.

17 R. Del Litto, V. Benessere, F. Ruffo, C. Moberg, *Eur. J. Org. Chem*., 2009, 1352-1356.

18 S. W. Krska, D. L. Hughes, R. A. Reamer, D. J. Mathre, Y. Sun, B. M. Trost, *J. Am. Chem. Soc.*, 2002, **124**, 12656-12657.

19 (a) T. Hayashi, A. Yamamoto, T. Hagihara, *J. Org. Chem.,* 1986, **51**, 723-727; (b) P. B. Mackenzie, J. Whelan, B. Bosnich, *J. Am. Chem. Soc.,* 1985, **107**, 2046-2054; (c) B. M. Trost, P. E. Strege, *J. Am. Chem. Soc.,* 1975, **97**, 2534.

20 (a) D. Dvorak, I. Stary, P. Kočovský, *J. Am. Chem. Soc.*, 1995, **117**, 6130–6131; (b) G. C. Lloyd-Jones, S. W. Krska, D. L. Hughes, L. Gouriou, V. D. Bonnet, K. Jack, Y. Sun, R. A. Reamer, *J. Am. Chem. Soc.*, 2004, **126**, 702-703.

21 R. R. Schrock, *Angew. Chem., Int. Ed.,* 2006, **45**, 3748-3759.

22 A. H. Hoveyda, R. R. Schrock, *Chem. Eur. J.*, 2001, **7**, 945-950.

23 J. B. Alexander, D. S. La, D. R. Cefalo, A. H. Hoveyda, R. R. Schrock, *J. Am. Chem. Soc*., 1998, **120**, 4041-4042.

24 S. S. Zhu, D. R. Cefalo, D. S. La, J. Y. Jamieson, W. M. Davis, A. H. Hoveyda, R. R. Schrock, *J. Am. Chem. Soc.*, 1999, **121**, 8251-8259.

25 (a) S. L. Aeilts, D. R. Cefalo, P. J. Bonitatebus, Jr. J. H. Houser, A. H. Hoveyda, R. R. Schrock, *Angew. Chem. Int. Ed.*, 2001, **40**, 1452-1456; (b) D. R. Cefalo, A. F. Kiely, M. Wuchrer, J. Y. Jamieson, R. R. Schrock, A. H. Hoveyda, *J. Am. Chem. Soc.*, 2001, **123**, 3139-3140.

26 For a review on Mo and W imido alkylidene complexes as olefin metathesis catalysts, see: R. R. Schrock, A. H. Hoveyda, *Angew. Chem. Int. Ed.*, 2003, **43**, 4592-4633 and references therein.

27 (a) T. S. Pilyugina, R. R. Schrock, P. Müller, A. H. Hoveyda, *Organometallics*, 2007, **26**, 831-837; (b) W. C. Peter Tsang, J. A. Jernelius, G. A. Cotez, G. S. Weatherhead, R. R. Schrock, A. H. Hoveyda, *J. Am. Chem. Soc.*, 2003, **125**, 2591-2596.

28 For representative examples, see: (a) G. S. Weatherhead, J. G. Ford, E. J. Alexanian, R. R. Schrock, A. H. Hoveyda, *J. Am. Chem. Soc*., 2000, **122**, 1828-1829; (b) I. Ibrahem, M. Yu, R. R. Schrock, A. H. Hoveyda, *J. Am. Chem. Soc*., 2009, **131**, 3844-3845; (c) G. A. Cortez, C. A. Baxter, R. R. Schrock, A. H. Hoveyda, *Org. Lett.*, 2007, **9**, 2871-2874.

29 D. S. La, E. S. Sattely, J. G. Ford, R. R. Schrock, A. H. Hoveyda, *J. Am. Chem. Soc.*, 2001, **123**, 7767-7778.

30 R. R. Schrock, *Chem. Rev.*, 2009, **109**, 3211-3226.

31 (a) S. J. Malcolmson, S. J. Meek, E. S. Sattely, R. R. Schrock, A. H. Hoveyda, *Nature*, 2008, 933-937; (b) E. S. Sattely, S. J. Meek, S. J. Malcolmson, R. R. Schrock, A. H. Hoveyda, *J. Am. Chem. Soc.*, 2009, **131**, 943-953; (c) S. J. Meek, S. J. Malcolmson, B. Li, R. R. Schrock, A. H. Hoveyda, *J. Am. Chem. Soc.*, 2009, **131**, 16407-16409.

32 (a) X. Solans-Monfort, E. Clot, C. Copéret, O. Eisenstein, *J. Am. Chem. Soc.*, 2005, **127**, 14015-14025; (b) A. Poater, X. Solans-Monfort, E. Clot, C. Copéret, O. Eisenstein, *J. Am. Chem. Soc.*, 2007, **129**, 8207-8216.

33 S. C. Marinescu, R. R. Schrock, B. Li, A. H. Hoveyda, *J. Am. Chem. Soc*. 2009, **131**, 58-59.

34 (a) J. Kolar (Halcon), US 3.350.422, US3.351.635, 1967; (b) M. N. Sheng, Zajaczek, (Arco), GB 1.136.923, 1968, 1, 923.

35 For recent reviews, see: (a) K. R. Jain, W. A. Herrmann, F. E. Kühn, *Coord. Chem. Rev*., 2008, **252**, 556-568; (b) A. J. Burke, *Coord. Chem Rev*., 2008, **252**, 170-175; (c) F. E. Kühn, A. M. Santos, M. Abrantes, *Chem. Rev.,* 2006, **106**, 2455-2475; (d) C. Freund, M. Abrantes, F. E. Kühn, *J. Organomet. Chem.,* 2006, **691**, 3718-3729; (e) F. E. Kühn, A. M. Santos, W. A. Herrmann, *Dalton Trans*, 2005, 2483-2491.

36 P. Besgse, H. Veschambre, *Tetrahedron*, 1994, **50**, 8885-8927.

37 H. B. Kagan, H. Mimoun, C. Mark, V. Schurig, *Angew. Chem. Int. Ed. Eng*., 1979, **18**, 485-486.

38 V. Schurig, K. Hintzer, U. Leyrer, C. Mark, *J. Organomet. Chem*., 1989, **370**, 81-96.

39 S. Park, K. Kim, S. S. Yoon, *Bull. Korean Chem. Soc*., 2000, **21**, 446-448.

40 W. A. Herrmann, J. J. Haider, J. Fridgen, G .M. Lobmaier, M. Spiegler, *J. Organomet. Chem*., 2000, **603**, 69-79.

41 X-Y. Wang, H-C. Shi, C. Sun, Z.-G. Zhang, *Tetrahedron*, 2009, **60**, 10993-10998.

42 S. Bellemin-Laponnaz, K. S. Coleman, *J. A. Osborn, Polyhedron*, 1999, **18**, 2533-2536.

43 A. A. Valente, A. D. Lopes, I. S. Gonçalves, A, J. E. Rodriguez-Borges, M. Pillinger, C. C. Romão, J. Rocha, X. García-Mera, *New. J. Chem*., 2001, **25**, 959-963.

44 F. E. Kühn, A. M. Santos, A. D. Lopes, I. S. Gonçalves, J. E. Rodríguez-Borges, M. Phillinger, C. C. Romão, *J. Organomet. Chem*., 2001, **621**, 207-217.

45 J. Fridgen, W. A. Herrmann, G. Eickerling, A. M. Santos, F. E. Kühn, *J. Organomet. Chem*., 2004, **689**, 2752-2761.

46 Y. Wang, Z. Wu, Z. Li, X. Zhou, *Tetrahedron Lett*., 2009, **50**, 2509-2511.

47 R. J. Cross, P. D. Newman, R. D. Peacock, D. Stirling, *J. Mol. Catal. A: Chemical*, 1999, **144**, 273–284.

48 A. K. Sah, C. P. Rao, P. K. Saarenketo, E. K. Wegelius, E. Kohlemainen, K. Rissanen, *Eur. J. Inorg. Chem*., 2001, 2773-2781.

49 J. Zhao, X. Zhou, A.M. Santos, E. Herdtweck, C.C. Romão, F.E. Kühn, *J. Chem. Soc., Dalton Trans*, 2003, 3736-3742.

50 I. S. Gonçalves, A. M. Santos, C. C. Romão, A. D. Lopes, J. E. Rodríguez-Borges, M. Pillinger, P. Ferreira, J. Rocha, F. E. Kühn, *J. Organomet., Chem*., 2001, **62**6, 1-10.

51 A. P. da Costa, P. M. Reis, C. Gamelas, C. C. Romão, B. Royo, *Inorg. Chim. Acta*, 2008, **361**, 1915-1921.

52 S. Gago, J. E. Rodríguez-Borges, T. A. M. Santos, J. Zhao, M. Pillinger, C. D. Nunes, Z. Petrovski, T. M. Santos, F. E. Kühn, C. C. Romão, I. S. Gonçalves, *J. Mol. Catal. A: Chemical*, 2005, **236**, 1-6.

53 E. P. Carreiro, G. Yong-En, A. J. Burke, *Inorg. Chim. Acta*, 2006, **359**, 1519-1523.

54 E. Carreiro, C. Monteiro, G. Yong-en, A. J. Burke, A. I. Rodrigues, *J. Mol. Catal. A: Chemical*, 2006, **260**, 295-298.

55 A. U. Barlan, A. Basak, H. Yamamoto, *Angew. Chem. Int. Ed*., 2006, **45**, 5849-5852.

56 (a) G. H. Hargaden, P. J. Guiry, *Chem. Rev*., 2009, **109**, 2505-2550; (b) H. A. McManus, P. J. Guiry, *Chem. Rev*., 2004, **104**, 4151-4202; (c) M. Gómez, G. Muller, M. Rocamora, *Coord. Chem. Rev*., 1999, **193-195**, 769-835.

57 S. Wood, S. Yoon, *J. Korean Chem. Soc*., 2000, **44**, 81-83.

58 J. A. Brito, H. Teruel, G. Muller, S. Massou, M. Gómez, *Inorg. Chim. Acta*, 2008, **361**, 2740-2746.

59 J. A. Brito, H. Teruel, G. Muller, S. Massou, M. Gómez, *Inorg. Chim. Acta*, 2008, **361**, 2740-2746.

60 J. A. Brito, H. Teruel, S. Massou, M. Gómez, *Magn. Reson. Chem*., 2009, **47**, 573–577.

61 M. Gómez, S. Jansat, G. Muller, G. Noguera, H. Teruel, V. Moliner, E. Cerrada, M. Hursthouse, *Eur. J. Inorg. Chem*., 2001, 1071-1076.

62 S. M. Bruno, B. Monteiro, M. S. Balula, F. M. Pedro, M. Abrantes, A. A. Valente, M. Pillinger, P. Ribeiro-Claro, F. E. Kühn, I. S. Gonçalves, *J. Mol. Catal. A: Chemical*, 2006, **260**, 11-18.

63 P. Neves, S Gago, C. C. L. Pereira, S. Figueiredo, A. Lemos, A. D. Lopes, I. S. Gonçalves, M. Pillinger, C. M. Silva, A. A. Valente, *Catal. Lett*., 2009, **132**, 94-103.

64 P. M. Reis, C. A. Gamelas, J. A. Brito, N Saffon, M. Gómez, B. Royo, *Eur. J. Inorg. Chem.*, 2011, 666-673.

65 M. Pratt, J. B. Harper, S. B. Colbran, *Dalton Trans*., 2007, 2746-2748.

66 M. Abrantes, A. Sakthivel, C. C. Romão, F. E. Kühn, *J. Organomet. Chem*., 2006, **691**, 3137-3145.

67 J. Zhao, E. Herdtweck, F. E. Kühn, *J. Organomet. Chem*., 2006, **691**, 2199-2206.

68 M. Abrantes, F. A. A. Paz, A. A. Valente, C. C. L. Pereira, S. Gago, A. E. Rodrigues, J. Klinowski, M. Pillinger, I. S. Gonçalves, *J. Organomet. Chem*., 2009, **694**, 1826-1833.

Chapter 2

OBJECTIVES

OBJECTIVES

It is well know that epoxides represent useful intermediates for the synthesis of fine chemicals including drugs and fragrances.[1] High-valent oxo-metal complexes have found applications as efficient catalysts for oxidation processes under homogeneous as well as heterogeneous conditions.[2] In particular, molybdenum systems are commercially applied for the production of propylene oxide using alkyl hydroperoxides as oxidants.[3] In spite of considerable efforts directed towards the development of enantioselective epoxidation protocols using chiral molybdenum catalysts,[4] little success has been achieved up to now.[5] The lability of the ligands coordinated to molybdenum center is probably the main reason why the attempts to develop enantioselective epoxidations fail, leading to low enantiomeric excesses in the most of cases.

During the last years, we have been studying the coordination of oxazoline ligands to molybdenum and their application in olefin epoxidations.[6,7] The activity trends observed for different catalytic systems developed by us proved that the coordination of a non-labile chiral ligand, such as oxazolinyl-pyridine ligands, appeared crucial to induce selectivity, in particular for the (*R*)-limonene epoxidation. As a result of these findings, it was considered to expand the studies to the coordination of monoanionic tridentate and bidentate oxazoline-based ligands to molybdenum. Therefore, the aim of this thesis is to prepare new *cis*-dioxomolybdenum(VI) complexes coordinated to non-labile chiral oxazoline ligands containing *N*- and/or *O*-donor centers, in order to obtain robust oxo-molybdenum(VI) catalysts.

In this context, the design of a new *N*,*N,O*-donor ligand is proposed. Bidentate and tridentate neutral ligands have been also envisaged, coming from oxazolinyl-pyridine derivatives. This kind of ligands can be easily prepared from commercially available reagents, following a suitable synthetic way (two or four steps). In addition, the corresponding *cis*-dioxomolybdenum(VI) complexes containing chiral bis(oxazolines) have been prepared in one-step synthesis, and fully characterized both in solution and solid state (see Chapter 3).

These new *cis*-dioxomolybdenum complexes containing chiral tridentate and bidentate anionic oxazoline-based ligands have been applied in alkene epoxidations, using organic solvents (see Chapter 5, section 5.3.1.).

Although many applications in metal-catalyzed organic transformations have been reported in the last two decades, few reports have been published concerning olefins epoxidations catalyzed by oxomolybdenum complexes in ionic liquid medium, being imidazolium-based ionic liquids the solvents of choice for the reported studies.[8,9,10] On the other hand, concerning enantioselective epoxidation in ionic liquids, only two contributions have been described up to now, involving imidazolium and pyridinium ionic liquids.[11,12] We decided to study the performance of our new *cis*-dioxomolybdenum complexes in olefin epoxidation reactions in imidazolium- and pyrrolidinium-based ionic liquids, in order to study the influence of the nature of the ionic liquid in the catalytic process (Chapter 5, section 5.3.2.).

With the purpose of using ^{95}Mo NMR spectroscopy as a tool to obtain structural information of molybdenum species in solution, we decided to carry out the analysis of ^{95}Mo NMR spectra corresponding to a series of oxomolybdenum(VI) complexes in order to study the correlation between the ^{95}Mo NMR chemical shift and the electron donor ability of some ligands present in these molybdenum complexes (Chapter 4).

In the last part of the catalytic study and with the aim to explore the potential of ionic liquids in palladium-catalyzed allylic substitutions, taking advantage of the large experience in this field, some chiral oxazoline-based ligands were preliminary tested in different allylic substitution reactions in pyrrolidinium-based ionic liquid (see Chapter 5, section 5.4.).

References

1 (a) B. Cornils, W. A. Herrmann Applied Homogeneous Catalysis with Organometallic Compounds Eds., Wiley-VCH, Weihneim, 2nd edition, 2002, vol. 1, pp. 412-426; (b) Q.-H. Xia, H.-Q. Ge, C.-P. Ye, Z.-M. Liu, K.-X. Su, *Chem. Rev*., 2005, **105**, 1603-1662; (c) F. E. Kühn, A. M. Santos, W. A. Herrmann, *Dalton Trans*., 2005, 2483-2491; (d) F. E. Kühn, J. Zhao, W. A. Herrmann, *Tetrahedron: Asymmetry*, 2005, **16**, 3469-3479.

2 J. M. Brégeault, *Dalton Trans*, 2003, 3289-3302.

3 (a) J. Kollar, Halcon, US Patents 3, 350, 422 and 3, 351, 635 1967; (b) M. N. Sheng, G. J. ZAjaczek, ARCO, GB Patent 1, 136, 923 1968.

4 For reviews, see: (a) K. R. Jain, W. A. Herrmann, F. E. Kühn, *Coord. Chem. Rev*., 2008, **252**, 556–568; (b) A. J. Burke, *Coord. Chem. Rev*., 2008, **252**, 170–175.

5 (a) F. E. Kühn, J. Zhao, W. A. Herrmann, *Tetrahedron: Asymmetry*, 2005, **16**, 3469-3479; (b) A. U. Barla, A. Basak, H. Yamamoto, *Angew. Chem. Int. Ed*., 2006, **45**, 5849-5852; (c) Y. Wang, Z. Wu, Z. Li, X.-G. Zhou, *Tetrahedron Lett*., 2009, **50**, 2509-2511.

6 M. Gómez, S. Jansat, G. Muller, G. Noguera, H. Teruel, V. Moliner, E. Cerrada, M. Hursthouse, *Eur. J. Inorg. Chem*., 2001, 1071-1076.

7 (a) J. A. Brito, M. Gómez, G. Muller, H. Teruel, J. C. Clinet, E. Duñach, M.A. Maestro, *Eur. J. Inorg. Che*m. 2004, 4278-4285; (b) J. A. Brito, H. Teruel, G. Muller, S. Massou, M. Gómez, *Inorg. Chim. Acta*., 2008, **361**, 2740-2746.

8 (a) A. A. Valente, Z. Petrovski, L. C. Branco, C. A. M. Afonso, M. Pillinger, A. D. Lopes, C. C. Romão, C. D. Nunes, I. S. Gonçalves, *J. Mol. Catal. A: Chemical*, 2004, **218**, 5-11; (b) F. E. Kühn, J. Zhao, M. Abrantes, W. Sun, C. A. M. Afonso, L. C. Branco, I. S. Gonçalves, M. Pillinger, C. C. Romão, Tetrahedron Lett., 2005, **46** 2005, 47-52; (c) D. Betz, A. Raith, M. Cokoya, F. E. Kühn, *ChemSusChem*, 2010, **3** 559-562; (d) M. Abrantes, P. Neves, M. M. Antunes, S. Gago, F. A. Almeida Paz, A. E. Rodrígues, M. Pillinger, I. S. Gonçalves, C. M. Silva, A. A. Valente, *J. Mol. Catal. A: Chemical,* 2010, **320** 19-26; (e) M. Herbert, A. Galindo,

F. Montilla, *Catal. Commun.* 2007, **8**, 987-990; (f) M. Herbert, E. Alvarez, D. J. Cole-Hamilton, F. Montilla, A. Galindo, *Chem. Commun*., 2010, **46**, 5933-5935.

9 (a) S.-F. Cai, L.-S. Wang, C.-L. Fan, *Molecules*, 2009, **14**, 2935-2946; (b) C. Bibal, J-C. Daran, S. Deroover, R. Poli, *Polyhedron*, 2010, **29**, 639-647; (c) S. Gago, S. S. Balula, S. Figuereido, A. D. Lopes, A. A. Valente, M. Pillinger, I. S. Gonçalves, *Appl. Catal. A: General*, 2010, **372**, 67-72; (d) P. Neves, C. C. L. Pereira, F. A. Almeida Paz, S. Gago, M. Pillinger, C. M. Silva, A. A. Valente, Romão, I. S. Gonçalves, *J. Organomet. Chem.*, 2010, **695**, 2311-2319; (e) W. R. Thiel, M. Jia, *Chem. Commun*. 2002, 2392-2393.

10 (a) M. Jia, A. Steifert, M. Berger, H. Giegengack, S. Schulze, W. R. Thiel, *Chem. Mater.,* 2004, **16**, 877-882; (b) M. Jia, A. Steifert, W. R. Thiel, *J. Catal*., 2004, 221, 319-324; (c) A. Castro, J. C. Alonso, P. Neves, A. A. Valente, P. Ferreira, *Eur. J. Inorg. Chem.* 2010, 602-607; (d) K. R. Jain, F. E. Kühn, *Dalton Trans*., 2008, 2221-2227; (e) K. A. Jain, W. A. Herrmann, F. E. Kühn, *Coord. Chem. Rev*., 2008, **252**, 556-568.

11 P. Neves, S. Gago, C. C. L. Pereira, S. Figuereido, A. Lemos, A. D. Lopes, I. S. Gonçalves, M. Pillinger, C. M. Silva, A. A. Valente, *Catal. Lett*., 2009, **132**, 94-103.

12 M. Abrantes, F. A. Almeida Paz, A. A. Valente, C. C. L. Pereira, S. Gago, A. E. Rodrígues, J. Klinowski, M. Pillinger, I. S. Gonçalves, *J. Organomet. Chem*., 2009, 694, 1828-1833.

Chapter 3 NEW CHIRAL LIGANDS AND THEIR *CIS*-DIOXOMOLYBDENUM(VI) COMPLEXES

Summary

This chapter describes the synthesis and characterization of novel *cis*-dioxomolybdenum(VI) complexes containing chiral ligands. In particular molybdenum complexes containing anionic *N*,*N*',*O*-tridentate oxazolinyl-pyridyl-phenolate (**A**), neutral *N,O*-bidentate pyridine-amide (**B**), neutral *N,N*-bidentate bis(oxazoline) (**C**) and monoanionic *N,N*-bidentate bis(oxazoline) (**D**) ligands. All molybdenum complexes were full characterized by NMR (^{1}H, ^{13}C and ^{95}Mo) and IR spectroscopy, mass spectrometry, elemental analysis and in some cases by X-ray diffraction studies on mono-crystals.

The work described in this chapter was entirely performed by the candidate except for ^{95}Mo NMR spectra which were performed by Marc Vedrenne and for X-ray diffraction analysis performed by Sonia Ladeira and Nathalie Saffon from University Paul Sabatier (Toulouse, France). Modelling studies were carried out by Prof. Montserrat Gómez from University Paul Sabatier (Toulouse, France).

3.1. Introduction

High-valent oxo-metal species have demonstrated the ability to catalyze the oxidation of a variety of organic substrates, by homogeneous as well as heterogeneous routes.[1] In particular, the Mo-catalyzed alkene epoxidation has received a lot of attention due to its industrial interest. The use of oxo-molybdenum complexes has been extensively explored over the last 40 years, beginning with homogeneous Mo(VI) catalysts applied in the Halcon and Arco processes.[2] Since then, considerable efforts have been directed towards the development of enantioselective epoxidation protocols using chiral molybdenum catalysts.[3] However, little success has been achieved up to now, and the synthesis of chiral molybdenum catalysts is still in its infancy.

Because of their ready accessibility, modular nature and applicability in a wide range of metal-catalyzed transformations, chiral oxazoline fragments have become one of the most successful and versatile ligands in asymmetric catalysis.[4] The large

majority of these ligands are readily prepared from chiral amino alcohols in few high-yielding synthetic steps. An important feature of these ligands is the incorporation of the stereogenic center on the carbon atom next to the metal-coordinated nitrogen, in close proximity to the metal active site. In addition, oxazolines have proved to be robust ligands under several reaction conditions.[4]

Some years ago, Gómez and co-workers described the preparation of the firsts oxazoline-dioxomolybdenum(VI) complexes of general formula *cis*-[MoO_2(κ^2-*N*,*O*-**L**)$_2$], containing an anionic chiral bidentate oxazolinyl-phenolate ligand, **L**.[5] These ligands are labile in solution and in consequence they cannot induce any selectivity in the Mo-catalyzed epoxidation reactions. However, dioxomolybdenum(VI) complexes containing neutral bidentate oxazolinyl-pyridine ligands were robust, without observing any ligand dissociation, and inducing diastereoselectivity in the (*R*)-limonene epoxidation.[6] The catalytic behavior observed for these systems, proved that the coordination of a non-labile chiral ligand appeared crucial to induce selectivity in the epoxidation process.[6] Based on these findings, we considered that *cis*-dioxomolybdenum(VI) complexes containing monoanionic tridentated ligands could be good candidates for Mo-catalyzed asymmetric epoxidation, since the expected robust coordination of the ligand to the molybdenum center could favor the stereo-selection in the asymmetric catalytic reaction.[6] In this context, the design of new *N*,*N,O*-donor and *N*,*N*-donor ligand is proposed. Bidentate and tridentate neutral ligands were also envisaged, coming from oxazolinyl-pyridine derivatives.

3.2. Experimental part

3.2.1. General

Syntheses were performed using standard Schlenk techniques under argon or nitrogen atmosphere. Ligands **C**[7] and **D**[7c,8] were prepared following procedures previously described in the literature. ^{1}H, ^{13}C and ^{95}Mo NMR spectra were recorded on Bruker Avance 300 and Bruker Avance 400 at 293 K. Chemical shifts were reported downfield from standards ($SiMe_4$ for ^{1}H and ^{13}C spectra; 1M Na_2MoO_4 (aqueous solution) at pH = 10 for ^{95}Mo spectra). IR spectra were carried out on

pellets of dispersed samples of the corresponding compounds in KBr and recorded on an IR Varian 640-IR FTIR spectrometer. Electrospray mass spectra (ESI-MS) were recorded on an API-ION TRAP(PO03MS) instrument, (ESI-HRMS) UPLC Xevo Q TOF (Waters) instrument, nitrogen was employed as drying and nebulizing gas. Chemistry ionization mass spectra were recorded on a GCT 1er Waters instrument, DCI CH_4. Optical rotations were determined on a Perkin Elmer 241 polarimeter. Elemental analyses were performed in the laboratories at ITQB. Modelling studies were carried out using the following software: SPARTAN'06 for Windows and Linux. Wavefunction, Inc. 18401 Von Karman Avenue, suite 370. Irvine, CA 92612, USA. The different geometries were optimized by means of density functional theory (DFT B3LYP) using 6-31G* polarization basis set and pseudopotentials. **X-Ray diffraction studies:** X-Ray data for complexes **1**, **3** and **4** were collected at low temperature (180 K for complexes **1** and **4**, and 193 K for complex **3**) using a microfocus source on a Bruker-Kappa APEX II diffractometer with molybdenum radiation (MoKα radiation (λ = 0.71073 Å)). The structure were solved by direct methods[9] and all non hydrogen atoms were refined anisotropically using the least-squares method on F2.[10] ORTEP view was generated from the corresponding software.[11] Crystal data and structure refinement are summarized in Table 3.1, Table 3.2 and Table 3.3. In chapten 7 are the crystal data for the three complexes. These data can also be obtained free of charge via www.ccdc.cam.ac.uk/conts/retrieving.htcm-3 (or from the CCDC, 12 Union Road, Cambridge CB2 1EZ, UK; fax: +44 1223 336033; e mail: deposit@ccdc cam ac uk).

3.2.2. Synthesis of ligands

3.2.2.1. Synthesis of 2-(6-(4,5-dihydro-4-isopropyloxazol-2-yl)pyridin-2-yl)ethanol, A

m-CPBA (*m*-chloroperbenzoic acid) (13.55 g, 70%, 55.0 mmol) was added to 2-(hydroxyethyl)pyridine (5.64 g, 45.8 mmol) in chloroform (150 mL) at 0 °C and stirred for 30 min. The suspension was then warmed at room temperature and stirred for 24 h. Residual *m*-CPBA was destroyed by the addition of *p*-formaldehyde (2.0 g, 66.6 mmol CH_2O). After being stirred for 2 h, ammonia was bubbled through the reaction

mixture for 10 min. The thick suspension which formed was dried with Na_2SO_4 and filtered. The filtrated was concentrated to dryness to yield a residue which was washed with dichloromethane (250 mL). Evaporation of the solvent gave 5.42 g (38.95 mmol, 85% yield) of 2-(hydroxyethyl)pyridine-N-oxide. ^{1}H NMR (400 MHz, CD_2Cl_2) δ: 3.20 (2H, t, 5.7 Hz, CH_2), 3.96 (2H, t, 5.7 Hz, CH_2), 5.81 (1H, s, O*H*), 7.16 (1H, td, 7.16, 2.13 Hz, C*H*), 7.29 (2H, m, C*H*) 8.24 (1H, d, 6.32 Hz, C*H*). ^{13}C{^{1}H} NMR (100 MHz, $CDCl_3$) δ: 33.5 (*C*H_2), 59.8 (*C*H_2), 123.2 (*C*H), 126.1 (*C*H), 126.5 (*C*H), 138.6 (*C*H), 149.9 (*C*).

To a solution of this *N*-oxide (470 g, 3.38 mmol) in CH_2Cl_2 (50 mL), *N*,*N*-dimethylcarbamoyl chloride (0.36 mL, 3.36 mmol) was added dropwise added; after 2.5 h, trimethylsilyl cyanide (0.54 mL, 4.03 mmol) was added. The mixture was stirred overnight at room temperature followed by 8 h under reflux and then cooled at room temperature; 1 equivalent each of *N*,*N*-dimethylcarbamoyl chloride and trimethylsilyl cyanide were again added. After an additional night of stirring at reflux, the reaction was quenched by addition of a saturated aqueous solution of Na_2CO_3 (25 mL). Both phases were separated, the aqueous layer was extracted with CH_2Cl_2 (2x15 mL) and the combined organic extracts were dried over anhydrous Na_2SO_4. Filtration and evaporation under reduced pressure of the solvent gave a brown-red oil which was purified by flash chromatography on silica gel (15x4 cm column, ethyl acetate:hexane = 1:1, followed by ethyl acetate) to give the expected nitrile 6-(2-hydroxyethyl)pyridine-2-carbonitrile product, isolated as a white solid (250 mg, 1.69 mmol, 50 %). IR(KBr): 2239 cm^{-1} (st, C≡N). ^{1}H NMR (400 MHz, CD_2Cl_2) δ: 3.07 (2H, t, 5.7 Hz, CH_2), 4.03 (2H, t, 5.7 Hz, CH_2), 7.43 (1H, d, 8.0 Hz, C*H*), 7.56 (1H, d, 7.8 Hz C*H*), 7.76 (1H, t, 7.8 Hz, C*H*). ^{13}C{^{1}H} NMR (100 MHz, $CDCl_3$) δ: 39.8 (*C*H_2), 61.2 (*C*H_2), 117.3 (*C*≡N), 133.2 (*C*), 126.7 (*C*H), 127.6 (*C*H), 137.7 (*C*H), 162.5 (*C*).

Compound 6-(2-hydroxyethyl)pyridine-2-carbonitrile (250 mg, 1.69 mmol) was mixed with (*R*)-2-amino-3-methylbutan-1-ol (262 mg, 2.54 mmol) and a pinch of $CuCl_2$ under dried conditions. The reaction mixture was stirred at 100 °C at reduced pressure overnight. Then dichloromethane (20 mL) was added to the reaction mixture, and the organic phase was washed with water (3x15 mL), dried with

anhydrous Na_2SO_4, and all the volatiles were evaporated under reduced pressure to yield the expected oxazoline **A** as a yellow oil (375 mg, 1.60 mmol, 94 %). $[\alpha]_D^{24}$ = -50 (c 0.3, $CHCl_3$). HRMS (DCI/CH_4, positive mode) found m/z: 235.1445; $C_{13}H_{18}N_2O_2$+H requires: 235.1447. IR(KBr): 1660 cm^{-1} (st, C=N); 3374 cm^{-1} (st, O-H). ^{1}H NMR (400 MHz, CD_2Cl_2) δ: 0.93 (3H, d, 6.7 Hz, C*H*$_3$), 1.04 (3H, d, 6.7 Hz, C*H*$_3$), 1.88 (1H, m, C*H*), 3.08 (2H, t, 5.6 Hz, C*H*$_2$) 4.08 (2H, t, 5.6 Hz, C*H*$_2$), 4.14 (1H m, C*H*), 4.19 (1H, pq, C*H*$_2$), 4.47, 4.50 (2H, dd, 9.01 Hz; 9.01 Hz, C*H*$_2$), 7.28 (1H, d, 7.91 Hz, C*H*), 7.70 (1H, pt, C*H*), 7.94 (1H, d, 7.7 Hz, C*H*). ^{13}C{^{1}H} NMR (100 MHz, CD_2Cl_2) δ: 18.5 (*C*H$_3$), 19.4 (*C*H$_3$), 33.1 (*C*H), 39.6 (*C*H$_2$), 62.1.9 (*C*H$_2$), 71.9 (*C*H$_2$), 73.2 (*C*H), 125.6 (*C*H), 137.4 (*C*H), 122.1 (*C*H), 146.9 (*C*), 160.8 (*C*), 162.9 (*C*=N).

3.2.2.2. Synthesis of *N*-(tetrahydrofuran-2-yl)picolinamide, B

In a 250 mL three-necked flask, (2*S*)-2-amino-1,4-butanediol (1.6 g; 15.4 mmol), 2-cyanopyridine (2.03 g; 19.5 mmol) and 0.318 g of potassium carbonate were successively introduced, followed by a solution of 10 mL glycerol in 18 mL of dry ethylene glycol. The resulting mixture was heated to 105 °C under nitrogen for 24 h. The reaction solution was extracted with CH_2Cl_2 (3x15 mL), washed with water (3x10 mL), the organic phase dried using anhydrous Na_2SO_4, filtered and the solvent was removed under reduced pressure. The remaining solid was then purified by flash chromatography (AcOEt:MeOH:NEt_3, 100:2:0.5) to yield **B** as a yellow oil (0.70 g; 3.64 mmol, 24.0%). $C_{10}H_{12}N_2O_2$ (192.21). MS (ESI, methanol, positive mode): 193 $[M+1]^+$. $[\alpha]_D^{26}$ = +150 (c 0.3, $CHCl_3$) IR(KBr): 1636 cm^{-1} (C=O). ^{1}H NMR (400 MHz, CD_2Cl_2): δ = 1.99 (m, 1H, C*H*$_2$), 2.31 (m, 1H, C*H*$_2$), 3.80 (m, 1H, C*H*$_2$), 3.87 (m, 1H, C*H*$_2$), 3.98 (m, 2H, C*H*$_2$), 4.73 (m, 1H, C*H*), 6.00 (s, 1H, NH), 7.43 (m, 1H, C*H*), 7.84 (m, 1H, C*H*), 8.19 (m, 1H, C*H*), 8.54 (m, 1H, C*H*); ^{13}C{^{1}H} NMR (100 MHz, CD_2Cl_2): δ = 164.1 (*C*=O), 149.6 (*C*), 148.1 (CH), 137.4 (*C*H), 126.3 (*C*H), 122.2 (*C*H), 77.4 (*C*H$_2$), 67.1 (*C*H$_2$), 50.2 (*C*H) 33.4 (*C*H$_2$).

3.2.2.3 Synthesis of 4,5-dihydro-2-(2-(4,5-dihydro-4-(methoxymethyl)-5-phenyloxazol-2-yl)propan-2-yl)-4-(methoxymethyl)-5-phenyloxazole, C

The synthesis of ligand **C** was performed according the method described in the literature, yielding 70%.[8] Purity was checked by IR and ^{1}H NMR spectroscopy: IR(KBr): 1650 cm^{-1} (st, C=N). ^{1}H NMR (400 MHz, CD_2Cl_2): δ = 1.68 (6H, s, C*H*$_3$), 3.39 (6H, s, C*H*$_3$), 3.47 (2H, dd 9.7, 6.9 Hz, C*H*$_2$), 3.67 (2H, dd 9.7, 4.4 Hz, C*H*$_2$), 4.16 (2H, td 9.7, 4.4 Hz, C*H*), 5.34 (1H, d 6.9 Hz, C*H*), 7.27 (10H, m, *Ph*).

3.2.2.4. Synthesis of (2E)-2-(4,5-dihydro-4-isopropyloxazol-2-yl)-2-(4-isopropyloxazolidin-2-ylidene) acetonitrile, D

The synthesis of ligand **D** was performed according to the method described in the literature, yielding 60 %.[7] Purity was checked by IR and ^{1}H NMR spectroscopy: IR(KBr): 2210 cm^{-1} (C≡N), 1649 cm^{-1} (st, C=N). ^{1}H NMR (400 MHz, CD_2Cl_2): δ = 0.90 (6H, d 6.7 Hz, C*H*$_3$), 0.97 (6H, d 6.7 Hz, C*H*$_3$), 1.73 (2H, m, C*H*), 3.87 (2H, m, C*H*), 4.16 (2H, dd, 8.7, 7.9 Hz, C*H*$_2$), 4.48 (2H, pt, 8.7 Hz, C*H*$_2$).

3.2.3. Synthesis of molybdenum complexes 1-5

3.2.3.1. Synthesis of [$MoO_2Cl(\kappa^3$-*N*,*N*',*O*-A)], 1

To a pale brown solution of **A** (326 mg, 1.39 mmol) in THF (10 mL), triethylamine (0.19 mL, 1.39 mmol) was added and the mixture was stirred for 30 minutes. The resulting solution was then transferred to a colourless solution of [MoO_2Cl_2(DME)][12] (384 mg, 1.33 mmol) in THF (20 mL) at -78 ºC. After few minutes, the solution turned violet with the formation of a precipitate. The mixture was stirred overnight at room temperature. The mixture was then filtered, the filtrate was concentrated to dryness and the remaining solid was purified by silica gel column using ethyl acetate as eluent. All the volatiles were then evaporated under reduced pressure to give a pale yellow solid. The solid obtained was successively washed with ether (3x10 mL) and pentane (3x10 mL). Recrystallization from CH_3CN afforded complex **1** as a light yellow solid (193 mg, 0.48 mmol, 35 %). $C_{13}H_{17}ClMoN_2O_4$ (396.68). Anal. Calcd: C, 39.36; H, 4.32; N, 7.06 %. Found: C, 39.24; H, 4.65; N, 6.50 %. MS (ESI, methanol,

positive mode) m/z 365 $[M\text{-}Cl]^+$. IR (KBr): 1661 cm^{-1} (st, C=N), 933 and 896 cm^{-1} (asymmetrical and symmetrical Mo=O streching). ^1H NMR (400 MHz, CD_2Cl_2) δ: 0.94 (3H, d, 6.8 Hz, C*H*$_3$), 0.98 (3H, d, 7.1 Hz, C*H*$_3$), 2.67 (1H, m, C*H*), 3.50 (2H, m, C*H*$_2$), 4.65 (^{1}H m, C*H*$_2$), 4.75 (2H, st, 8.5 Hz, C*H*$_2$), 4.90 (1H, m, NC*H*), 5.14 (2H, m, C*H*$_2$), 7.67 (1H, d, 7.91 Hz, C*H*), 7.90 (1H, d, 7.50 Hz, C*H*), 8.07 (1H, pt, C*H*) ppm. $^{13}C\{1H\}$ NMR (100 MHz, CD_2Cl_2) δ: 14.9 (*C*H$_3$), 18.8 (*C*H$_3$), 29.1 (*C*H), 38.6 (*C*H$_2$), 70.9 (N-*C*H), 73.9 (*C*H$_2$), 75.4 (*C*H$_2$), 124.0 (*C*H), 130.5 (*C*H), 140.3 (*C*H), 140.6 (*C*), 159.6 (*C*), 167.2 (*C*=N) ppm. ^{95}Mo NMR (26.08 MHz, CD_2Cl_2) δ: +67.5 ppm.

3.2.3.2 Synthesis of $[MoO_2(\kappa^3\text{-}N,N',O\text{-}A)]_2(\mu\text{-}O)]$, 2

Treatment of complex **1** with wet $CHCl_3$ for 15 min afforded complex **2** as a crystalline yellow solid in quantitative yield. $C_{27}H_{37}N_4O_9Mo_2$ (753.48). Anal. Calcd: C 42.29, H 4.64, N 7.59. Found: C 42.28, H 5.08, N 7.63. IR (KBr): 1592 cm^{-1} (C=N), 938 and 911 cm^{-1} (asymmetrical and symmetrical Mo=O streching), 805 cm^{-1} (st, Mo-O-Mo).^1H NMR (400 MHz, CD_2Cl_2) δ: 1.01 (6H, pd, 4.2 Hz, C*H*$_3$), 2.94 (1H, m, C*H*), 3.59 (2H, m, C*H*$_2$), 4.79 (2H, st, 8.5 Hz, C*H*$_2$), 4.93 (1H, m, NC*H*), 4.98 (1H, m, C*H*$_2$), 5.20 (1H, m, C*H*$_2$), 7.66 (1H, d, 7.91 Hz, C*H*), 7.88 (1H, d, 7.68 Hz, C*H*), 8.07 (1H, pt, C*H*).

3.2.3.3. Synthesis of $[MoO_2Cl_2(\kappa^2\text{-}N,O\text{-}B)]$, 3

To a THF solution (10 mL) of $[MoO_2Cl_2]$ (181 mg, 0.91 mmol), the picolinamide ligand **B** (203 mg, 1.06 mmol) in THF (5 mL) was added at -78 ºC. After 2 h, the solvent was removed under reduced pressure and the remaining solid was washed with ether (3x10 mL). Recrystallization from CH_3CN:ether (1:4) afforded compound **3** as a light orange solid (291 mg, 0.82 mmol, 90 %). $C_{10}H_{12}Cl_2N_2O_4Mo_2$ (391.06). MS (ESI, methanol, positive mode) m/z 390 $[M\text{-}Cl+CH_3OH+2H]^+$. IR (KBr): 1626 cm^{-1} (st, C=O), 950 and 914 cm^{-1} (asymmetrical and symmetrical Mo=O streching). ^1H NMR (400 MHz, CD_3CN): δ = 2.16 (m, 1H, C*H*$_2$), 2.45 (m, 1H, C*H*$_2$), 3.81 (dd, 14.0, 8.5 Hz, 1H, C*H*$_2$), 3.89-4.07 (m, 4H, C*H*$_2$), 4.86 (m, 1H C*H*), 7.98 (pt, 6.1, 1H, C*H*), 8.41 – 8.35 (m, 2H, C*H*), 8.92 (s 1H, N*H*), 9.42 (pd, 5.2 Hz, 1H, C*H*) ppm. $^{13}C\{^1H\}$ NMR (100 MHz, CH_3CN): δ: 33.3 (*C*H$_2$), 55.3 (*C*H), 68.2 (*C*H$_2$), 73.3 (*C*H$_2$), 126.2 (*C*H),

131.7 (*C*H), 143.2 (*C*H), 145.4 (*C*), 152.5 (*C*H), 168.0 (*C*=O) ppm. ^{95}Mo NMR (26.08 MHz, CD_3CN): δ: +189.7 ppm.

3.2.3.4. Synthesis of [$MoO_2Cl_2(\kappa^2$-*N*,*N*-C)], 4

The bis-oxazoline **C** (147 mg, 0.35 mmol) dissolved in THF (5 mL) was added to a THF solution (15 mL) of [MoO_2Cl_2(DME)][12] (100 mg, 0.35 mmol) at -78 ºC. After stirring overnight at room temperature, the solvent was removed under reduced pressure. The solid obtained was successively washed with ether (3x10 mL) and pentane (3x10 mL). Crystallization from CH_3CN afforded a light yellow solid (130 mg, 0.21 mmol, 60 %). HRMS (ESI, THF, positive mode) found m/z: 581.0885 [M-Cl]+; $C_{25}H_{30}ClMoN_2O_6$ requires 581.0860. IR(KBr): 1654 cm^{-1} (st, C=N), 937 and 909 cm^{-1} (asymmetrical and symmetrical Mo=O streching). ^{1}H NMR (400 MHz, CD_2Cl_2) δ: 1.70 (s, 6H, C*H*$_3$), 3.42 (s, 6H, C*H*$_3$), 3.93 (dd, 2H, 10.24 and 3.05 Hz, C*H*$_2$), 4.04 (dd, 2H, 10.29 and 4.61 Hz, C*H*$_2$), 5.00 (m, 2H, C*H*), 5.70 (d, 2H, 4.88 Hz, C*H*), 7.41 (m, 10H, CH) ppm. ^{13}C{^{1}H} NMR (75 MHz, CD_2Cl_2) δ: 24.2 (*C*H$_3$), 40.0 (C), 58.7 (*C*H$_3$), 72.2 (*C*H$_2$), 75.0 (N*C*H), 83.9 (*C*H), 126.4 (*C*H), 128.9 (*C*H), 129.3 (*C*H), 138.2 (*C*), 171.1 (*C*=N) ppm. ^{95}Mo NMR (26.08 MHz, CD_2Cl_2) δ: +136.6 ppm.

3.2.3.5. Synthesis of [$MoO_2Cl(\kappa^2$-*N*,*N*-D)], 5

A solution of ligand **D** (304 mg, 1.15 mmol) in THF (20 mL) was added to a solution of [MoO_2Cl_2] (227 mg, 1.14 mmol) in THF (15 mL) at -78 °C. The reaction mixture was permitted to warm up to room temperature and stirred for 2 h. All volatiles were removed under reduced pressure to yield an orange solid which was washed with diethyl ether (3x10 mL) to yield **5** as a yellow-orange solid (340 mg, 0.80 mmol, 70 %). $C_{14}H_{20}ClN_3O_4Mo$ (425.72): Anal. calcd.: C 39.50, H 4.74, N 9.87. Found: C 40.70, H 5.00, N 9.60. MS (ESI, THF, negative mode) m/z (%) = 462 [M+Cl]$^-$.IR (KBr): 2221 cm^{-1} (st, C≡N), 1601 cm^{-1} (st, C=N), 957 and 918 cm^{-1} (asymmetrical and symmetrical Mo=O streching).^{1}H NMR (400 MHz, CD_3CN) δ: 0.92 (pt, 8.1 12H, C*H*$_3$), 1.96 (m, 2H, C*H*), 4.18 (pq, 8.7, 14.9, Hz, 2H, C*H*$_2$), 4.66 (pt, 6.6 Hz, 2H, C*H*$_2$), 4.86 (m, 2H, C*H*) ppm. ^{13}C{^{1}H} NMR (100 MHz, CH_2Cl_2) δ: 18.1 (*C*H$_3$), 30.0 (*C*H), 32.5

(*C*H), 47.7 (*C*=C), 62.2 (*C*H_2), 72.6 (*C*H_2), 118.0 (*C*≡N), 161.0 (*C*=C), 171.5 (*C*=N) ppm. ^{95}Mo NMR (26.08 MHz, CD_3CN) δ: +126.8 ppm.

3.3. Results and discussion

3.3.1. Synthesis and characterization of the ligand A and its *cis*-dioxomolybdenum(VI) complexes, 1 and 2.

The 2,6-difunctionalized oxazolinyl-pyridine ligand **A** was obtained in a three-step sequence from commercially available 2-pyridine ethanol, previously activated by treatment with *m*-CPBA (*m*-chloroperbenzoic acid). This intermediate was further modified by cyanation reaction using trimethylsilyl cyanide to give 6-(2-hydroxyethyl)pyridine-2-carbonitrile in 50% yield. The nitrile derivative led to the formation of the oxazoline heterocycle in 90% yield, by condensation with L-valinol ((*S*)-2-amino-3-methylbutan-1-ol) catalyzed by copper dichloride as depicted in Scheme 3.1. Compound **A** was isolated as a white solid (in an overall yield of 36%) and characterized by NMR spectroscopy and mass spectrometry.

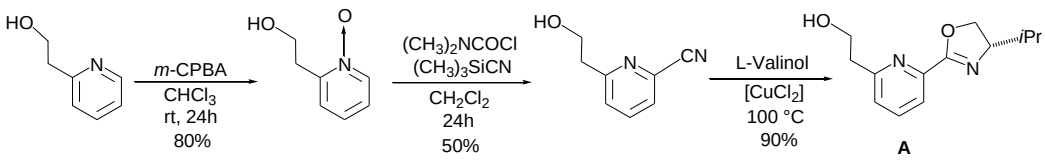

Scheme 3.1. Synthesis of ligand **A** following a three-step synthetic strategy.

The IR spectrum of **A** showed a very strong absorption band at 1660 cm^{-1}, due to the imine bond (C=N) stretching of the oxazoline heterocycle. Its HRMS spectrum (Cl, CH_4) spectrum displayed a molecular peak at m/z 235.1445, corresponding to the $[M + H]^+$ fragment. The new ligand showed a specific rotation of $[\alpha]_D^{24}$ = -50 (c 0.3, $CHCl_3$). The ^{1}H NMR spectrum showed two doublets at δ 0.93 and 1.04 and a multiplet at δ 1.88 assigned to the methyl and methinic groups of the isopropyl group, respectively; two triplets at δ 3.08 and 4.08 assigned to the CH_2 groups of the ethyl group; three signals corresponding to the oxazoline ring: one at 4.14 (the proton on the asymmetric C atom) and other two signals at δ 4.19 and 4.47 (the diastereotopic

methylenic protons), as well as the characteristic signals for the pyridyl protons at δ 7.28; 7.70 and 7.94 (Figure 3.1).

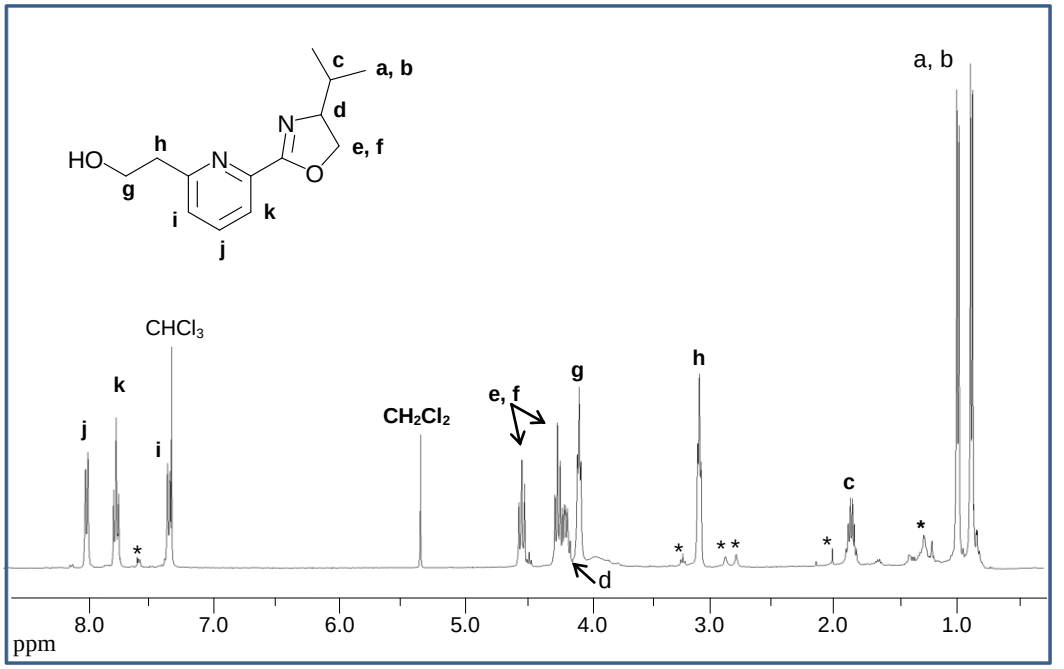

Figure 3.1. ^{1}H NMR spectrum (400 MH_Z, CD_2Cl_2, 298 K) of ligand **A** (* = impurities).

Treatment of the previously described ligand **A** with [MoO_2Cl_2(DME)] (DME = dimethoxyethane) in the presence of triethylamine gave the corresponding enantiomerically pure dioxo complex [$MoO_2Cl(\kappa^3$-*N,N,O*-**A**)] (**1**) isolated as a yellow solid after purification by column chromatography (Scheme 3.2).

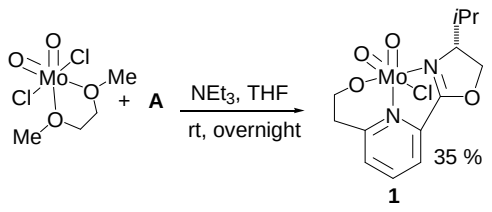

Scheme 3.2. Synthesis of the mono-metallic complex **1** containing the chiral ligand **A**.

Complex **1** was easily hydrolyzed in wet deuterated solvents, giving the μ-oxo bimetallic molybdenum complex $[MoO_2(\kappa^3\text{-}N,N,O\text{-}\mathbf{A})]_2(\mu\text{-}O)$ (**2**), indicating that compound **1** is rather sensitive to moisture and decomposes readily in the presence of traces of water (Scheme 3).

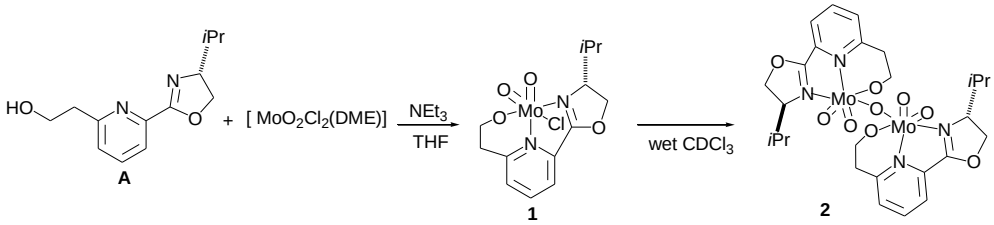

Scheme 3.3. Synthesis of the bimetallic molybdenum complex **2**.

The IR spectrum of complex **1** showed two strong bands at 938 and 911 cm^{-1} attributed to the asymmetric and symmetric Mo=O stretches for a *cis*-$[MoO_2]^{2+}$ moiety, respectively.[5,6,13,14] Complex **2** exhibited along with the two characteristic bands for Mo=O moiety (911 and 938 cm^{-1}), a new absorption band due to the Mo-O-Mo group (805 cm^{-1}), in accordance with related dioxo-μ-oxo molybdenum(VI) compounds described in the literature.[6a,15,16] Results of elemental analysis were consistent with their composition. The corresponding mass spectrum was also performed to characterized complex **1**; positive ion ESI-MS experiments in methanol showed the molecular ion peak at m/z 365 $[M\text{-}Cl]^+$.

The structure of $[MoO_2Cl(\kappa^3\text{-}N,N,O'\text{-}\mathbf{A})]$ (**1**) was established by single-crystal X-ray diffraction analysis. The molecular view and selected bond lengths and angles are shown in Figure 3.2. The structure revealed a six-coordinate Mo atom in a distorted octahedral surrounding, with a *mer* coordination of the tridentate ligand, rendering the ligand skeleton almost planar. The molybdenum oxo groups showed the expected mutual *cis* configuration which are in *trans* position to the pyridinic nitrogen atom and chloro ligand.

The *trans* disposition of the oxo group with the chloro atom is unexpected for this type of complexes, since related tridentate N_2O phenolate complexes of tungsten adopt a distorted octahedral structure with the two nitrogen donor atoms being located *trans* to the oxo groups, and with the phenolate oxygen opposite to the chloride ligand.[17]

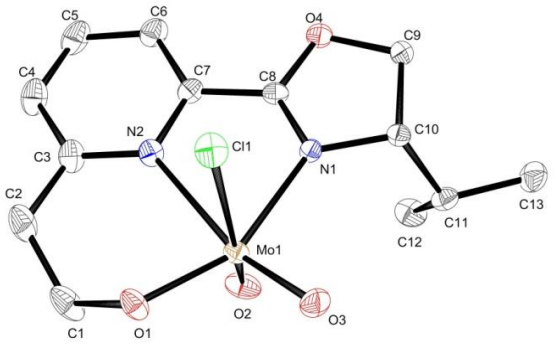

Figure 3.2. Molecular view of compound **1** with ellipsoids representing 50% probability. H atoms are omitted for clarity. Selected bond distances (Å) and angles (º): Mo(1)-O(1) 1.8800(19), Mo(1)-O(2) 1.6965(19), Mo(1)-O(3) 1.700(2), Mo(1)-Cl(1) 2.5264(9), Mo(1)-N(1) 2.188(2), Mo(1)-N(2) 2.374(2), N(1)-Mo(1)-N(2) 71.61(9), O(1)-Mo(1)-O(3) 106.84(9), O(1)-Mo(1)-N(2) 83.67(8), Cl(1)-Mo(1)-O(2) 161.13(8).

Although a number of X-ray diffraction studies have been reported concerning the bidentated coordination of pyridine and quinoline derivatives, only three bimetallic dioxomolybdenum(VI) complexes have been described containing anionic tridentate ligands.[18,19] Therefore, complex **1** represents the first X-ray characterization for a monometallic molybdenum complex bearing a *N*,*N*',*O*-tridentated ligand. The Mo-Cl bond was relatively long (2.52 Å) because of the strong *trans* influence of the oxo ligand; the expected range of Mo-Cl bond distances in *cis*-dioxo Mo(VI) complexes are 2.36-2.41 Å.[20] The Mo=O bond lengths (Mo-O2, 1.6965(19) and Mo-O3, 1.700(2)) as well the Mo-O single bond distance are in the expected range of *cis*-dioxo Mo(VI) complexes and Mo(VI) alkoxides, respectively.[21,22] Crystal data are summarized in Table 3.1.

Table 3.1. Crystal data and structure refinement for complex **1**.

Empirical formula	$C_{13}H_{17}ClMoN_2O_4$
Formula weight	396.68
Temperature	180(2) K
Wavelength	0.71073 A
Crystal system	Orthorhombic
Space group	P 21 21 21
Unit cell dimensions	a = 8.3931(18) α= 90°
	b = 9.447(2) A β= 90°
	c = 20.148(5) A γ = 90°
Volume	1597.6(6) $Å^3$
Z	4
Density (calculated)	1.649 Mg/m^3
Absorption coefficient	1.003 mm^{-1}
F(000)	800
Crystal size	0.34 x 0.10 x 0.06 mm^3
Theta range for data collection	5.19 to 26.35º
Limiting index	-10<=h<=10, -11<=k<=11, -25<=1<=25
Reflections collected	8118
Independent reflections	3183 [R(int) = 0.0262]
Completeness to theta = 26.35°	98.8 %
Max. and min. transmission	0.9423 and 0.7266
Refinement method	Full-matrix least-squares on F^2
Data / restraints / parameters	3183 / 0 / 192
Goodness-of-fit on F^2	1.068
Final R indices [I>2sigma(I)]	R1 = 0.0232, wR2 = 0.0487
R indices (all data)	R1 = 0.0299, wR2 = 0.0492
Absolute structure parameter	-0.04(3)
Largest diff. peak and hole	0.647 and -0.415 e.$Å^{-3}$

Concerning the characterization of **1** in solution, its ^{1}H NMR spectrum at 298 K showed, as expected, the signals corresponding to the (hydroxyalkyl) pyridinooxazoline ligand shifted to lower fields upon coordination (Figure 3.3). The $^{13}C\{^1H\}$ NMR spectrum also proved that the ligand is bound to the dioxomolybdenum core, displaying the signal of the pyridine carbon close to the nitrogen atom shifted downfield compared to that of the free ligand (free ligand δ: 122.1 (*C*H), 125.6 (*C*H), 137.4 (*C*H), and 162.9 (*C*=N) ppm vs coordinated ligand δ: 124.0 (*C*H), 130.5 (*C*H), 140.3 (*C*H) and 167.2 (*C*=N)).

Complex **2** showed a very close ^{1}H NMR spectrum to complex **1**, which is not surprising due to the similarity between them (Figure 3.4).

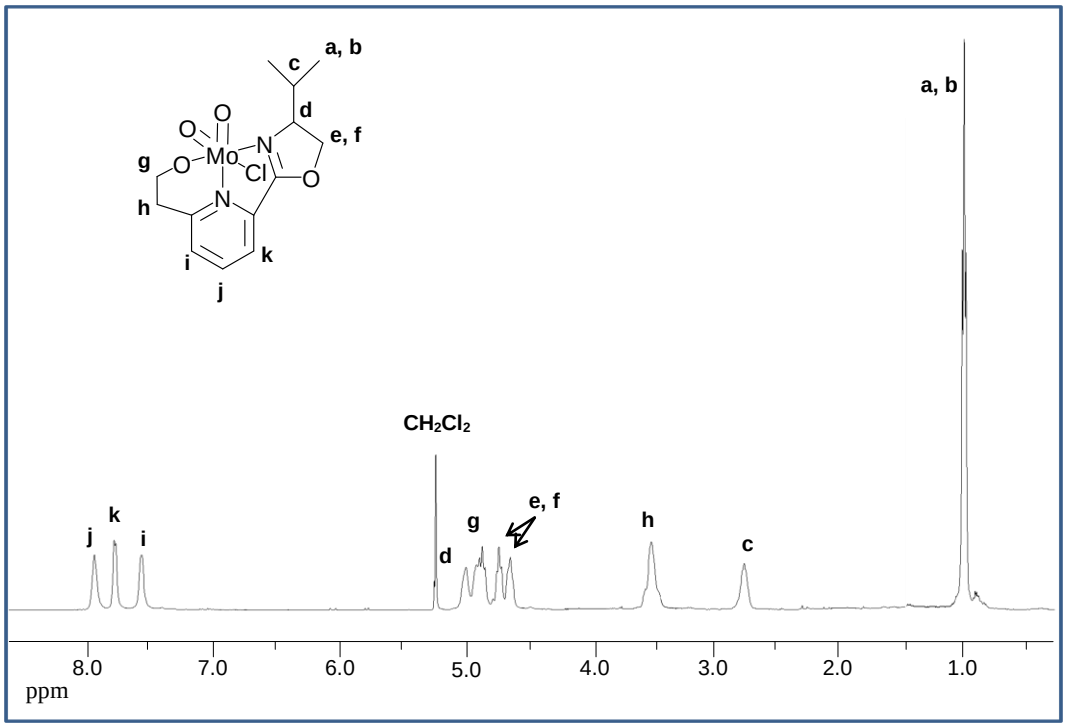

Figure 3.3. ^{1}H NMR (400 MHz, CD_2Cl_2, 298 K) spectrum of complex **1**.

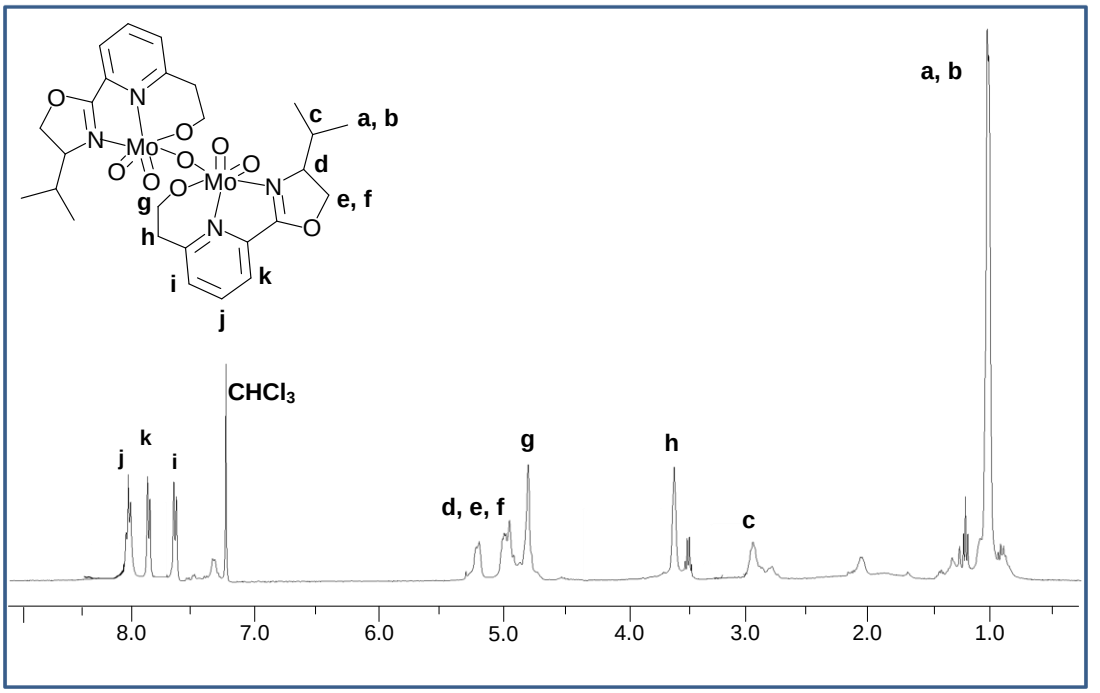

Figure 3.4. ^{1}H NMR (400 MHz, CD_2Cl_2, 298 K) spectrum of complex **2**.

A variable temperature ^{1}H NMR study of complex **1** (298 K - 193 K) evidenced up to three isomers at 273 K in a relative ratio of 3/1/1 (Figures 3.5). The origin of these isomers can be probably due to the two arrangements of the tridentate ligand in a pseudo-octahedral environment, giving meridional and facial isomers. Due to the polyhedron chirality, the *mer* isomer leads to two diastereoisomers because of the optically pure oxazoline moiety. The *fac* arrangement can form three different stereoisomers.

In order to rationalize these experimental observations, a modelling study was carried out, optimizing the different geometries by means of density functional theory (DFT B3LYP) (Figure 3.6). The two *mer* stereo-isomers represent the lowest energy conformations (**1**-*mer*1 corresponds to the isomer analyzed by X-ray diffraction, see above), while the three *fac* isomers show higher energy than those exhibited by the *mer* ones. Based on this modelling, the three isomers observed by ^{1}H NMR can be then associated to **1**-*mer*1, **1**-*mer*2 and **1**-*fac*1

The ^{95}Mo NMR spectrum of **1** containing the *N*,*N*',*O*-tridentated anionic ligand **A** showed one sharp symmetrical peak (width at middle height: 358 Hz) at +67.5 ppm at room temperature. This could point at the presence of a single species in solution.

However, the ^{1}H NMR spectrum shows the presence of more than one species in solution at low temperature; which leads to think that the electronic behavior between the isomers could probably be very similar and the different isomers appear like a single species in the molybdenum spectrum.

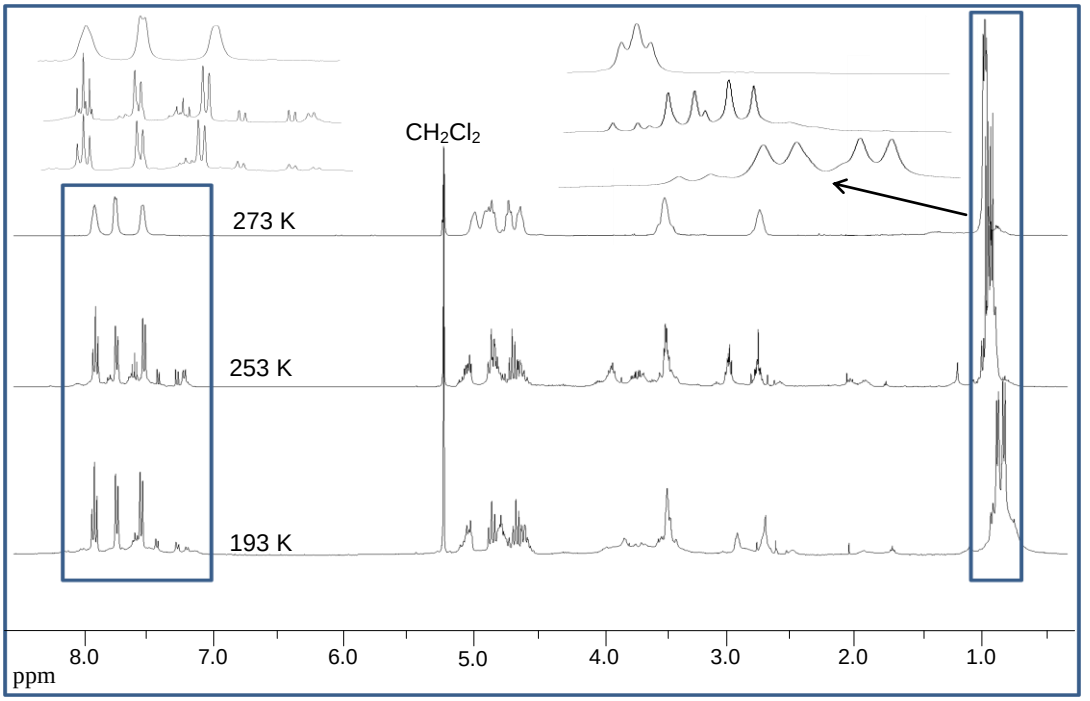

Figure 3.5. ^{1}H NMR (400 MHz, CD_2Cl_2) **s**pectra of **1** recorded at different temperatures (193-298 K).

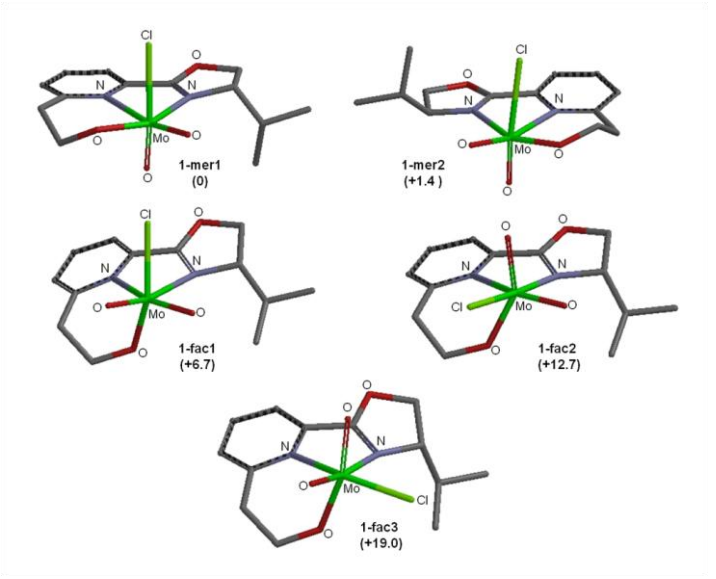

Figure 3.6. Modelled isomers for complex **1** (DFT). In brackets, relative energies in kcal/mol.

3.3.2. Synthesis and characterization of the pyridine-amide ligand B and its *cis*-dioxomolybdenum(VI) complex 3.

The pyridine-amide ligand **B** was prepared by reaction of 2-cyanopyridine with (2*S*)-2-amino-1,4-butanediol as depicted in Scheme 3.4. Compound **B** was isolated as yellow oil in a moderated yield (23%). This methodology usually leads to the formation of the corresponding oxazolinyl-pyridine ligands,[23] however in our case, the formation of **B** is favored (Scheme 3.4). Even changing the basicitiy of the medium, lowering the temperature and shortening the time, formation of the oxazoline was never observed.

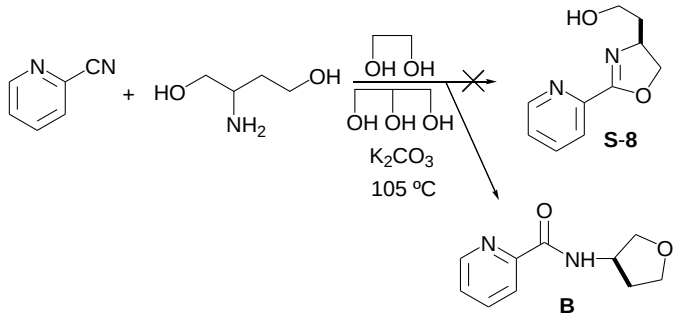

Scheme 3.4. Synthesis of pyridine-amide **B**.

J. McGarvey and co-workers proposed a rearrangement of the oxazoline heterocycle bearing a hydroxo group under basic conditions (Scheme 3.5).[24] This rearrangement involves a reversible cyclization process, which cannot explain our experimental observations.

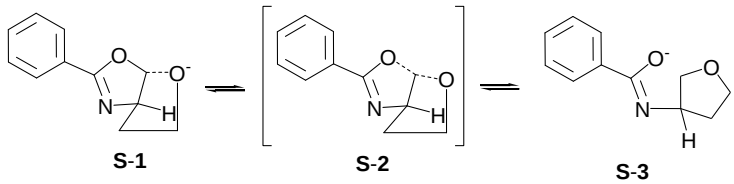

Scheme 3.5. Rearrangement of the oxazoline **I** to generate the amide **II**.

Then, we propose the mechanism shown in Scheme 3.6. The formation of the amide **B** under basic conditions can be explained on the basis of the relative high acidity of the primary alcohols and mainly by the higher nucleophilic character of the alkoxyde

group (intermediate **S-4** in Scheme 3.6) in relation to the iminol (intermediate **S-6**) in Scheme 3.6).

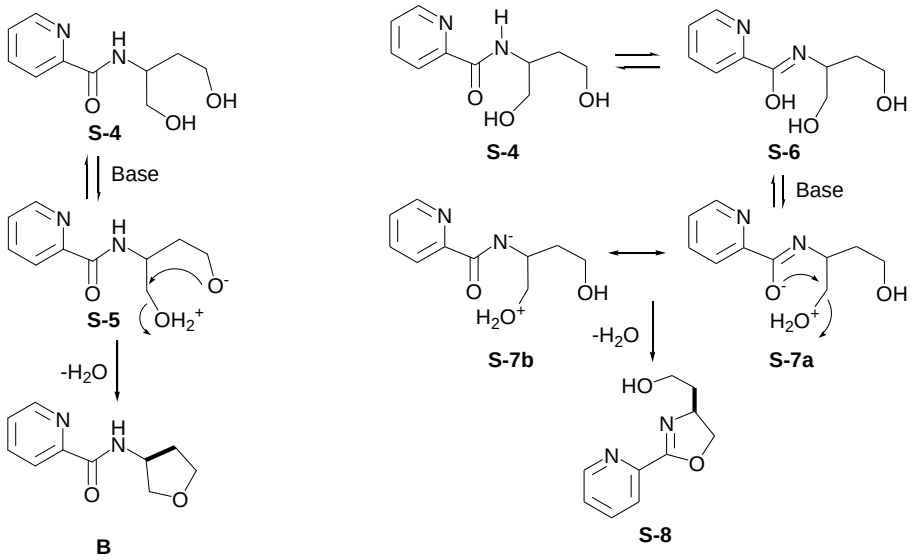

Scheme 3.6. Proposed mechanism for the formation of oxazoline **S-8** (right) and amide **B** (left).

The IR spectrum of ligand **B** showed the characteristic functional group absorptions, in particular: a very strong band at 1626 cm^{-1} for the carbonyl bond C=O. The ESI-MS spectrum showed a peak at m/z 193, corresponding to $[M + H]^+$. This new ligand showed a specific rotation of $[\alpha]_D^{26}$ = +150 (c 0.3, $CHCl_3$). For ligand **3,** the ^1H NMR spectrum displayed six signals at 1.99 and 2.31 ppm (diastereotopic methylenic protons), 3.80, 3.87, 3.98, 4.73 ppm (enantiotopic proton) assigned to the inequivalent protons of the furanyl ring, four resonances at 7.42, 7.82, 8.18 and 8.53 for the pyridyl protons, and a broad singlet signal at 6.00 ppm assigned to the N-H proton (Figure 3.7).

$[MoO_2Cl_2]$ reacts with one equivalent of **B** to form complex **3** in nearly quantitative yield (Scheme 3.7). This complex was obtained as an air stable crystalline orange solid and was full characterized by multinuclear (^1H, $^{13}C\{^1H\}$ and ^{95}Mo) NMR and IR spectroscopy, mass spectrometry, elemental analysis and X-ray diffraction analysis.

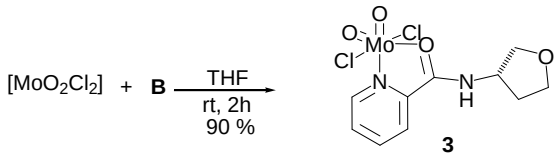

Scheme 3.7. Synthesis of mono-metallic complex **3** containing the chiral ligand **B**.

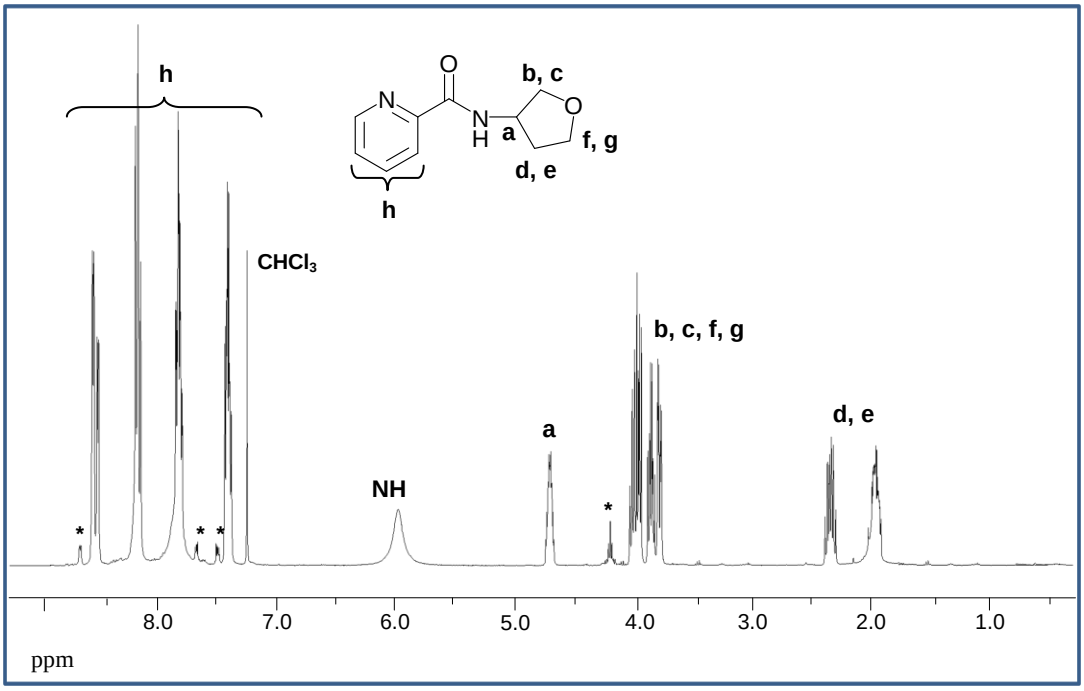

Figure 3.7. ^{1}H NMR (400 MHz, CD_2Cl_2, 298 K) spectrum of ligand **B** (* = impurities).

In the solid state, the IR spectrum of **3** exhibited a strong band around 1626 cm^{-1} attributed to the carbonyl amide bond (C=O) along with two strong bands at 950 and 914 cm^{-1} characteristic of the asymmetric and symmetric Mo=O stretching vibrations of the *cis*-$[MoO_2]^{2+}$ fragment, respectively.[5,6,13,14]

Figure 3.8 shows the molecular structure of **3** determined by X-ray diffraction analysis, including selected bond distances and angles. Crystal data are summarized in Table 3.2.

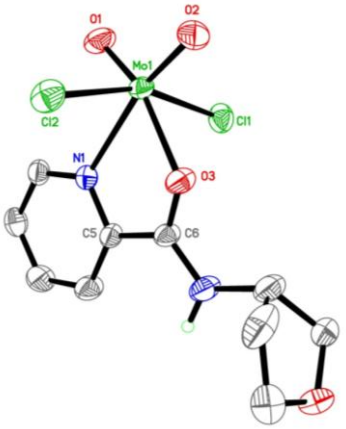

Figure 3.8. Molecular view of compound **3** with ellipsoids representing 50% probability. H atoms are omitted for clarity. Selected bond distances (Å) and angles (º): Mo(1)-O(1) 1.690(2), Mo(1)-O(2) 1.693(2), Mo(1)-Cl(1) 2.3991(8), Mo(1)-Cl(2) 2.3629(8), Mo(1)-N(1) 2.350(2), Mo(1)-O(3) 2.1871(19), N(1)-Mo(1)-O(3) 69.37(7), O(1)-Mo(1)-O(2) 106.04(12), Cl(1)-Mo(1)-Cl(2) 160.51(3).

Table 3.2. Crystal data and structure refinement for complex **3**.

Empirical formula	$C_{10}H_{12}Cl_2MoN_2O_4$
Formula weight	391.06
Temperature	193(2) K
Wavelength	0.71073 Å
Crystal system	Monoclinic
Space group	P2(1)
Unit cell dimensions	a = 8.4049(2) Å α= 90° b = 18.4313(4) Å β= 101.8820(10)° c = 9.3117(2) Å γ = 90°
Volume	1411.60(5) $Å^3$
Z	4
Density (calculated)	1.840 Mg/m^3
Absorption coefficient	1.317 mm^{-1}
F(000)	776
Crystal size	0.60 x 0.40 x 0.08 mm^3
Theta range for data collection	2.21 to 30.30°
Index ranges	-11<=h<=11, -26<=k<=26, -13<=l<=13
Reflections collected	26678
Independent reflections	8259 [R(int) = 0.0268]
Completeness to theta = 30.30°	99.7 %
Absorption correction	Semi-empirical from equivalents
Max. and min. transmission	0.9020 and 0.5054
Refinement method	Full-matrix least-squares on F^2
Data / restraints / parameters	8259 / 172 / 397
Goodness-of-fit on F^2	1.012
Final R indices [I>2sigma(I)]	R1 = 0.0275, wR2 = 0.0669
R indices (all data)	R1 = 0.0299, wR2 = 0.0685
Absolute structure parameter	-0.03(3)
Largest diff. peak and hole	0.603 and -0.573 e.$Å^{-3}$

The molecular structure of **3** revealed an octahedral coordination with the molybdenum atom coordinating to the pyridine nitrogen atom and the carbonyl oxygen atom of the chelating ligand, and with two chlorine atoms *trans* to each other, and two oxo groups in relative *cis* position. This geometric arrangement is comparable to that found in related *cis*-dioxomolybdenum containing bidentate ligands.[25] Mo-Cl, Mo=O and Mo-O bond lengths were within the expected range of values.[21,26]

For complex **3,** the ^{1}H NMR spectrum showed, as expected, the signals corresponding to the pyridine-amide ligand shifted to lower fields upon coordination (Figure 3.9), being the protons corresponding to the pyridine ring and the iminic proton those showing important effect upon coordination (free ligand δ: 6.00 (NH), 7.43 (C*H*), 7.84 (C*H*), 8.19 (C*H*), 8.54 (C*H*) ppm vs coordinated ligand: 8.92 (N*H*), 7.98 (C*H*), 8.41 – 8.35 (C*H*), 9.42 (C*H*) ppm).

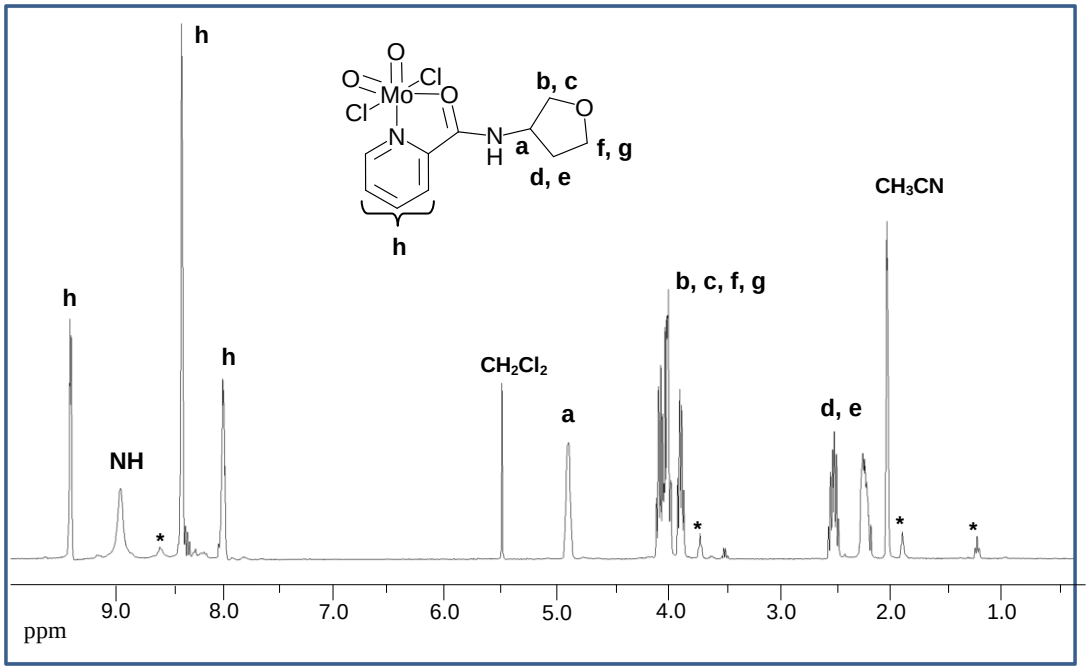

Figure 3.9. ^{1}H NMR (400 MHz, CD_2Cl_2, 298 K) spectrum of complex **3** (* = impurities).

Its ^{13}C NMR spectrum demonstrated that the ligand is bound to the dioxomolybdenum core. Thus, the signal for the carbon atom of the carbonyl group was found at δ 168.0, shifted downfield compared to that of the free ligand which appears at δ 164.3.

The ^{95}Mo NMR spectrum of complex **3** showed one sharp symmetrical peak at δ +189.7 (width at middle height: 217 Hz). The sharp peak points to the presence of one isomer in solution.

3.3.3. Synthesis and characterization of molybdenum complexes 4 and 5 containing oxazoline ligands C and D.

The new mono-metallic dioxomolybdenum(VI) complexes **4** and **5** containing the chiral oxazoline-based ligands **C** and **D** respectively, were prepared by treatment of $[MoO_2Cl_2]$ and $[MoO_2Cl_2(DME)]$ (DME = dimethoxyethane) with the corresponding ligand in THF at room temperature (Schemes 3.8 and 3.9)

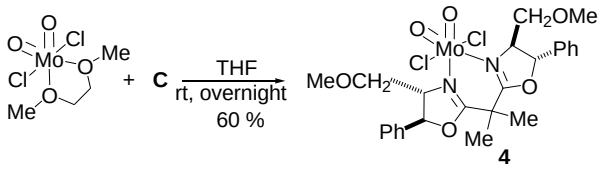

Scheme 3.8. Synthesis of mono-metallic complex **4** containing chiral ligand **C**.

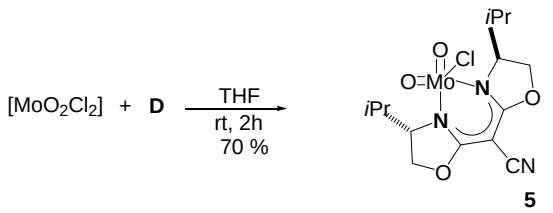

Scheme 3.8. Synthesis of mono-metallic complex **5** containing chiral ligand **D**.

In the solid state, IR spectra of **4** and **5** exhibited a very strong band around 1650 cm^{-1} due to the oxazoline imine bond (for **4**, 1654 cm^{-1} and for **5**, 1601 cm^{-1}); both

complexes showed two strong bands in the range of 890-940 cm^{-1} corresponding to asymmetric and symmetric Mo=O stretching vibrations[5,6,13,14] (for **4**, 939 and 910 cm^{-1}; for **5**, 957 and 918 cm^{-1}).

The structure of $[MoO_2Cl_2(\kappa^2\text{-}N,N\text{-}\mathbf{C})]$ (**4**) was established by single-crystal X-ray diffraction analysis (Figure 3.10). This structure represents the first example reported in the literature for dioxomolybdenum(VI) complexes containing bis(oxazolines).[27,28] A distorted octahedral arrangement around the metal atom was observed, with both chlorine atoms in a relative *trans* position. Nitrogen atoms were thus *trans* placed in relation to the oxo groups, leading to relatively long Mo-N bond distances (Mo-N1 = 2.326 Å and Mo-N2 = 2.309 Å), due to the oxo *trans* influence as previously observed for other oxomolybdenum(VI) complexes containing oxazoline ligands.[5,6a] The six-membered metallacycle adopts a very flat conformation; the deviation of each atom from the equatorial plan constituted by the six atoms of the ring is very small (Mo1: 0.057 Å; N1: -0.13 Å; C3: 0.065 Å; C4: 0.10 Å; C7: -0.15 Å; N2: 0.056 Å). The angle between both heterocycle oxazoline rings is *ca.* 22°. Crystal data are summarized in Table 3.2.

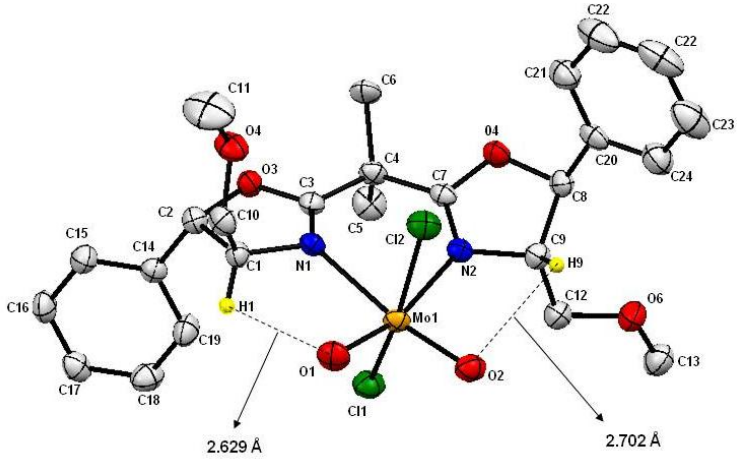

Figure 3.10. Molecular view of compound **4** with ellipsoids representing 50% probability. H atoms are omitted for clarity. Selected bond distances (Å) and angles (º): Mo(1)-O(1) 1.686(2), Mo(1)-O(2) 1.695(2), Mo(1)-Cl(1) 2.383(1), Mo(1)-Cl(2) 2.368(1), Mo(1)-N(1) 2.326(2), Mo(1)-N(2) 2.309 (2), N(1)-Mo(1)-N(2) 76.41(8), O(1)-Mo(1)-O(2) 105.35(11), Cl(1)-Mo(1)-Cl(2) 160.57(3).

Table 3.3. Crystal data and structure refinement for complex **4**.

Empirical formula	$C_{25}H_{30}Cl_2MoN_2O_6$
Formula weight	621.35
Temperature	180(2) K
Wavelength	0.71073 Å
Crystal system	Monoclinic
Space group	P2(1)
Unit cell dimensions	a = 11.8113(2) Å α= 90° b = 14.5654(4) Å β= 105.570(2)° c = 16.3202(2) Å γ = 90°
Volume	2704.63(17) $Å^3$
Z	4
Density (calculated)	1.526 Mg/m^3
Absorption coefficient	0.724 mm^{-1}
F(000)	1272
Crystal size	1.60 x 0.04 x 0.04 mm
Theta range for data collection	5.19 to 26.37°
Index ranges	-10<=h<=14, -18<=k<=17, -20<=1<=17
Reflections collected	17498
Independent reflections	10545 [R(int) = 0.0241]
Completeness to theta = 26.37°	98.8 %
Absorption correction	Semi-empirical from equivalents
Max. and min. transmission	0.9716 and 0.3904
Refinement method	Full-matrix least-squares on F^2
Data / restraints / parameters	10545 / 1 / 657
Goodness-of-fit on F^2	1.030
Final R indices [I>2sigma(I)]	R1 = 0.0294, wR2 = 0.0590
R indices (all data)	R1 = 0.0340, wR2 = 0.0612
Absolute structure parameter	-0.026(18)
Largest diff. peak and hole	0.332 and -0.313 $e.Å^{-3}$

The ^{1}H NMR spectrum of **4** only exhibited one set of signals indicating a C_2 symmetry for the bidentate ligand upon coordination (Figure 3.11). The non-aromatic protons of the heterocycle are down-fielded in relation to the free ligand, in particular the C-H close to the nitrogen atom ($\Delta\delta$ = +0.78 ppm); this deshielding can be attributed to the interaction of the proton with the oxo groups as shown by the average interatomic distance H…O=Mo from the crystallographic data (2.61 Å), in agreement with previous observations for oxo- and peroxo-molybdenum(VI) complexes.[5,6]

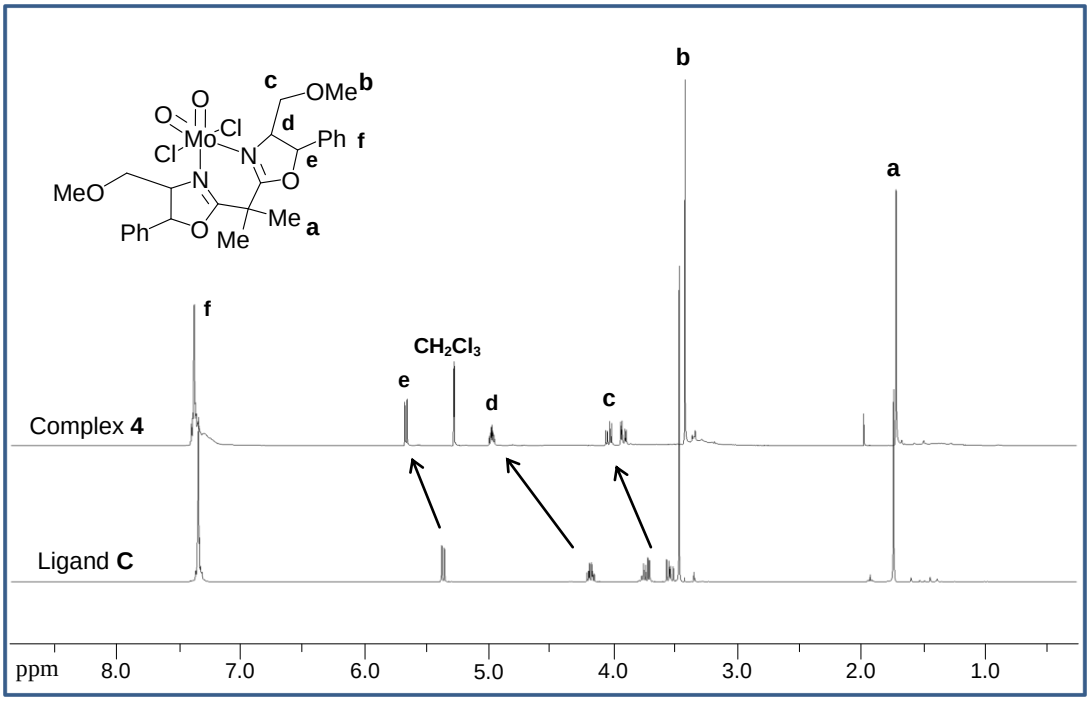

Figure 3.11. ^{1}H NMR (400 MHz, CD_2Cl_2, 298 K) spectrum of ligand **C** and complex **4**.

The ^{95}Mo NMR spectrum of **4** in solution showed one symmetric signal (width at middle height: 700 Hz) at +136.6 ppm, pointing to the presence of only one isomer in solution in agreement with other related oxomolybdenum(VI) complexes containing bis(oxazoline) ligands.[29] Comparing with analogous structures containing bipyridine ligands, *e.g.* [MoO_2Br_2(4,4'-*t*Bu-bipyridine)] which shows a chemical shift at +243.3 ppm,[30] the up-fielded shift observed for complex **4** indicates a lower electron-donor ability of the bis(oxazoline) than that exhibited by related bipyridine ligands, which induces a lower electronic density around the metallic center (see Chapter 4).[31]

Molybdenum complexes bearing monoanionic bisoxazolinate ligands have not been reported so far in the literature, despite the interesting catalytic results displayed by complexes incorporating these monoanionic ligands.[32] The reaction of the cyano-bis(oxazoline) **D**, prepared as previously described in the literature,[7c,8] with [MoO_2Cl_2] affords complex **5** in quantitative yield (Scheme 3.8). The proposed structure of **5** is in accordance with the analytical data derived from NMR and IR

spectroscopy, elemental analysis and mass spectrometry. ^{1}H NMR spectra of **5** showed a single set of resonances for the bidentated ligand (Figure 3.12).

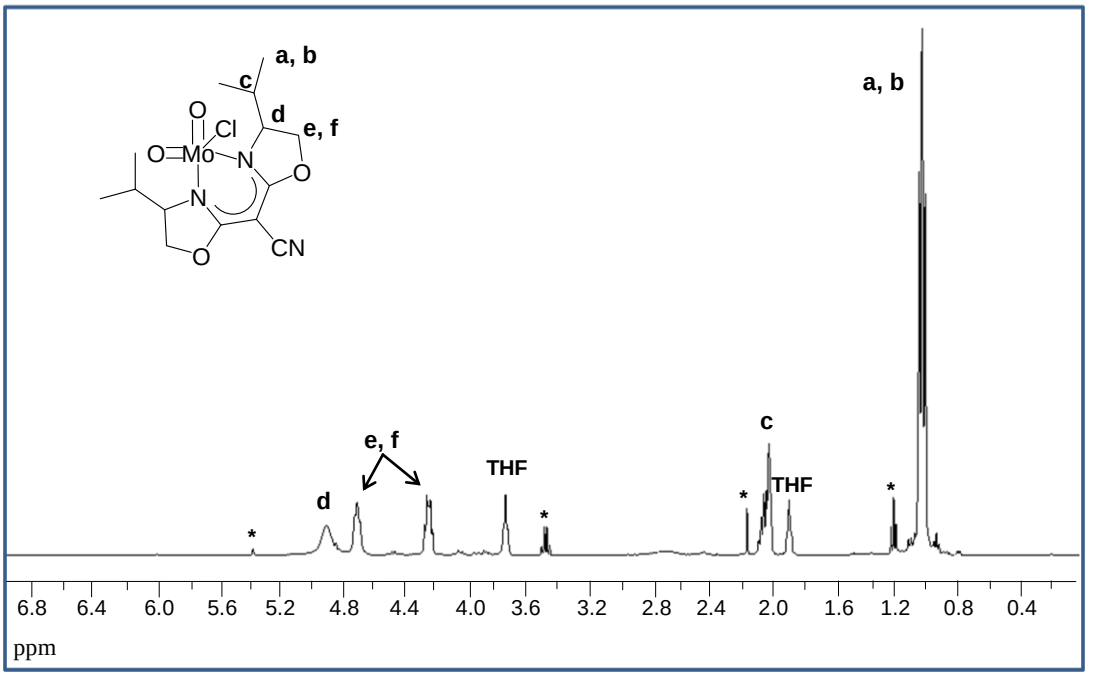

Figure 3.12. ^{1}H NMR (400 MHz, CD_2Cl_2, 298 K) spectrum of ligand **C** and complex **5** (* = impurities).

Electrospray ionization mass spectrum of an acetonitrile solution of **5** showed a peak at m/z 462 in the negative ion mode corresponding to $[M+Cl]^-$. The ^{95}Mo NMR spectrum of **5** in solution showed one symmetric signal (width at middle height: 945 Hz) at +126.8 ppm.

It is noteworthy that the chemical shift, δ_M, for molybdenum compounds is usually defined relative to an external standard, $\delta_M = \delta_{ref} - \delta$. For ^{95}Mo NMR, the standard corresponds to a solution of Na_2MoO_4 (pH + 11, 1 mol/L). On basis of theoretical calculations,[33] it should be expected that for good donor ligands the metal atom turns rich in electronic population and the chemical shift increases.

Therefore, comparing the ^{95}Mo NMR of the three dioxomolybdenum complexes containing oxazoline-based ligands **A**, **C** and **D**, the most electron rich metal center corresponds to complex **4** (+136.6 ppm), followed by **5** (+126.8 ppm) and **1** (+67.5

ppm) (Figure 3.13). The molybdenum complex **3**, containing the amide ligand **B**, exhibits the highest chemical shift (+189.7 ppm), pointing to the electron richness of the metal center (Figure 3.13).

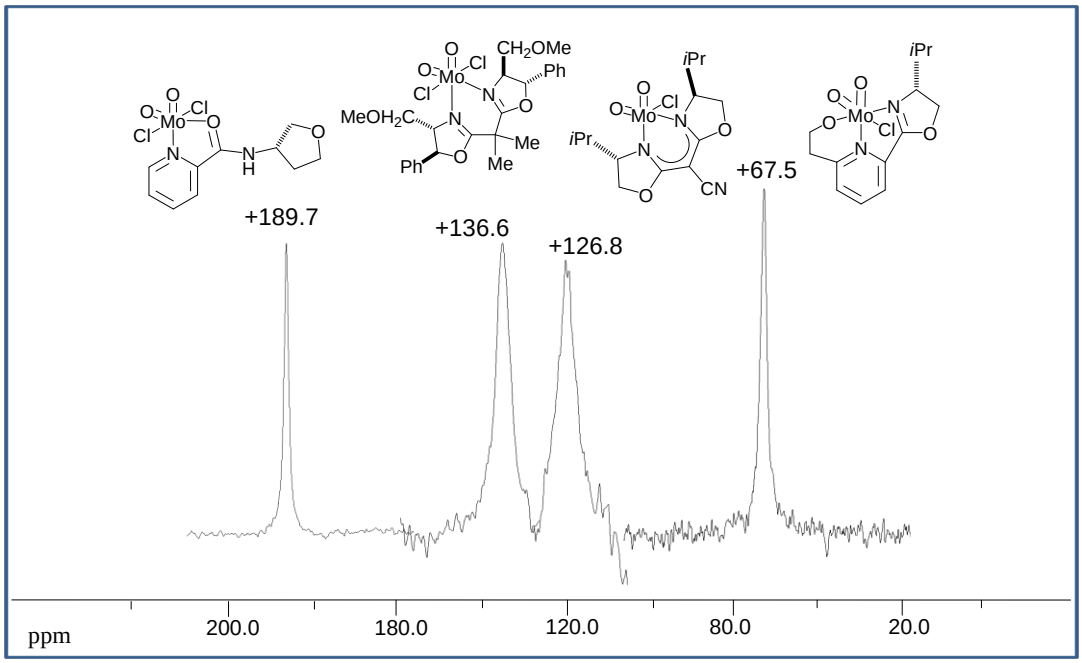

Figure 3.13. ^{95}Mo NMR (26.08 MHz, CD_2Cl_2, 298 K) spectra of complexes **1** and **3**-**5**.

3.4. Conclusions

In conclusion, novel *cis*-dioxomolybdenum(VI) complexes containing optically pure chiral ligands were synthesized and fully characterized both in solution and solid state. All the new *cis*-dioxomolybdenum complexes characterized by X ray diffraction (complex **1** ([$MoO_2Cl(\kappa^3$-*N*,*N*',*O*-**A**)], complex **3** [$MoO_2Cl_2(\kappa^2$-*N*,*O*-**B**)], complex **4** [$MoO_2Cl_2(\kappa^2$-*N*,*N*-**C**)]) showed a distorted octahedral coordination with both oxo ligand in relative *cis* position. For complex **5**, [$MoO_2Cl(\kappa^2$-*N*,*N*-**D**)] the proposed structure taking into account data derived from NMR and IR spectroscopy, elemental analysis and mass spectrometry, corresponds to a trigonal bypyramid arrangement around the metal center.

Complex **1** ([$MoO_2Cl(\kappa^3$-*N*,*N*',*O*-**A**)]) represents the first X-ray characterization of a monometallic molybdenum complex bearing a *N*,*N*',*O*-tridentate ligand, showing an unusual arrangement with the chloride ligand *trans* to one oxo group with a relatively long distance in the Mo-Cl bond (2.52 Å), as a result of the strong *trans* influence of the oxo ligand. Similarly, complex **4** represents the first X-ray structure reported for a Mo(VI) complex containing a bis(oxazoline) ligand.

Complex **1** showed in solution the presence of at least 3 isomers at low temperature, probably due to meridional and facial isomers arrangements. On the other hand, complexes **3** and **4** showed the presence of only one isomer in solution.

Complex **1** was rather sensitive to moisture, decomposing to produce a bimetallic species $[MoO_2(\kappa^3$-*N,N,O*-**A**$)]_2(\mu$-O). Complexes **4** and **5** were also very sensitive to moisture, in contrast to complex **3**, which exhibited high stability under moisture and air conditions.

3.5. Acknowledgments

We wish to acknowledge M. C. Almeida and Dr. A. Coelho for providing data from the Mass Spectrometry and Elemental Services at ITQB. The Bruker Avance III MHz spectrometer is part of the National NMR Network and was purchased in the framework of the National Program for Scientific Reequipment, contract REDE/1517/RMN/2005, with funds from POCI 2010 (FEDER) and Fundação para a Ciência e a Tecnologia (FCT).

3.6. References

1 (a) R. H. Holm, *Coord. Chem. Rev.* 1990, **100**, 183-221; (b) A. Sakthivela, J. Zhaoa, G. Raudaschl-Sieber, M. Hanzlik, A. S. T. Chiang, F. E. Kühn, *Appl. Catal. A: General*, 2005, **281**, 267-273; (c) F. E. Kuhn, A. M. Santos, W. A. R. Herrmann, *Dalton Trans*., 2005, 2483-2491; (d) C. Maurya, D. D. Mishra, S. N. Rao, R. Verma, N. N. Rao, *Ind. J. Chem*., 1997, **36A**, 599-601.

2 (a). M. N. Sheng, Zajaczek (Arco), GB 1.136.923.1968,1, 923; (b) J. Kolar, (Halcon), US 3.350.422, US3.351.635,1967.

3 K. R. Jain, W. A. Herrmann, F. E. Kühn, *Coord. Chem. Rev*., 2008, **252**, 556-568; (b) A. J. Burke, *Coord. Chem. Rev*., 2008, **252**, 170-175.

4 (a). G. C. Hargaden, P. J. Guiry, *Chem. Rev*., 2009, **109**, 2505-2550; (b) H. A. McManus, P. J. Guiry, *Chem. Rev*., 2004, **104**, 4151-4202; (c) M. Gómez, G. Muller, M. Rocamora, *Coord. Chem. Rev*., 1999, **193-195**, 769-835.

5 M. Gómez, S. Jansat, G. Muller, G. Noguera, H. Teruel, V. Moliner, E. Cerrada, M. Hursthouse, *Eur. J. Inorg. Chem*., 2001, 1071-1076.

6 (a) J. A. Brito, M. Gómez, G. Muller, H. Teruel, J. C. Clinet, E. Dunãch, M. A. Maestro, *Eur. J. Inorg. Chem*., 2004, 4278-4285; (b) J. A. Brito, M. Gómez, H. Teruel, *Inorg. Chim. Acta*, 2008, **361**, 2740-2746.

7 (a) V. K. Aggarwal, L. Bell, M. P. Coogan, P. Jubault, *J. Chem. Soc. Perkin Trans*., 1998, 11, 2037-2042; (b) K. Hallman, A. Frölander, T. Wondimagegn, M. Svensson, C. Moberg, PNAS, 2004, 101, 5400-5404; (c) K. A. Nolin, R. W. Ahn, D. Toste, *J. Am. Chem. Soc.* 2005, **127**, 12462-12463.

8 E. J. Corey, Zhe Wang, *Tetrahedron Lett*., 1993, **34**, 4001-4004.

9 G.M. Sheldrick, SHELXS-97, Acta Crystallogr. A46 1990, 467–473.

10 G.M. Sheldrick, SHELXL-97 Program for Crystal Structure Refinement, University of Göttingen, 1997.

11 ORTEP3 for Windows: L.J. Farrugia, J. Appl. Crystallogr. 30 (1997) 565.

12 B. Kamenar, M. Penavi, B. Korpar-olig, B. Markovi, *Inorg. Chim. Acta*., 1982, **65**, L245-L247.

13 (a) F. E. Kühn, A. M. Santos, A. D. Lopes, I. S. Gonçalves, J. E. Rodríguez-Borges, M. Pillinger, C. C. Romão, *J. Organomet. Chem*., 2001, **621**, 207-217; (b) A. A. Valente, I. S. Gonçalves, A. D. Lopes, J. E. Rodríguez-Borges, M. Pillinger, C. C. Romão, J. Rocha, X. García-Mera, *New. J. Chem*., 2001, **25**, 959-963.

14 P. M. Reis, C. A. Gamelas, J. A. Brito, N. Saffon, M. Gómez, B. Royo, *Eur. J. Inorg. Chem*. 2011, 666-673.

15 H. Arzoumanian, R. Bakhtchadjian, G. Agrifoglio, H. Krentzien, J-C. Daran, *Eur. J. Inorg. Chem*., 1999, 2255-2259. (b) H. Arzoumanian, R. Bakhtchadjian, R. Atencio, A. Briceno, G. Verde, G. Agrifoglio, *J. Mol. Catal. A: Chem.*, 2006, **260**, 197-201.

16 C. C. L. Pereira, S. S. Balula, F. A. A. Paz, A. A. Valente, M. Pillinger, J. Klinowski, I. S. Gonçalves, *Inorg. Chem*., 2007, **46**, 8508-8510.

17 Y. Wong, J. Ma, F. Xue, T. C. W. Mak, D. K. P. Ng, *Organometallics*, 1999, **18**, 5075-5079.

18 (a) M. Bakir, I. Hassa, O. Green, *J. Coord. Chem*., 2006, **59**, 1953-1962; (b) J. M. Mitchell, N. S. Finney, *J. Am. Chem. Soc*., 2001, **123**, 862-869; (c) B. Piggot, S. F. Wong, D. Williams, *J. Inorg. Chim. Acta*, 1988, **141**, 275-279.

19 (a) Y. Wong, D. K. P. Ng, H. K. Lee, *Inorg. Chem*., 2002, **41**, 5276-5285.

20 (a) A. Lehtonen, R. Sillanpää, *Eur. J. Inorg. Chem*., 2006, 2878-2884; (b) M. E. Judmaier, A. Wallner, G. N. Stipicic, K. Kirchner, J. Baumgartner, F. Belaj, *Inorg. Chem*. 2009, **48**, 10211-10221.

21 F. E. Kühn, A. D. Lopes, A. M. Santos, E. Herdtweck, J. J. Haider, C. C. Romão, A. G. Santos, *J. Mol. Catal. A: Chemical*, 2000, **151**, 147-160.

22 (a) L. M. R. Hill, M. K. Taylor, V. W. L. Ng, C. G. Young, *Inorg. Chem.* 2008, **47**, 1044-1052; (b) T. A. Hanna, C. D. Incarvito, A. L. Rheingold, *Inorg. Chem.* 2000, **39**, 630-631; (c) J. M. Hawkins, J. C. Dewan, K. B. Sharpless, *Inorg. Chem*., 1986, **25**, 1503-1505; (d) J. M. Berg, R. H. Holm, *J. Am. Chem. Soc*., 1985, **107**, 917-925.

23 G. Balavoine, J. C. Clinet, I. Lellouche, *Tetrahedron Lett*., 1989, **30**, 5141-5144.

24 K. J. Wilson, M. Sabat, G. J. McGarvey, *J. Org. Chem*., 1993, **58**, 6180-6181.

25 A. Günyar, D. Betz, M. Drees, E. Herdtweck, F. E. Künk, *J. Mol. Catal. A: Chemical*, 2010, **331**, 117-124.

26 M. S. Saraiva, S. Quintal, F. C. M. Portugal, T. A. Lopes, V. Félix, J. M. F. Nogueira, M. Meireles, M. G. B. Drew, M. J. Calhorda, *J. Organomet. Chem*., 2008, **693**, 3411-3418.

27 Only one structure has been previously reported corresponding to a Mo(III) complex containing a bis(oxazoline) derived of oxalic acid: F. Stoffelbach, P. Richard, R. Poli, T. Jenny, C. Savary, *Inorg. Chim. Acta,* 2006, **359**, 4447-4453.

28 J. A. Brito, S. Ladeira, E. Teuma, B. Royo, M. Gómez, *Appl. Catal. A: General*, 2011, **398**, 88-95.

29 F. E. Kühn, A. M. Santos, A. D. Lopes, I. S. Gonçalves, J. E. Rodríguez-Borges, M. Phillinger, C. C. Romão, *J. Organomet. Chem*., 2001, **621**, 207-217.

30 H. Arzoumanian, G. Agrifoglio, H. Krentzien, M. Capparelli, *J. Chem. Soc., Chem*. *Commun*., 1995, 655-656.

31 J. A. Brito, H. Teruel, S. Massou, M. Gómez, *Magn. Reson. Chem*., 2009, **47**, 573-577.

32 S. Dagorne, S. Bellemin-Laponnaz, A. Maisse-François, *Eur. J. Inorg. Chem*., 2007, 913-925.

33 H. Teruel, A. Sierralta, *J. Mol. Catal.*, *A: Chemical.* 1996, **107**, 379-383.

Chapter 4 ^{95}Mo NMR SPECTROSCOPY: A USEFUL TOOL FOR STRUCTURAL STUDIES IN SOLUTION

This chapter originated the following publication:

J. A. Brito, H. Teruel, S. Massou, M. Gómez

Magn. Reson. Chem., 2009, **47**, 573–577

Summary

Oxomolybdenum(VI) complexes containing diverse ligands from an electronic and topological point of view have been analyzed by means of ^{95}Mo NMR spectroscopy in solution with the purpose of using this technique as a tool to study their coordination chemistry and reactivity. The relationship between the electronic density on the metal tuned by the electron-donor ability of the coordinated ligands and the ^{95}Mo chemical shift has been proved for mono- and bimetallic complexes showing a hexa- or hepta-coordination around the metal center. The different origins of the signal broadening (associated either to the symmetry of the metallic polyhedron or to the presence of isomers or to the ligand de-coordination) have been also considered to rationalize the obtained data.

The work described in this chapter was entirely performed by the candidate except for the ^{95}Mo NMR spectra which were performed by Dr. Stéphane Massou and Marc Vedrenne from University Paul Sabatier (Toulouse, France), and the preparation of ligand **J** which was prepared in the group of Prof. M. Etienne.

4.1. Introduction

Transition metal oxo compounds are involved in oxygen transfer reactions in both biological[1] and industrial processes.[2] In particular, the interest in molybdenum-catalyzed olefin epoxidations is closely related with the development of homogeneous Mo(VI) catalysts in the Halcon and Arco processes in 1960s.[3] However, the epoxidation mechanism keeps on as a controversial subject.[4] In the last years, we have been especially interested in the use of oxomolybdenum(VI) catalysts containing chiral oxazoline ligands, which are robust species towards oxidation reactions. The obtained results concerning the catalytic selectivity led us to study the coordination chemistry of Mo(VI) complexes in solution by means of ^{1}H NMR.[5,6] Similarly, ^{95}Mo NMR can also be a helpful technique to understand the reactivity of molybdenum(VI) complexes, because of the significant dependence of the chemical shift with the electronic environment and coordination geometry around the molybdenum atom.[7] From a mechanistic point of view, we have evidenced the olefin interaction with the metal center by ^{95}Mo NMR spectroscopy.[8]

Herein we report a ^{95}Mo NMR analysis of mono- and bimetallic oxo- and oxoperoxo-Mo(VI) complexes in solution, containing mono- and poly-dentate *N*-donor ligands (Figure 4.1), in order to prove the convenience of this technique to obtain information about the coordination chemistry in solution.

4.2. Experimental part

4.2.1. General

^{95}Mo NMR spectra were acquired on a Bruker Avance II spectrometer equipped with a 5-mm z-gradient TXO probe. The ^{1}H and the ^{95}Mo frequencies were 400.13 and 26.08 MHz, respectively. From 10 to 50 mg of molybdenum compounds were dissolved in 600 µl of deuterated acetone, depending on their solubility. The solvent deuterium resonance was used to accurately adjust the magnetic field. The ^{95}Mo chemical shift was referenced to 1 M Na_2MoO_4 in D_2O (pH = 11). Spectra were recorded at 298 K unless otherwise stated. To suppress acoustic ringing, an echo pulse sequence was used with an echo delay of 20 µs and a 90º pulse length of 14 µs. The spectral width was 50 kHz, the acquisition time was 157 ms, and 250000 transients were accumulated with a relaxation delay of 100 ms. Therefore, the total experimental time was 19 h and a very high signal-to-noise ratio was obtained for signals with narrow resonances. An exponential window function was applied with a line broadening of 20–200 Hz before Fourier transform to obtain an optimum signal-to-noise ratio. For calculation of half-height widths, Lorentzian deconvolutions were applied using TOPSPIN 1.3 software. Ligands **A**,[9] **B**[10], **C**,[11] **D**,[9c,12] **G**,[13] (*R*)-**H** and (*S*)-**I**,[6] and complexes **1**,[9,10] **3**,**5**,[10] **4**,[9] **7**,[14] **8**, **17**,[8] **9**–**10**,[6] **11**,[15] **12**,[16] **14**, **15**[17] and **16**[5] were prepared according to reported methods. Complexes **6**[18] and **13**[19] were prepared following the methodology described for related compounds.

4.3. Results and Discussion

4.3.1. ^{95}Mo NMR study of oxomolybdenum(VI) complexes

For the present study, several oxomolybdenum(VI) complexes were chosen (**1**-**13**) containing bidentate donor ligands: 2,2'-bipyridine and 4,4-ditert-butyl-2,2-bipyridine (**E**–**F**), the amide ligand **B** and also oxazoline derivatives (neutral, **C** and **G**, and

anionic, **A**, **D, H** and **I**, ligands), with the aim of studying the coordination behavior in solution due to their potential as homogeneous catalytic precursors, mainly for oxidation processes (Figure 4.1).

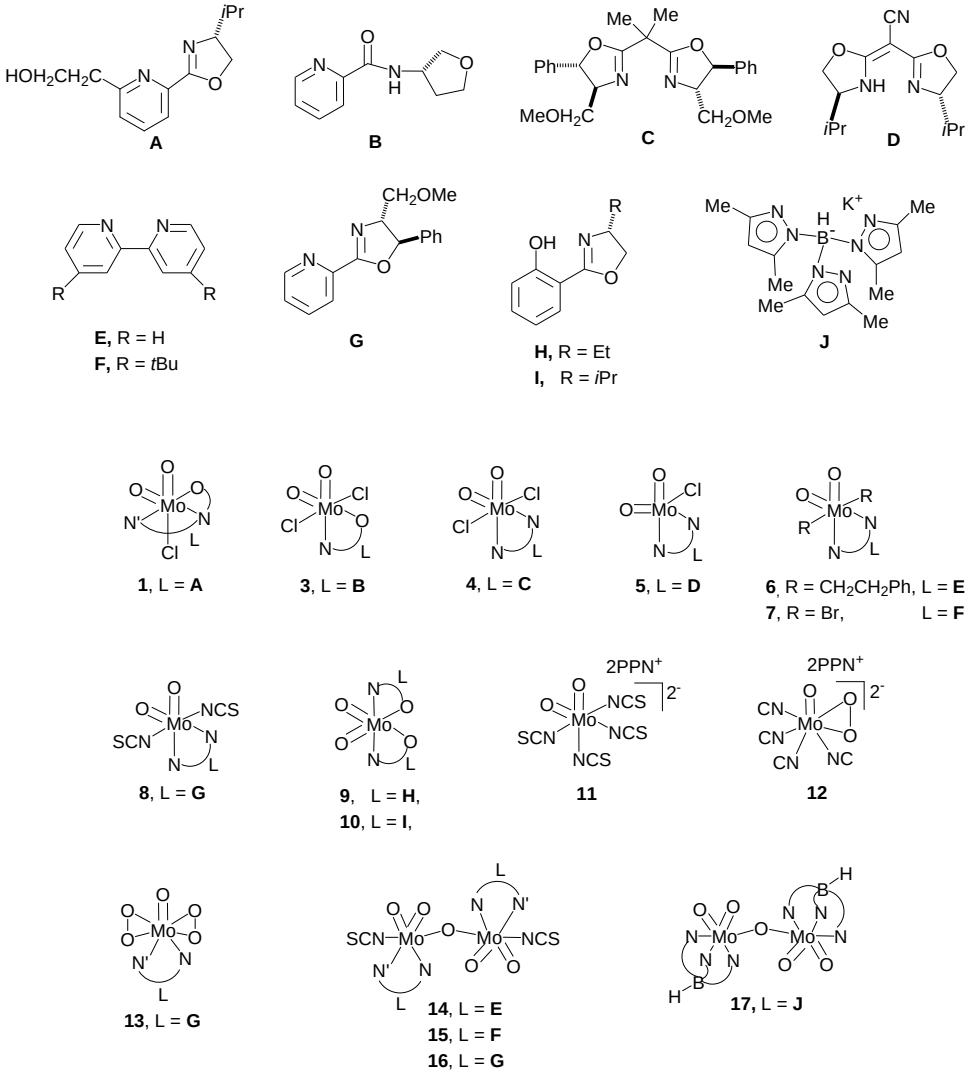

Figure 4.1. Oxomolybdenum(VI) complexes (**1**–**17**) containing monodentated (Br, alkyl, CN, NCS) and polydentated (**A**–**J**) ligands. PPN^+ = bis(triphenylphosphine)iminium cation.

The solid state structures of the monometallic **1, 3, 4**, **6**, **11**[6,9,10,14,15] and bimetallic **14**-**17**[8,17] complexes show a distorted octahedral geometry around the metal atom, while for the heptacoordinated compounds **12** and **13**, the ligands are placed around the molybdenum center giving a pseudopentagonal bipyramidal geometry.[5,16] The

proposed structure for complex **5**, taking into account mass spectrometry and NMR data corresponds to a trigonal bipyramid arrangement around the metal center (see Chapter 3, section 3.2.3.5.). The chemical shifts observed cover a wide range (*ca.* 1100 ppm, from +500 to −600 ppm), depending on the electronic density on the metal by modulation of the coordinated ligands (Table 4.1 and Figure 4.2).

Table 4.1. ^{95}Mo NMR data (26.08 MHz, 298 K, acetone-d_6) for oxomolybdenum(VI) complexes

Entry	Complex	Chemical shift (ppm)	Full width at middle height (Hz)[a]
1	**1**	+67.5	358
2	**3**	+189.7	217
3	**4**	+136.6	700
4	**5**	+126.8 +306.6	900 2200
5	**6**	+493.9	44
6	**7**[b]	+243.3	1190
7	**8**	−93.7	319
8	**9**	+49.2 −58.5[c]	1491 152
9	**10**	+53.9 −60.7[c]	1059 99
10	**11**	+125.0	295
11	**12**	−597	51
12	**13**	−136.5	780
13	**14**[d]	−73.8	146
14	**16**	−76.0	647
15	**17**	−64.3	565

[a] Calculated by lorentzian deconvolution. [b] δ = +196.8 ppm has been previously reported for complex **7** (Ref. [14]). [c] Resonance corresponding to the partial de-coordination of the ligand occurred in solution. [d] δ = −45, −57 ppm has been previously reported for complex **15** (Ref. [17]).

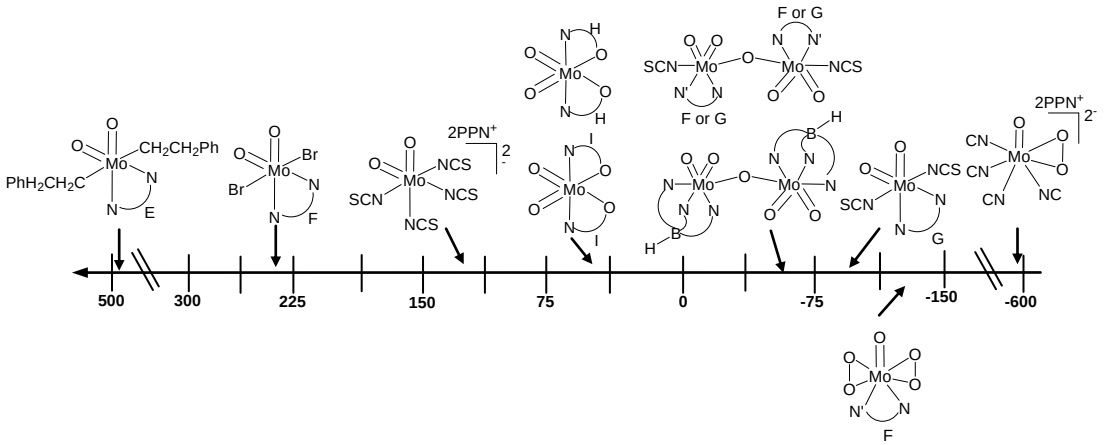

Figure 4.1. ^{95}Mo NMR (CD_3COCD_3, 26.08 MHz, 298 K) data of oxomolybdenum(VI) complexes. Chemical shift scale from +500 to −600 ppm.

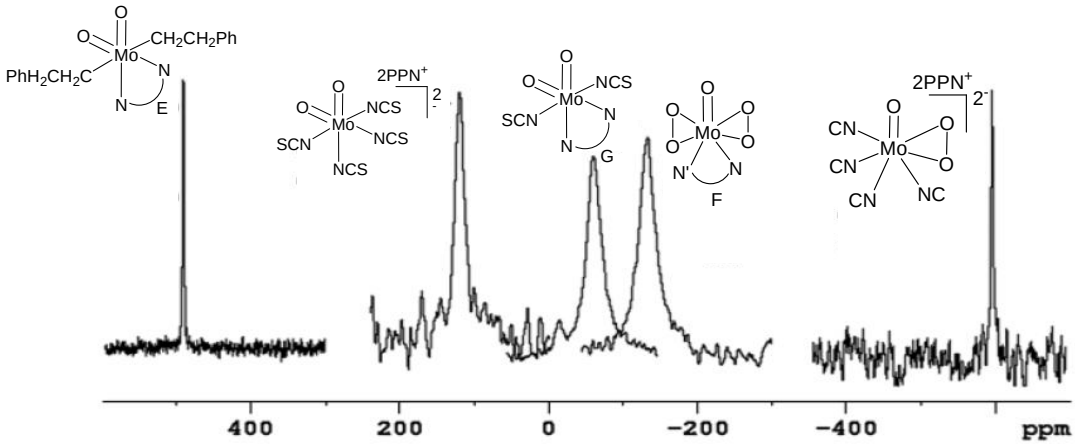

Figure 4.3. Selected ^{95}Mo NMR (CD_3COCD_3, 26.08 MHz, 298 K) data of oxomolybdenum(VI) complexes for comparison of the signal broadening [300 ppm (7824 Hz) width used for each].

As proposed by theoretical calculations,[20,21] a correlation between chemical shift and electronic density on molybdenum(VI) ion can be inferred. When electron-donor ligands are involved, the resonances are shifted to lower fields. Therefore, for the hexacoordinated complexes, **6** shows a higher chemical shift than that observed for **7** (+493.9 (R = CH_2CH_2Ph) vs +243.3 (R = Br) ppm, entries 5 and 6 in Table 4.1), due to the higher electron-donor properties of the alkyl (**6**) than that exhibited by the bromide group (**7**).[22] In agreement with this electronic trend, the chemical shift of **11**, containing isothiocyanate ligands besides the two oxo groups showing all of them a significant electron-withdrawing character, is effectively shifted to high field (+125 ppm, entry 10 in Table 4.1).

Concerning the complexes containing oxazoline ligands, the higher chemical shifts are observed for compounds **4** and **5** with neutral and anionic bis-oxazoline ligands respectively (*ca.* +136 ppm, entry 3, and +126.8 ppm, entry 4 Table 4.1). Compounds containing anionic ligands **A**, **H** and **I** displayed resonances at +67.5 for **1**) ppm, +49.9 ppm (for **9**), +53.9 ppm, (for **10**) (entries 1, 8 and 9 in Table 4.1) while the lowest chemical shifts were displayed by those compounds containing neutral oxazolinyl-pyridine ligands (-93.7 and -76 ppm for **8** and **16,** entries 7 and 14

respectively Table 4.1). This result is consistent with the higher electronic density of the molybdenum atom in **4** and **5** when compared to **8** and **16**. In relation to these two latter compounds, the chemical shift difference between them ($\Delta\delta$ = 17.7 ppm) could be explained by the presence of the oxo bridge group in the bimetallic complex **16** (formally replacing one of the isothiocyanate ligands in the monometallic compound **8**), leading to an increase of the electron density on the molybdenum atom. It is worth mentioning that the bipyridine **F** (4,4-ditertbutyl-2,2-bipyridine) and the oxazolinyl-pyridine **G** show similar electronic capabilities.

Close chemical shifts are found for bimetallic complexes **15** (containing **F**) and **16** (containing **G**) showing related structures (*ca.* −75 ppm for **15** and **16**, entries 13 and 14 in Table 4.1). For the heptacoordinated complexes **12** and **13**, the same electronic trend was found. The cyano derivative **12** shows the lowest chemical shift of the compounds considered here (−597.6 ppm, entry 11 in Table 4.1), whereas the chemical shift of the oxobis(peroxo) complex **13** containing weak electron-withdrawing groups is shifted to higher fields (−136.5 ppm, entry 12 in Table 4.1). Concerning the line width of the signals, the range of values is also wide. The full width values at middle height (FWMH) are in the range of 44 to 1491 Hz (Table 4.1).

In Figure 4.3, some selected spectra are showed in order to compare the signal broadening for different kind of complexes. Symmetrical environment around the metal, together with the presence of non-labile coordinated ligands, leads to narrow resonances, as those observed for complexes **6** (FWMH = 44Hz, entry 5 in Table 4.1) and **12** (FWMH = 51 Hz, entry 11 in Table 4.1). However for compounds showing similar structures like the bimetallic complexes **15** and **16**, narrower resonance is observed for **15** (FWMH = 146Hz, entry 13 in Table 4.1) than that corresponding to **16** (FWMH = 647 Hz, entry 14 in Table 4.1). This is probably due to the lower symmetry of the oxazolinyl-pyridine **G** (complex **16**) than that exhibited by the bipyridine derivative **F** (complex **15**). When the tridentated tris(pyrazolyl)borate is involved (complex **17**), the signal is also relatively broad (FWMH = 565 Hz, entry 15 Table 4.1) in agreement with a symmetry loss of ligand **J** upon coordination to the metal center. The main relaxation mechanism of ^{95}Mo is the electric quadrupole

relaxation. This effect depends on the magnitude of the electric field gradient around the ^{95}Mo nucleus. Thus, less symmetric molecules have shorter relaxation time and, consequently spectra with broader lines are obtained.[23] On the other hand, the broadening of the signals can point to the presence of isomers showing close chemical shifts. Therefore, when **9** and **10** are solubilized, two resonances are observed showing an important chemical shift difference between them ($\Delta\delta$ > 100 ppm, entries 8 and 9 in Table 4.1), due to the partial nitrogen de-coordination of the bidentated *N*,*O* oxazolinylphenolate ligand as shown in their ^{1}H NMR spectra.[6]

The ^{95}Mo resonance at high field (-58.5 and −60.7 ppm for **9** and **10** respectively; entries 8 and 9 in Table 4.1) is narrower than that observed at low field (+49.2 and +53.9 ppm for **9** and **10** respectively; entries 8 and 9 in Table 4.1). The broad signal (half height width of 1059 and 1491 Hz for **9** and **10**, respectively; entries 8 and 9 in Table 4.1) can be partly explained by the mixture of isomers obtained for each of these compounds containing the *N*,*O*-oxazolinylphenolate coordinated as a bidentated ligand, due to the three relative arrangements of the iminic nitrogen and the oxo groups around the metal atom. In addition, owing to the asymmetrical environment of the polyhedron (Δ and Λ disposition) each of these possibilities is in fact a pair of diastereomers;[6] therefore, six diastereomers are plausible formed showing close ^{95}Mo chemical shifts.

When the nitrogen atom is de-coordinated from the molybdenum atom, the number of diastereomers decreases, leading to narrow signals at −58.5 (**9**) and −60.7 (**10**) ppm with half-height widths of 152 and 99 Hz, respectively. This up-fielded shift is in agreement with the electron-donation decrease towards the molybdenum atom when the partial substitution of the oxazoline ligand by the solvent occurs. In order to check the isomeric composition at different temperatures, a VT NMR study in deuterated dichloromethane for **10** was carried out (193–298 K; for ^{1}H NMR spectra, see Figure 4.4) This analysis evidenced no significant isomeric distribution changes by both ^{1}H and ^{95}Mo NMR (Figure 4.5). It is important to note that even using a non-coordinating solvent (like dichloromethane), the partial de-coordination of the ligand takes place. Concerning the ^{95}Mo NMR spectra at low temperature (243 K), the

broadening of the resonance at low field could be related to an internal motion decrease, leading to a less symmetric environment around the metallic center for the isomers formed.

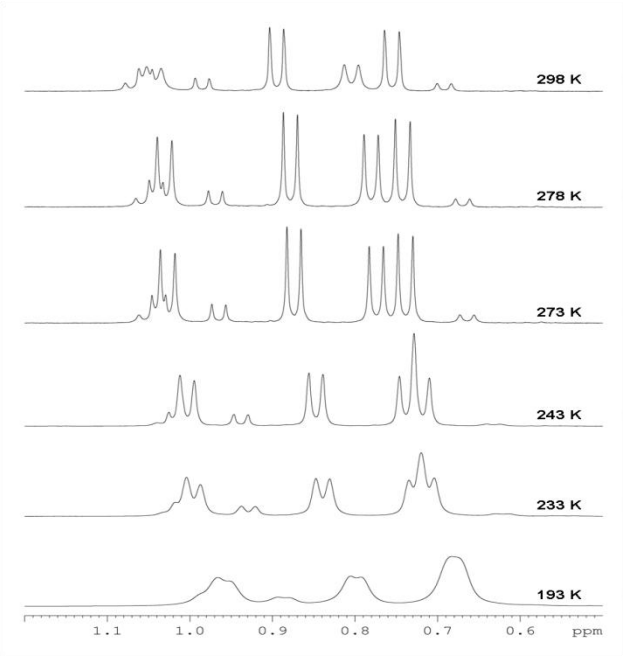

Figure 4.4. Methyl region of ^{1}H NMR (400 MHz, CD_2Cl_2) spectra of **10** recorded at different temperatures (193-298 K).

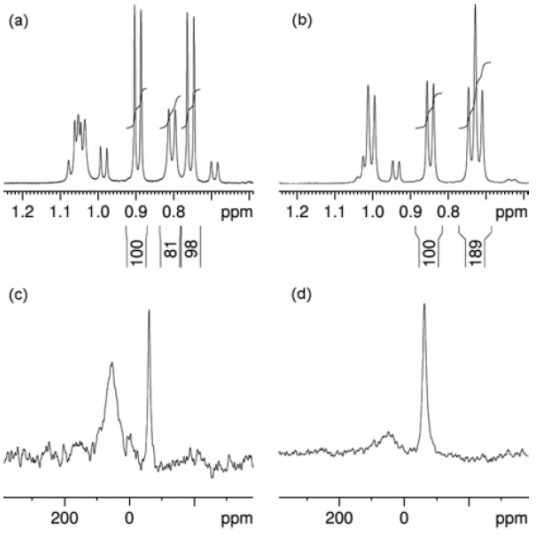

Figure 4.5. ^{1}H (400 MHz, (a) and (b)) and ^{95}Mo (26.08 MHz, (c) and (d)) NMR spectra of **10** in deuterated dichloromethane: (a) and (c) recorded at 298 K; (b) and (d) at 243 K.

4.3.2. Application of ^{95}Mo NMR to a coordination study

A previous work of monometallic dioxomolybdenum(VI) complexes containing hemi-labile anionic oxazolinyl-phenolate ligand like **H** and **I**[5] showed that the high activities produced in olefin epoxidations (olefin = cyclooctene and (*R*)-limonene) can be attributed to the partial de-coordination of the chiral ligand, losing the possibility to induce asymmetry in the epoxidation process.[5] In contrast, the presence of robust spectator ligands like oxazolinyl-pyridine **G**, leads to less active catalysts.[8] Therefore **13** is less active than **10** for both olefins (for cyclooctene: 15% versus 95% conversion; for (*R*)-limonene: 22% versus 79% conversion). Among the bimetallic-based catalytic systems **14**, **16** and **17**, all of them containing inert ligands (**E =** 2,2'-bipyridine, **G** = an oxazolinyl-pyridine and **J** = a tris(3,5-dimethylpyrazol-1-yl)borate, respectively), **16** was the most active system, while **17** was completely inactive for both olefins (for cyclooctene epoxidation: 17%, 36%, and 0% conversion for **14**, **16** and **17** respectively; for (*R*)-limonene epoxidation: 24%, 64%, and 0% conversion for **14**, **16** and **17** respectively). The tremendous difference observed between **16** and **17** is associated to the lack of labile positions in **17**, in contrast to **16**, which contains a coordination position occupied by an isothiocyanate group. However the difference in activity observed for **14** and **16**, coordinated to **G** and **E**, respectively, can be associated to the higher π-acceptor ability of 2,2'-bipyridine **E** than the oxazolinyl-pyridine **G**, leading to a lability decrease for the isothiocyanate group and consequently a lesser catalytic activity for **14**. The activity trends observed for the different catalytic systems studied point to the requirement of both a labile position on the coordination metallic sphere in order to be active and the presence of a robust chiral ligand to induce asymmetry in the catalytic process. Comparing the catalytic activity of the bimetallic complex **16** and the monometallic complex **13** in (*R*)-limonene epoxidation, catalyst **16** has superior activity and selectivity (50% vs 20 % conversion for **16** and **13** respectively) (*trans*/*cis*-*endo* epoxide = 4/1 for **16** and 1/1 for **13**, see Scheme 4.1). This behavior can be explained by the inertness of complex **13** due to the non-labile ligands around the metal center, and probably the partial de-coordination of **G** during the catalytic reaction makes the system active.

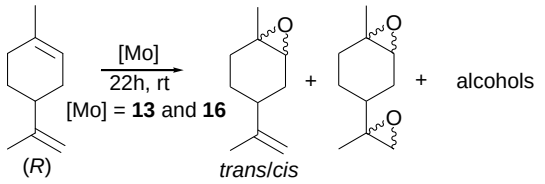

Scheme 4.1. (*R*)-limonene epoxidation catalyzed by **13** and **16** using TBHP as oxidant.

In contrast, the bimetallic complex **16** contains a labile ligand (isothiocyanate) and a robuts ligand **G**, inducing diastereoselectivity in the (*R*)-limonene epoxidation. This selectivity induction seems to be plausible when the olefin is coordinated to the metal. Attempts to isolate complexes derived from **16** containing cyclooctene or limonene, in the presence of silver hexafluorophosphate, were unsuccessful, only observing the precipitation of AgNCS. Conductivity measurements of **16** in the presence of a large excess of (*R*)-limonene (Λ_M = 80 cm^{-1} mol^{-1} Ω^{-1}) or pyridine (Λ_M = 102 cm^{-1} mol^{-1} Ω^{-1}) in acetonitrile showed the formation of 1:1 electrolytes. In contrast, in neat acetonitrile, the conductivity was lower (Λ_M = 20 cm^{-1} mol^{-1} Ω^{-1}), showing the formation of ionic species but in low concentration. These data are in agreement with the substitution of one isothiocyanate group by the olefin or pyridine.

In a previous work, the ^{95}Mo NMR technique was used to evidence the formation of molybdenum intermediate species formed upon treatment of **16** (Figure 4.6) with olefin.[8,24] After addition of one equivalent of (*R*)-limonene to a solution of complex **16** in $CDCl_3$, a new signal appeared at down field (-77 ppm) in relation to the neat complex (-93 ppm), increasing in intensity with time. The signals were attributed to a bimetallic Mo species containing two different molybdenum atoms, one coordinated to the olefin (-77 ppm), and the other one to the isothiocyanate group (-93 ppm); the deshielding observed is due to an electronic density increase at the molybdenum atom probably due to the coordination of the olefin to the metal center favored by the dissociation of the isothiocyanate ligand. This study demonstrates that ^{95}Mo NMR technique represents a useful tool for structural studies and also, for helping to elucidate catalytic mechanisms.

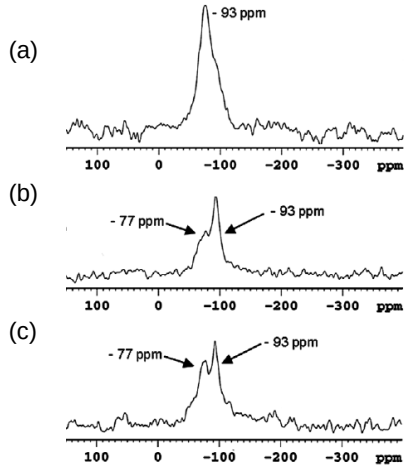

Figure 4.6. ^{95}Mo NMR spectra ($CDCl_3$, 26.08 MHz): (a) complex **16**; (b) **16** + (*R*)-limonene, after 15 min of the olefin addition; (c) **16** + (*R*)-limonene after 48 h of the olefin addition (results from ref. [8,24]).

4.4. Conclusions

In this work, we could prove the efficiency of the ^{95}Mo NMR as a tool to get information about the behavior of oxomolybdenum(VI) complexes in solution. The detailed study of 16 molybdenum compounds containing mono- and polydentated coordinated ligands showing different electron-donor nature, has permitted to establish a chemical shift scale depending on the ligand donor-electronic characteristics and consequently to look into the electronic density on the metal atom. From a structural point of view, the analysis of the resonance width leads to the discussion of the symmetry environment around the metal atom and the presence of isomers in solution. What is more important, the research described here has evidenced the convenience of the ^{95}Mo NMR to obtain structural information about catalytic intermediates, a key aspect for mechanistic studies in solution, as shown in the coordination of (*R*)-limonene to the bimetallic complex **16**.

4.5. Acknowledgments

The authors thank CNRS, Université Paul Sabatier (Actions Ponctuelles de Coopération grant for HT) and Fundação para a Ciência e Tecnologia (doctoral grant SFRH/BD/30917/2006 for JAB) for financial support.

4.6. References

1 R. H. Holm, *Coord. Chem. Rev*., 1990, **100**, 183-221.

2 (a) B. Cornils, W. A. Herrmann *Applied Homogeneous Catalysis with Organometallic Compounds*, Eds:, Wiley-VCH: Weinheim, 2nd edition, 2002, vol. 1, pp 412-426; (b) For organometallic Mo(VI) derivatives, see: F. E. Kühn, A. M. Santos, M. Abrantes, *Chem. Rev*., 2006, **106**, 2455-2475.

3 (a) M. N. Sheng, Zajaczek (Arco), GB 1.136.923, 1968; (b) J.Kolar (Halcon), US 3.350.422, US3.351.635, 1967.

4 (a) H. Mimoun, *Angew.Chem. Int. Ed. Engl*., 1982, **21**, 734-750; (b) K. B. Sharpless, J. M. Townsen, D. R. Williams, *J. Am. Chem. Soc.,* 1972, **94**, 295-296; (c) K. A. Jørgensen, R. Hoffmann, *Acta Chem. Scand., Ser. B,* 1986, **40**, 411-419; (d) P. Macchi, A. J. Schultz, F. K. Larsen, D. B. Iversen, *J. Phys. Chem. A*, 2001, **105**, 9231-9242.

5 J. A. Brito, M. Gómez, G. Muller, H. Teruel, J. C. Clinet, E. Duñach, M. A. Maestro, *Eur. J. Inorg. Chem*., 2004, 4278-4285.

6 M. Gómez, S. Jansat, G. Muller, G. Noguera, H. Teruel, V. Moliner, E. Cerrada, M. Hursthouse, *Eur. J. Inorg. Chem*., 2001, 1071-1076.

7 M. Minelli, J. H. Enemark, R. T. C. Brownlee, M. J. O'Connor, A. G. Wedd, *Coord. Chem. Rev*., 1985, **68**, 169-278.

8 J. A. Brito, H. Teruel, G. Muller, S. Massou, M. Gómez, *Inorg. Chim. Acta*. 2008, **361**, 2740-2746.

9 J. A. Brito, S. Ladeira, E. Teuma, B. Royo, M. Gómez, *Appl. Catal. A: General*, 2011, **398**, 88–95.

10 J. A. Brito, N. Saffon, M. Gómez, B. Royo, *Curr. Inorg chem*., accepted.

11 (a) V. K. Aggarwal, L. Bell, M. P. Coogan, P. Jubault, *J. Chem. Soc. Perkin Trans*., 1998, **11**, 2037-2042; (b) K. Hallman, A. Frölander, T. Wondimagegn, M. Svensson, C. Moberg, PNAS, 2004, 101, 5400-5404; (c) K. A. Nolin, R. W. Ahn, D. Toste, *J. Am. Chem. Soc.* 2005, **127**, 12462-12463.

12 E. J. Corey, Z. Wang, *Teaahedron Lett*., 1993, **34**, 4001-4004.

13 G. Balavoine, J. C. Clinet, I. Lellouche, *Tetrahedron Lett*., 1989, **30**, 5141-5144.

14 H. Arzoumanian, G. Agrifoglio, H. Kretzein, M. Capparelli, *J. Chem. Soc., Chem. Commun*., 1995, 655-656.

15 H. Arzoumanian, R. López, G. Agrifoglio, *Inorg. Chem.,* 1994, **33**, 3177-3179.

16 H. Arzoumanian, J. F. Pétrignani, M. Pierrot, F. Ridouane, J. Sánchez, *Inorg. Chem*., 1988, **27**, 3377-3381.

17 H. Arzoumanian, R. Bakhtchadjian, G. Agrifoglio, H. Kretzien, J. C. Daran, Eur. *J. Inorg. Chem.*, 1999, 2255-2259.

18 G. N. Schrauzer, L. A. Hughes, E. O. Schlemper, F. Ross, D. Ross, *Organometallics*, 1983, **2**, 1163-1166.

19 E. O. Schlemper, G. N. Schrauzer, L. A. Hughes, *Polyhedron*, 1984, **3**, 377-.

20 H. Teruel, A. Sierralta, *Polyhedron,* 1996, **15**, 2215-2221.

21 H. Teruel, A. Sierralta, *J. Mol. Catal.*, *A: Chemical*, 1996, **107**, 379-383.

22 For dioxo-dihalo molybdenum compounds containing diimine ligands, ^{95}Mo chemical shifts are also comprise in the range 207–265 ppm: F. E. Kühn, A. D. Lopes, A. M. Santos, E. Herdtweck, J. J. Haider, C. C. Romão, A. G. Santos, *J. Mol. Catal. A: Chemical*, 2000, **151**, 147-160.

23 R. T. C. Brownlee, M. J. O'Connor, B. P. Shehan, A. G. Wedd, *J. Magn. Reson.*, 1985, **61**, 516-525.

24 This ^{95}Mo NMR study was part of a previous work carried out in the Universitat de Barcelona under the supervision of Prof Montserrat Gómez and it is only showed here as an example of the useful tool that represents ^{95}Mo NMR.

Chapter 5 APPLICATIONS OF CHIRAL OXOMOLYBDENUM(VI) COMPLEXES IN CATALYSIS

This chapter originated the following publications:

J. A. Brito, N. Saffon, M. Gómez, B. Royo
Curr. Inorg. Chem., 2011, *Accepted*.
J. A. Brito, S. Ladeira, E. Teuma, B. Royo, M. Gómez
Appl. Catal. A: General, 2011, **398**, 88–95.

Summary

The new molybdenum complexes **1**-**5** (Figure 5.1) were found to be efficient catalysts in olefin epoxidation reactions affording high activities and good chemoselectivity. These monometallic complexes (**1** and **3**-**5**), together with the bimetallic system **16** previously prepared in our group, were used as catalytic precursors in the epoxidation of cyclooctene, (*R*)-limonene, and *trans*-β-methylstyrene in organic medium as well in imidazolium- and pyrrolidinium-based ionic liquids. They exhibited high chemoselectivity towards the epoxide formation, mainly for cyclooctene and (*R*)-limonene epoxidation, without formation of the corresponding diols. In [BMP][NTf_2] (BMP = butyl methyl pyrrolidinium; NTf_2 = bis(trifluoromethanesulfonyl)amide), complex 1**6** exclusively gave *trans*-(*R*)-limonene 1,2-epoxide, while monometallic catalytic systems led to a mixture of *trans- and cis*-(*R*)-limonene 1,2-epoxide. ^{95}Mo NMR studies helped to understand the different catalytic behavior of 1**6** and **4** in ionic liquid medium.

With the aim to explore the effect of ionic liquids in allylic substitutions, the chiral ligands **A** and **C** were preliminary tested in different Pd-catalyzed allylic substitution reactions in pyrrolidinium-based ionic liquid.

The work described in this chapter was entirely performed by the candidate except for the ^{95}Mo NMR spectra which were performed by Marc Vedrenne from University Paul Sabatier (Toulouse, France).

5.1. General introduction

Epoxides represent useful intermediates for the synthesis of fine chemicals including drugs and fragrances.[1] High-valent oxo-metal complexes have found applications as efficient catalysts for oxidation processes under homogeneous as well as heterogeneous conditions.[2] In particular, molybdenum systems are commercially applied to the production of propylene oxide using alkyl hydroperoxides as oxidants.[3] With the aim to overcome the metal leaching using homogeneous catalysts, several methodologies have been developed in order to immobilize the

catalyst and reuse them without loss of catalytic efficiency. One of these approaches consists in the use of biphasic systems to preserve the homogeneous advantages of the catalysts.[4] Ionic liquids (ILs) solvents, exhibiting negligible vapor pressure, thermal stability and high polarity, being their physico-chemical properties easily tuneable depending on the nature of the ions involved, turn into a convenient substitute to volatile organic solvents and a suitable medium to immobilize the catalyst.[5] These features confer them a wide number of applications in organic synthesis, mainly in catalysis.[6] IL phase containing the active catalyst could be readily reused without significant loss of catalytic activity,[7] fact particularly interesting for asymmetric catalysis, due to the high added value of the chiral catalysts.[8] The pioneering work in this field was published by Chauvin and co-workers in 1995, concerning the use of *N*,*N*'-dialkylimidazolium salts in biphasic catalysis for Rh-catalyzed olefin hydroformylation, isomerisation and asymmetric hydrogenation, demonstrating the feasibility to recover the catalyst.[9] However, the first works using neat ILs appeared later, in 2000, when Song's team reported that *N*,*N*'-dialkylimidazolium derivatives could be appropriated solvents to perform enantioselective alkene epoxidations[10] and ring opening of epoxides.[11] Although many applications in metal-catalyzed organic transformations have been reported in the last two decades as stated by the literature mentioned above, few reports have been published concerning the olefin epoxidation catalyzed by oxomolybdenum complexes in ionic liquid medium, being imidazolium-based ionic liquids (Im-ILs) the solvents of choice for the most studies. The first article was published in 2004 by A. A. Valente and co-workers where cyclooctene epoxide was obtained in several imidazolium-based ionic liquids using dioxomolybdenum(VI) complexes as catalytic precursors, getting a better catalyst recycling for that containing a tridentate amine.[12] F. E. Kühn, C. C. Romão and co-workers evaluated the catalytic behavior of cyclopentadienyl-molybdenum complexes for cyclooctene epoxidation in Im-ILs, demonstrating the importance of the anion nature in the subsequent ring opening giving the corresponding diol.[13] The catalytic activity could be improved and the selectivity tuned using cyclopentadienyl ansa-bridged molybdenum complexes in the appropriate Im-IL.[14] Under microwave-assisted heating in [BMI][BF_4], cyclopentadienyl molybdenum complexes led to the exclusive formation of olefin

epoxide.[15] Recently F. Montilla, A. Galindo and co-workers have studied olefin epoxidation catalyzed by oxodiperoxo- and dioxoperoxo-molybdenum(VI) complexes in Im-ILs using urea-epoxide and hydrogen peroxide as oxidants.[16] Oxodiperoxomolybdenum(VI) complexes have also become active in the epoxidation of oleate derivatives using hydrogen peroxide as oxidant in Im-ILs, being reused up to five consecutive runs with slight loss of activity.[17] With the aim to improve the immobilization of the catalyst in the ionic liquid phase, R. Poli, C. Bibal and co-workers have used Mo(VI) complexes containing Schiff base ligands tagged with sulfonated groups, but after the third recycling the activity considerably decreases.[18] Different molybdenum precursors have been recently applied in olefin epoxidation using Im-ILs and 1-butyl-4-methylpyridinium tetrafluoroborate, without observing remarkable differences between both kind of ILs.[19] To the best of our knowledge, only heterogenized oxomolybdenum complexes onto supports such as mesoporous silicates[20] have led to reasonable recycling although somewhat activity loss is observed comparing with the corresponding homogenous systems.[21] Concerning enantioselective epoxidation in ILs, only two contributions have been reported up to now (involving imidazolium and pyridinium derivatives), using a dioxomolybdenum(VI) complex containing a chiral tetradentate bis(oxazoline) ligand[22] and an aminoacid-pendant arm-cyclopentadienylmolybdenum(II) complex,[23] but asymmetric induction could not be achieved in any case.

Based on previous experience with oxomolybdenum complexes containing oxazoline ligands in epoxidation of olefins in organic solvents,[24,25] it was planned to study the performance of this type of complexes in olefin epoxidation reactions in ionic liquid medium. The bimetallic complex **16** (Figure 5.2) was previously described as an efficient catalyst for cyclooctene epoxidation and what is more interesting, leading to an important diastereomeric induction for the epoxidation of (*R*)-limonene.[25] Besides this system containing a bidentated oxazolinyl-pyridine ligand (**G**) (Figure 5.2), we have employed the two new dioxomolybdenum complexes containing tridentate oxazolinyl-pyridine **A** and bis(oxazoline) **C** ligands, complexes **1** and **4** respectively (Figure 5.1) synthesized in this thesis. In addition to Im-ILs, we have used for the first

time in these processes pyrrolidinium-based ILs as solvents in order to study the influence of the nature of the ionic liquid in the catalytic process.

Pd-catalyzed asymmetric allylic substitution has been intensely investigated over the last decade.[26] Besides a high level of asymmetric induction, the advantages of this process include the tolerance of a wide range of functional groups and a great flexibility in the type of bonds that can be formed, for example, C-C, N-C, P-C or O-C bonds. However, catalyst recycling is also of major concern in asymmetric allylic substitution reactions. There are few examples of application of ionic liquid in this type of reactions.[27] A significant increase in enantioselectivity has been observed in ILs compared to organic solvents.[28] The enantioselectivity has been preserved after few runs, however a decrease in product yield after consecutive runs continues to be one of the main problems. With the aim to explore the potential application of oxazoline ligands **A** and **C** in allyllic substitution reactions using ionic liquids as solvent, some preliminary catalytic studies were performed.

5.2. Experimental part

5.2.1. General

All syntheses and manipulations were performed using standard Schlenk techniques under an argon atmosphere. The ionic liquids [BMI][PF_6] 99.5%, [BMI][NTf_2] 99% and [BMP][NTf_2] 99% were purchased from Solvionic and heated at 70 °C under vacuum overnight before use. *tert*-Butylhydroperoxide (TBHP) was purchased from Aldrich as *ca*. 5.5 M solution in *n*-decane over molecular sieves. [MoO_2Cl_2] and cyclooctene were purchased from Aldrich, (*R*)-limonene from Sigma-Aldrich and *trans*-β-methylstyrene from Acros Organics. H_2O_2 (aq) (30 %) was purchased from VWR Prolabo. Ligands **C**,[29] **G**[30] and complex **16**[25a] were obtained following the procedures previously described. GC routine analyses were carried out using a Perkin Elmer Clarus 500 gas chromatograph (25 m × 0.32 mm methyl siloxane with 5% of phenyl siloxane (BPX5 column) with a FID detector and Perkin Elmer Clarus 5605 mass spectrometer. For epoxidation reactions, enantiomeric excesses were determined by HPLC at 25 °C on a Waters Alliance 2695 HPLC separation module

with a Waters 996 PDA detector. For allylic alkylation and allylic phosphination reactions, enantiomeric excesses were determined on PIC solution Supercritical fluid chromatography SFC with a UV PDA detector at 35 °C. ICP-MS were done by an independent analytical laboratory (Antellis) from Toulouse (France).

5.2.2. General procedure for epoxidation experiments in organic solvent

The catalytic reactions were performed in a reaction vessel equipped with a magnetic stirrer and immersed in an oil bath at the appropriate temperature. The molybdenum catalytic precursor (0.01 mmol of Mo: 4.0 mg for **1**; 3.8 mg for **2**; 6.2 mg for **3**; 6.2 mg for **4**; 4.3 mg for **5**) was dissolved in 2 mL of solvent ($CHCl_3$ when the oxidant used was a solution of *tert*-butylhydroperoxide in *n*-decane (TBHP) and EtOH when H_2O_2 was used as oxidant). 1 mmol of olefin (110 mg for cyclooctene; 136 mg for (*R*)-limonene; 136 mg for *trans*-β-methylstyrene) was then added, followed by a *ca*. 5.5 M *tert*-butylhydroperoxide solution in *n*-decane over molecular sieves (or 0.36 mL; 2.00 mmol) of H_2O_2 (30%)). The mixture was then stirred for a period of time depending on the epoxidation reaction. The catalytic mixture was then quenched by addition of MnO_2 and Na_2SO_4 in order to destroy peroxides and remove water, and filtered through Celite. Analyses of organic products were performed by gas chromatography.

5.2.3. General procedure for epoxidation experiments in ionic liquid as solvent

The molybdenum catalytic precursor (0.01 mmol of Mo: 4.0 mg for **1**; 6.2 mg for **4**; 0.025 mmol of Mo: 11.6 mg for 1**6**) was dissolved in 1 mL of ionic liquid ([BMI][PF_6], [BMI][NTf_2] or [BMP][NTf_2]) and CH_2Cl_2 (2.5 mL for [BMI][PF_6] and 1.5 mL for [BMI][NTf_2] and [BMP][NTf_2]). 1 mmol of olefin (110 mg for cyclooctene; 136 mg for (*R*)-limonene) was then added, followed by a *ca*. 5.5 M *tert*-butylhydroperoxide aqueous solution (for **1** and **4**, 0.36 mL, 2.00 mmol; for 1**6**, 0.27 mL, 1.50 mmol). After reaction, several solvent extractions were performed with diethyl ether (14x1 mL). 0.5 mL of the extracted sample was then quenched by addition of MnO_2 and Na_2SO_4 in order to destroy peroxides and remove water, and then diluted with diethyl

ether (up to 1.5 mL). The resulting slurry was then filtered on Celite and eluted with diethyl ether. Analyses of organic products were performed by gas chromatography.

5.2.4. General procedure for the recycling of the catalyst in ILs

The epoxidation was performed under the same reaction conditions as described in section 5.2.3. The upper organic phase was separated and the IL phase was extracted with ether (14x1 mL). The collected organic layers were assembled and injected into the GC to evaluate the cyclooctene conversion. The IL phase was then dried under vacuum for 2 h to remove traces of ether and *t*BuOH formed in the catalytic run. The IL phase was reused in the consecutive cycle with a new charge of cyclooctene and TBHP as it was in the first cycle. The same extraction procedure was re-applied for each consecutive cycle.

5.2.5. General procedure for Pd-catalyzed allylic substitutions.

Pd-catalyzed allylic alkylation: The ligand (0.0125 mmol of oxazoline: 3.0 mg for **A**; 5.3 mg for **C**) and $[Pd(\eta^3\text{-}C_3H_5)(\mu\text{-}Cl)]_2$ (0.01 mmol, 2.0 mg) were dissolved in 1 mL of [BMPy][NTf_2] and stirred for 30 min. *rac*-3-Acetoxy-1,3-diphenylpropene (0.5 mmol, 126 mg) followed by dimethylmalonate (1.5 mmol, 198 mg) and [*N*,*O*-bis (trimethylsilyl)acetamide] BSA (1.5 mmol, 305 mg) were then added. The reaction mixture was stirred for 8h at 40 °C. The reaction was extracted with pentane (10x1mL), the sample was filtered through SiO_2, and the solvent was evaporated under reduced pressure. The conversion was determined by ^1H NMR and the enantiomeric excesses were determined by SFC on an AD-H column 20 % MeOH at 35 ºC; 4 mL/min pressure out 100 bar CO_2 using *t*BuOH as solvent.

Pd-catalyzed allylic phosphination: The ligand (0.0125 mmol of oxazoline, 5.3 mg for **C**) and $[Pd(\eta^3\text{-}C_3H_5)\text{-}(\mu\text{-}Cl)]_2$ (0.0076 mmol, 1.52 mg) were dissolved in 1 mL of [BMPyr][NTf_2]. *rac*-3-Acetoxy-1,3-diphenyl-1-propene (0.151 mmol, 38 mg) dissolved in 0.2 mL of CH_2Cl_2 was then added and the mixture was stirred for 30 min under reduced pressure to remove the CH_2Cl_2. Diphenyl phosphine $HPPh_2$ (0.151 mmol, 28 mg) was then added at 40 ºC and the mixture stirred for 48 h. The product was

then extracted with ether (5x1 mL) and S_8 was added. The mixture was stirred 30 min at room temperature, filtered and the solvent removed under reduced pressure. The samples were analyzed by ^{1}H and ^{31}P NMR. Enantiomeric excesses were determined by SFC on a Chiralcel AD-H column, MeOH 15% as eluent, at 35 ºC in a flow of 4 cm^3/min under 100 bar CO_2.

Pd-catalyzed allylic sulfonylation: The ligand (0.0125 mmol of oxazoline, 3.0 mg for **A**; 5.3 mg for **C**) and $[Pd(\eta^3\text{-}C_3H_5)\text{-}(\mu\text{-}Cl)]_2$ (0.01 mmol, 2 mg) were dissolved in 1 mL of [BMPyr][NTf_2] and stirred for 30 min. *rac*-3-Acetoxy-1,3-diphenyl-1-propene (0.5 mmol, 126 mg) dissolved in 0.2 mL of CH_2Cl_2 was added, followed by *p*-toluene sulfonic acid sodium salt (0.7 mmol mg, 125 mg) and the mixture was stirred at 100 ºC for 24 h. The reaction was extracted with pentane (10x1 mL), the sample was filtered through SiO_2, and the solvent evaporated under reduced pressure. The conversion was determined by ^{1}H NMR.

Pd-catalyzed allylic amination: Ligand **C** (0.0125 mmol, 5.3 mg) and $[Pd(\eta^3\text{-}C_3H_5)\text{-}(\mu\text{-}Cl)]_2$ (0.01 mmol) were dissolved in 1 mL of [BMP][NTf_2] and stirred for 30 min at 40 ºC. *rac*-3-Acetoxy-1,3-diphenyl-1-propene (0.5 mmol, 126 mg) dissolved in 0.2 mL of CH_2Cl_2 was added followed by benzylamine (0.7 mmol, 75 mg). The mixture was stirred at 100 ºC for 24 h and then extracted with pentane (10x1 mL), filtered through SiO_2, and the solvent evaporated under reduced pressure. The conversion was determined by ^{1}H NMR. Enantiomeric excesses were determined by SFC on a Chiralcel OJ-H column, MeOH 30% and 0.3% DEA as eluent, at 40 ºC in a flow of 4 cm^3/min under 100 bar CO_2.

5.3. Catalytic Studies in Olefin Epoxidation

5.3.1. Catalytic Studies in Olefin Epoxidation in organic solvent

Complexes **1**-**3** and **5** (Figure 5.1) were tested as catalysts for olefin epoxidation using *cis*-cyclooctene, (*R*)-limonene and *trans*-β-methylstyrene as substrates, and

tert-butyl hydroperoxide (TBHP in *n*-decane) as oxidant in chloroform at 55 °C (Scheme 5.1)

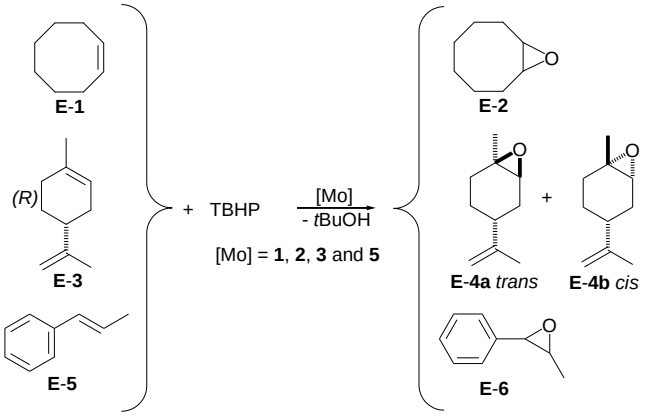

Scheme 5.1. Mo-catalyzed olefin epoxidation in organic solvent.

The formation of the corresponding epoxides was analyzed by GC. As shown in Table 5.1, complexes **1**-**3** and **5** were efficient catalysts towards oxidation of cyclooctene affording quantitative conversion towards the corresponding epoxide. Comparing the activity of complexes **1** and **5**, both containing oxazoline-based ligands, higher activity was achieved by **1**, giving quantitative conversion of the epoxide in 30 min with a turnover frequency (TOF) of 469 h^{-1} (calculated at 10 min). Catalysts **1** and **2** exhibited identical activity (entries 1 and 3, Table 5.1) , indicating that the μ-oxo bimetallic dimer **2** and the monometallic **1** are readily converted to a common active species. Similar results were described by Finney and co-workers.[31] Complex **3** bearing the pyridino amido ligand led to the best TOF (6125 h^{-1}, calculated at 10 min) without observing any induction period (entry 4, Table 5.1).

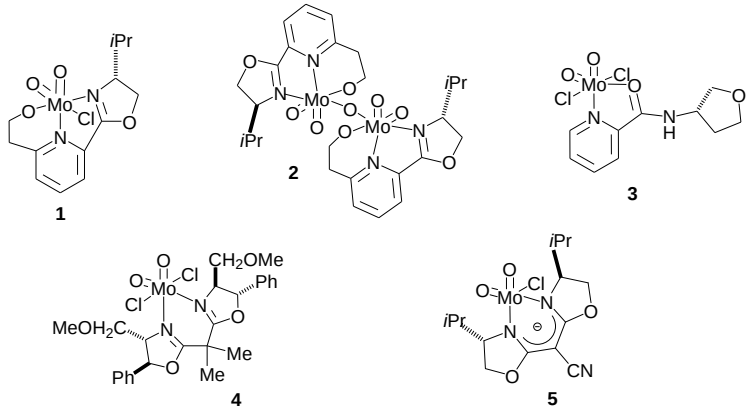

Figure 5.1. Molybdenum complexes **1**-**5** applied in olefin epoxidations using $CHCl_3$ as solvent.

Complexes **1**, **3** and **5** were also active using H_2O_2 as oxidant; the epoxidation of cyclooctene with H_2O_2 (30% in water) carried out in EtOH afforded moderate yield of the corresponding epoxide in a selective manner with the three catalysts (entries 2, 5 and 7, respectively in Table 5.1). However, no further conversion of cyclooctene was observed after 24 h of reaction, indicating low stability of the catalysts under the reaction conditions. This study was further extended to the catalytic epoxidation of (*R*)-limonene with TBHP under similar conditions. All complexes displayed good activity achieving quantitative conversions towards 1,2-(*R*) limonene epoxide in few hours (entries 8-10, Table 5.1). However, no diastereoisomeric induction of (*R*)-limonene took place even lowering the temperature at 25 °C. Next, we investigated the epoxidation of *trans*-β-methylstyrene, a model substrate for *trans*-olefins, in order to explore the capability of these catalytic precursors to promote asymmetric induction. Quantitative formation of the corresponding epoxide was formed in nearly racemic mixture (≤6% ee) when complex **1** was used as catalyst (entry 11, Table 5.1).

Table 5.1. Olefins epoxidation catalyzed by complexes **1**-**3**, **5**.[a]

Entry	Catal.	Olefin	Oxidant/solvent	t (h)	Yield(%)[b]	*trans*/*cis* (%)
1	**1**	cyclooctene	TBHP/$CHCl_3$	1	100	-
2	**1**	cyclooctene	H_2O_2/EtOH	22	42	-
3	**2**	cyclooctene	TBHP/$CHCl_3$	1	100	-
4	**3**	cyclooctene	TBHP/$CHCl_3$	0.33	99	-
5	**3**	cyclooctene	H_2O_2/EtOH	16	50	-
6	**5**	cyclooctene	TBHP/$CHCl_3$	3	96	-
7	**5**	cyclooctene	H_2O_2/EtOH	22	32	-
8	**1**	(*R*)-limonene	TBHP/$CHCl_3$	1	94	52/48
9	**3**	(*R*)-limonene	TBHP/$CHCl_3$	0.33	99	50/50
10	**5**	(*R*)-limonene	TBHP/$CHCl_3$	3	91	51/49
11	**1**	*trans*-β-methylstyrene	TBHP/$CHCl_3$	4	83	-
12	**3**	*trans*-β-methylstyrene	TBHP/$CHCl_3$	1	60	-
13	**5**	*trans*-β-methylstyrene	TBHP/$CHCl_3$	4	28	-

[a] Results from dupliclated reactions. All reactions were carried out using a catalyst:substrate:oxidant ratio 1:100:200 in $CHCl_3$ when TBHP is used as oxidant and in EtOH for H_2O_2 at 55 **º**C, unless otherwise stated. [b] Conversion determined by GC.

No improvement in the enantioselectvity was observed by either lowering the reaction temperature or using toluene as solvent instead of chloroform. For

complexes **3** and **5**, no asymmetric induction was obtained even at low conversions (entries 12 and 13, Table 1). However, in all cases the catalytic reaction was chemoselective, exclusively leading to the corresponding epoxide.

5.3.2. Catalytic studies in olefin epoxidation in ionic liquid

Olefin epoxidations (cyclooctene, (*R*)-limonene and *trans*-β-methylstyrene) using *tert*-butylhydroperoxide (TBHP) in *n*-decane as oxidant, were also carried out in ionic liquids, in the presence of catalysts, **1**, **4** and **16** (Figure 5.2); for comparative purposes, reactions in dichloromethane were also evaluated. Complexes **1**, **4**, and **16** and TBHP were soluble in all the solvents tested; olefins were immiscible in the three ionic liquids tested, [BMI][PF_6], [BMI][NTf_2] and [BMP][NTf_2] (BMI = 1-butyl-3-methyl-imidazolium; BMP = butyl methyl pyrrolidinium; NTf_2 = bis(trifluoromethanesulfonyl)amide). Cyclooctene epoxidation was chosen as benchmark reaction in order to compare the activity of complex **16** in different media (Scheme 5.2). In all cases, the olefin was exclusively converted into cyclooctene epoxide without observing the formation of by-products (Table 5.2).

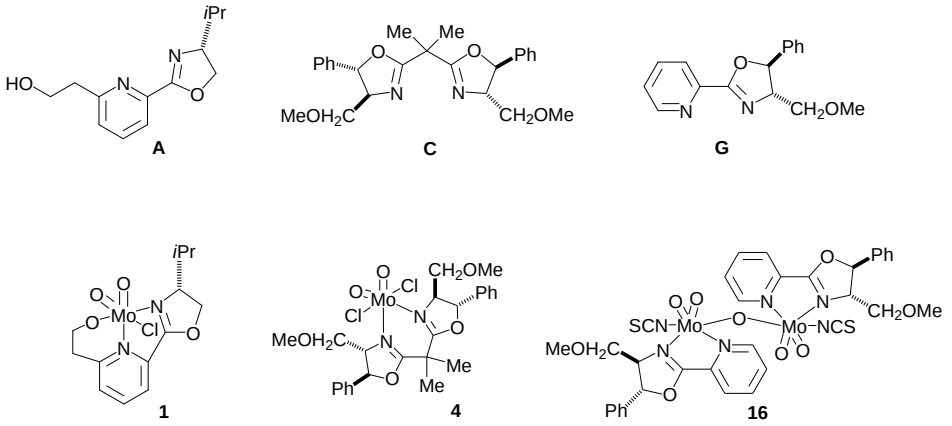

Figure 5.2. Oxazoline-based ligands (**A**, **C** and **G**) and their corresponding dioxomolybdenum(VI) complexes (**1**, **4** and 1**6**).

Under the same catalytic conditions, higher activity was observed in dichloromethane than in the neat ionic liquids, [BMI][PF_6], [BMP][NTf_2] and

[BMI][NTf_2] (entries 1-4, Table 5.2), probably due to phase transfer limitations because cyclooctene is immiscible with these ionic liquids.

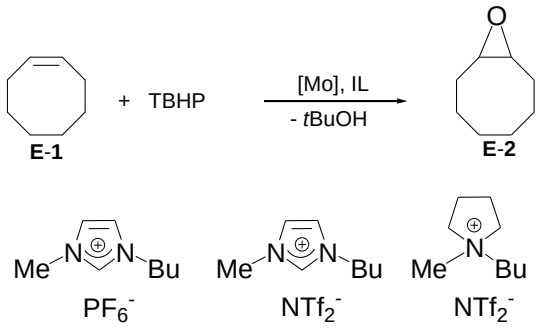

Scheme 5.2. Mo-catalyzed cyclooctene epoxidation in different ionic liquids, [BMI][PF_6], [BMI][NTf_2] and [BMP][NTf_2].

When the reaction was carried out in the presence of dichloromethane as co-solvent (addition of the necessary amount in order to get one single phase), the activity in IL/CH_2Cl_2 was slightly higher than that observed in dichloromethane (entries 1 vs 5, 7 and 9, Table 5.2). Comparing imidazolium-based IL containing two different anions, PF_6 and NTf_2, no remarkable differences were observed (entries 5 and 9, Table 5.2), in contrast to the benefit effect previously reported using [BMI][NTf_2].[13,32]

Table 5.2. Cyclooctene epoxidation catalyzed by bimetallic dioxomolybdenum complex **16** in different solvents.[a]

Entry	Solvent	Co-solvent	T (°C)	Oxidant	Conv.(%)[b]
1	CH_2Cl_2	-	40	TBHP	78
2	[BMI][PF_6]	-	55	TBHP	42
3	[BMP][NTf_2]	-	55	TBHP	63
4	[BMI][NTf_2]	-	55	TBHP	72
5	[BMI][PF_6]	CH_2Cl_2[c]	55	TBHP	85
6	[BMI][PF_6]	CH_2Cl_2[d]	40	TBHP	74
7	[BMP][NTf_2]	CH_2Cl_2[d]	55	TBHP	90
8	[BMP][NTf_2]	CH_2Cl_2[d]	40	TBHP	68
9	[BMI][NTf_2]	CH_2Cl_2[d]	55	TBHP	87
10[e]	[BMI][NTf_2]	CH_2Cl_2[d]	30	TBHP	74
11[e]	[BMP][NTf_2]	CH_2Cl_2[d]	30	TBHP	67
12[e]	[BMP][NTf_2]	CH_2Cl_2[d]	40	TBHP	80
13[e]	[BMP][NTf_2]	CH_2Cl_2[d]	30	H_2O_2	4

[a] Results obtained from duplicated tests. Reaction conditions: 1 mmol cyclooctene, 1.5 mmol TBHP in *n*-decane (*ca.* 5.5 M) and 0.025 mmol Mo for 4 h in 1 mL of solvent. [b] Determined by GC; only cyclooctene epoxide was formed. [c] 2.5 mL of dichloromethane. [d] 1.5 mL of dichloromethane. [e] Reaction for 22h.

The reaction monitoring carried out during 6 hours evidenced that the reaction did not progress after 2h of reaction using imidazolium-based ILs (up to *ca.* 85% conversion), however in the pyrrolidinium IL, the reaction smoothly advanced during the reaction time, pointing to a higher catalyst stability in [BMP][NTf_2] than in imidazolium-based ILs (Figure 5.3).

At lower temperatures and longer times, the catalytic system in [BMP][NTf_2]/CH_2Cl_2 was also active, giving 67% substrate conversion after 22 h at 30 °C, achieving 80% conversion at 40 °C (entries 11 and 12, Table 5.2). Hydrogen peroxide was used instead of TBHP, but unfortunately the system was almost inactive (entry 13, Table 5.2). For the following studies, [BMP][NTf_2] was chosen as ionic liquid due to the higher catalyst stability and the lower amount of co-solvent required in comparison with imidazolium-based ILs.

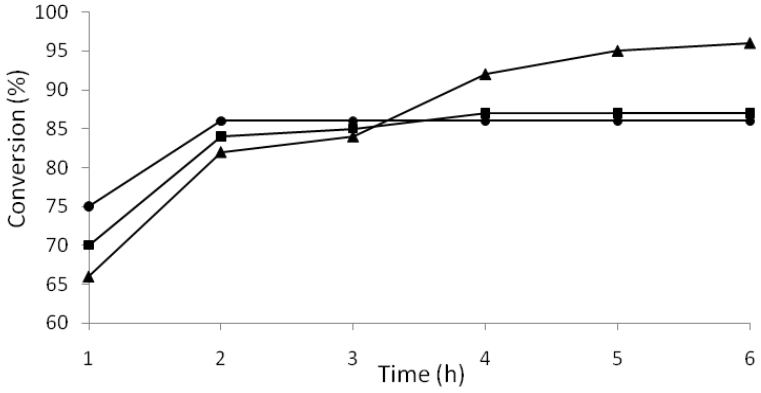

Figure 5.3. Cyclooctene epoxidation monitoring using the catalyst **16** in [BMI][PF_6]/CH_2Cl_2 (●), [BMI][NTf_2]/CH_2Cl_2 (■) and [BMP][NTf_2]/CH_2Cl_2 (▲); conversions based on the substrate.

The catalytic system **16** in [BMP][NTf_2] was recycled up to three times at 40 ºC preserving its catalytic behavior (Figure 5.4). The same trend was observed when re-additions of olefin and oxidant were done; this fact clearly points to a catalyst deactivation with the recycling. In [BMI][PF_6], the catalyst could be reused up to 5 times without loss of activity working at 40 ºC; but at higher temperature (55 ºC), the recycling was not effective (activity loss after the first run), probably due to the lower activity of NHC–molybdenum species formed in the imidazolium-based ionic liquid (see below).

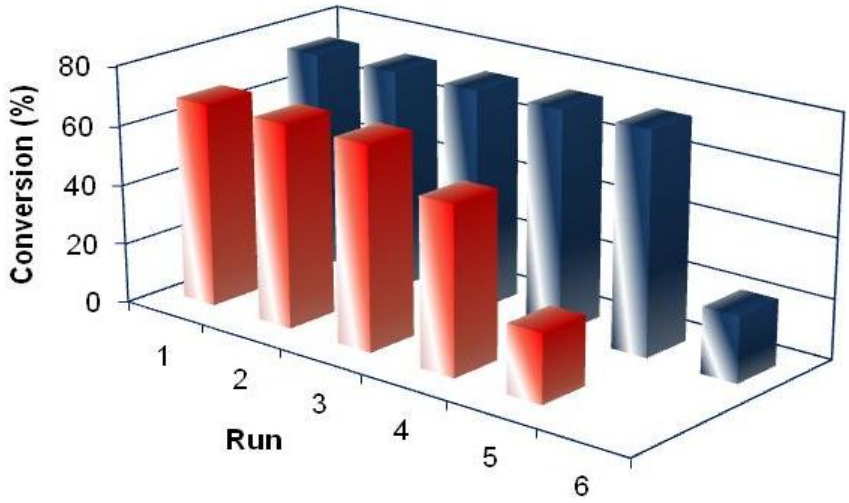

Figure 5.4. Recycling experiments using complex **16** as catalyst in [BMP][NTf_2]/CH_2Cl_2 (red) and [BMI][PF_6]/ CH_2Cl_2 (blue). For reaction conditions, see entries 8 (red) and 6 (blue) of Table 5.2, and section 5.2.4.

The monometallic complexes [$MoO_2Cl(\kappa^3$-*N*,*N*',O-**A**)] (**1**) and [$MoO_2Cl_2(\kappa^2$-*N*,*N*-**C**)] (**4**), were also tested in cyclooctene epoxidation using [BMP][NTf_2] as ionic liquid. These catalytic systems exhibited higher activity than that observed using **16** (entries 2-3 vs 1, Table 5.3), obtaining nearly quantitative conversion of epoxide after 1 h of reaction when **4** was applied as catalyst (entry 2, Table 5.3). The activity observed in dichloromethane for **1** and **4** (entries 4 and 5, Table 5.3) was somewhat higher than that in [BMP][NTf_2]/CH_2Cl_2, as stated for complex **16** (see above). When the molybdenum precursor [MoO_2Cl_2(DME)], precursor for the synthesis of **1** and **4**, was used as catalyst, quantitative conversion of epoxide was obtained after 1 hour of reaction, giving 15% of alcohol (entry 6, Table 5.3). The presence of oxazoline-based ligands in the catalysts avoids the epoxide opening. Effectively, [MoO_2Cl_2(DME)] in the absence of oxazoline ligand gave formation of the corresponding diol even at short times of reaction (after 10 minutes of reaction, 7% of the diol was observed), showing a lower chemoselectivity than that exhibited by complexes **1**, **4** and **16** which exclusively gave the epoxide.

Table 5.3. Cyclooctene epoxidation catalyzed by dioxomolybdenum complexes **1**, **4** and **16**.[a]

Entry	Catalyst	Solvent	Conv. (%)[b]	Epoxide yield[b,c]
1	**1**	$[BMP][NTf_2]/CH_2Cl_2$	87	87 (0)
2	**4**	$[BMP][NTf_2]/CH_2Cl_2$	98	98 (0)
3	**16**	$[BMP][NTf_2]/CH_2Cl_2$	81	81 (0)
4	**1**	CH_2Cl_2	94	94 (0)
5	**4**	CH_2Cl_2	100	100 (0)
6	$[MoO_2Cl_2(DME)]$	$[BMP][NTf_2]/CH_2Cl_2$	100	85 (15)

[a] Results obtained from duplicated tests. Reaction conditions: 1 mmol cyclooctene, 1.5 mmol TBHP in *n*-decane (*ca*. 5.5 M) and 0.025 mmol Mo in 1 mL of $[BMP][NTf_2]$ and 1.5 mL of CH_2Cl_2, at 55 °C for 1 h. [b] Determined by GC. [c] In brackets, diol yield.

The cyclooctene epoxidation was monitored during one hour of reaction for the three catalysts, **1**, **4** and **16** (Figure 5.5). During the first 30 minutes, complexes **1** and 1**6** showed a similar catalytic activity (after 10 minutes of reaction: TOF for **1**, 74 h^{-1}; for **16**, 82 h^{-1}), while catalyst **4** was clearly less active (TOF for **4**, 12 h^{-1}). However, the activity of **4** increased faster at longer times (after 1 h, 98% conversion) than that observed for the other two systems, in particular for **16**. It is noteworthy that the catalytic system **4** preserved its activity after the recharge of olefin and oxidant after one hour of reaction (90% conversion without formation of by-products).

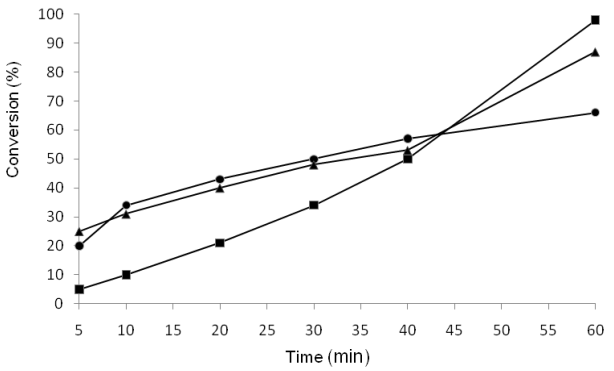

Figure 5.5. Cyclooctene epoxidation monitoring using complexes **1** (▲), **4** (■), and **16** (●) as catalysts in $[BMP][NTf_2]/CH_2Cl_2$; conversions based on the substrate.

(*R*)-Limonene and *trans*-β-methylstyrene epoxidations were chosen to evaluate the diastereo- and enantio-selectivity induced by the dioxomolybdenum(VI) complexes **1** and **4**, containing optically pure ligands.

Concerning (*R*)-limonene epoxidation (Scheme 5.3), complex **16** led to the formation of the corresponding 1,2-epoxide with 42% conversion in [BMP][NTf_2] at 30 ºC for 22 h (entry 5, Table 5.4). This activity was lower than that observed in dichloromethane (entry 5 vs 4, Table 5.4). However, the diasteroselectivity was remarkably higher in [BMP][NTf_2] than in the organic solvent, obtaining exclusively the *trans* isomer in IL. Increasing the catalyst load (olefin/Mo = 20), the activity remained practically invariable, but the formation of the diol clearly increased (entry 6, Table 5.4). This behavior can be associated to the increase of the rate for the epoxide ring-opening in the presence of higher amount of catalyst. In [BMI][PF_6], the activity was similar to that obtained in dichloromethane, but with a low diastereoselectivity induction (entry 7, Table 5.4). However, in [BMI][NTf_2] the activity and diastereoselectivity were similar to those found in the pyrrolidinium-based ionic liquid (entry 8 vs 4, Table 5.4), but the chemoselectivity was lower (*ca*. epoxide:diol ratio = 1:1). This fact points to a higher rate of the epoxide ring-opening for the *cis* isomer than for the *trans* one.

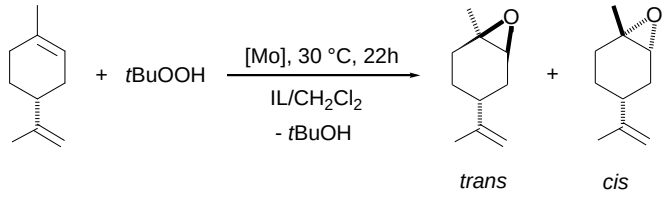

Scheme 5.3 Mo-catalyzed (*R*)-limonene epoxidation in IL using dichloromethane as co-solvent.

Monometallic complexes **1** and **4** were highly active, giving more than 80% olefin conversion, but with a very low diastereoselectivity (entries 4 and 5, Table 5.4); at shorter times, no changes in the selectivity were observed. The addition of free ligand in the catalytic mixture for the system containing complex **4**, did not lead to a selectivity improvement, giving an activity decrease (entry 2 vs 3, Table 5.4).

Table 5.4. (*R*)-limonene epoxidation catalyzed by dioxomolybdenum complexes **1**, **4** and **16**.[a]

Entry	Catalyst	Solvent	Conv. (%)[b]	Epoxide yield (%)[b,c]	*trans*/*cis* ratio[b]
1	**1**	[BMP][NTf_2][e]	82(57)[h]	82 (0)	60/40(60/40)[h]
2	**4**	[BMP][NTf_2][e]	89(47)[h]	89 (0)	60/40(60/40)[h]
3[i]	**4**	[BMP][NTf_2][e]	57	57 (0)	50/50
4	**16**	CH_2Cl_2	87	62 (18)[d]	80/20
5	**16**	[BMP][NTf_2][e]	42	38 (4)	100/0
6	**16**	[BMP][NTf_2][e]	37[f]	18 (19)	100/0
7	**16**	[BMI][PF_6][g]	64	58 (6)	54/46
8	**16**	[BMI][NTf_2][e]	44	24 (20)	100/0

[a] Results obtained from duplicated tests. Reaction conditions: 1 mmol (*R*)-limonene, 1.5 mmol TBHP in *n*-decane (*ca.* 5.5 M) and 0.025 mmol Mo in 1 mL of solvent, at 30 °C for 22h. [b] Determined by GC. [c] In brackets, diol yield. [d] 18% diol and 7% double epoxide. [e] 1 mL of [BMP][NTf_2] and 1.5 mL of CH_2Cl_2 at 30 °C for 22h. [f] 0.050 mmol Mo used. [g] 1 mL of [BMI][PF_6] and 2.5 mL of CH_2Cl_2. [h] In brackets, data at 3h of reaction. [i] Reaction in the presence of 0.10 mmol of free ligand (Mo/**C** ratio = 1/5).

This behavior points to a coordination competition between the olefin and/or oxidant and ligand towards the metal; partial or total ligand dissociation during the epoxidation in the absence of ligand excess could not be observed by the NMR monitoring (see below).

In relation to the chemoselectivity, mono-metallic catalytic systems only gave the 1,2-epoxide, in contrast to the bimetallic system **16** which also led to alcohol formation even if in low yield (up to 6%, entries 5 and 7, Table 5.4). It is noteworthy that alcohol formation is more favored in dichloromethane than in ionic liquid (entry 4 vs 5 and 7, Table 5.4). The corresponding 8,9-epoxide (or the double epoxide) was never observed, in contrast to that obtained in organic solvents.[25a]

In order to understand the effect of the ionic liquid in the epoxidation selectivity, a ^{95}Mo NMR study was carried out. Complex **16** was stable at 35 °C for a long period (at least for one week) in [BMP][NTf_2]/dichloromethane, even in the presence of (*R*)-limonene (see Figure 5.6), exhibiting one signal at -66.5 ppm (width at middle height: 1100 Hz; the large width is due to the presence of several isomers due to the relative position of the two oxazolinyl-pyridine ligands (**G**) in the bimetallic structure; see reference [25a] for a detailed structural discussion).

However in [BMI][PF_6]/dichloromethane, a new broad signal can be distinguished at *ca*. 120 ppm which becomes more intense after the olefin addition (+123 ppm, width

at middle height: 600 Hz) (see Figure 5.7). This low-fielded shift points to an electronic density increase around the metallic center.[35] This behavior, in contrast to that observed using pyrrolidinium-based ionic liquid [BMP][NTf_2], can be due to the formation of Mo-NHC carbene bond by partial de-coordination of the chiral ligand; the presence of the olefin favors the de-coordination of the isothiocyanate group in agreement with that observed in neat dichloromethane.[25b] With the aim to evidence the formation of Mo-carbene bond, ^{13}C NMR spectrum for complex **16** was recorded in [BMI][NTf_2], observing the appearance of new signals in the region 170-165 ppm corresponding to the C=N and plausible Mo-C(NHC) bonds[33] (see Figure 5.8), in agreement with the low-fielded signal observed by ^{95}Mo NMR (see Figure 5.7). This fact also explains the higher activity of the catalyst at relative long times in [BMP][NTf_2], in contrast to that observed in imidazolium-based ionic liquids for the cyclooctene epoxidation (see above kinetics profile, Figure 5.3).

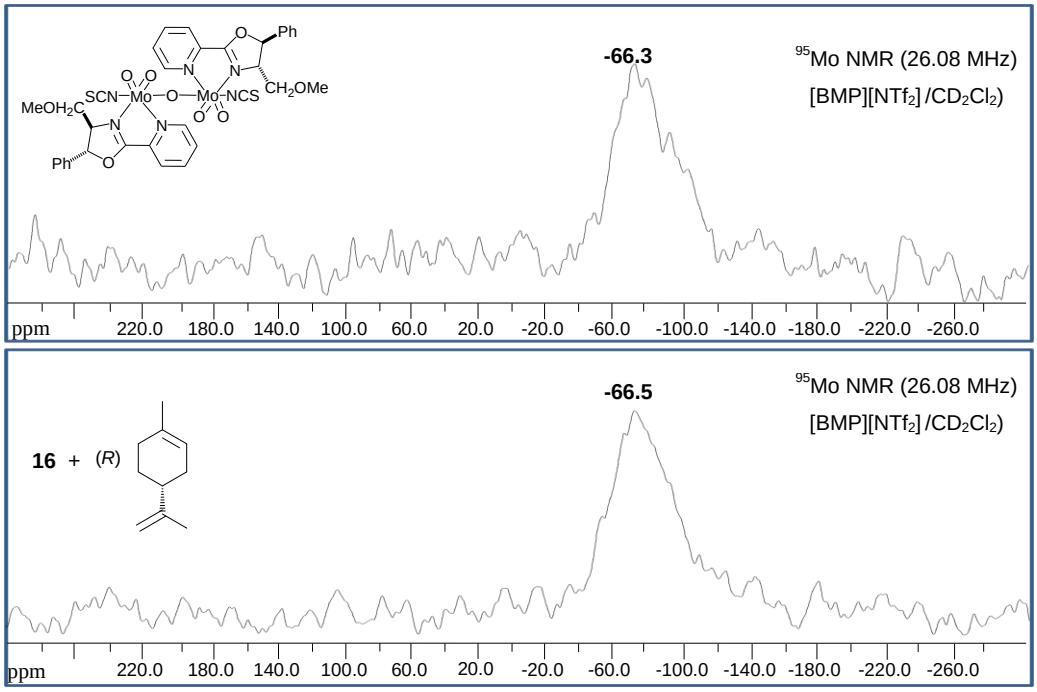

Figure 5.6. ^{95}Mo NMR spectra (26.08 MHz, 308 K) of complex **16** in [BMP][$NTf]_2/CD_2Cl_2$ (top) and in the presence of (*R*)-limonene (down).

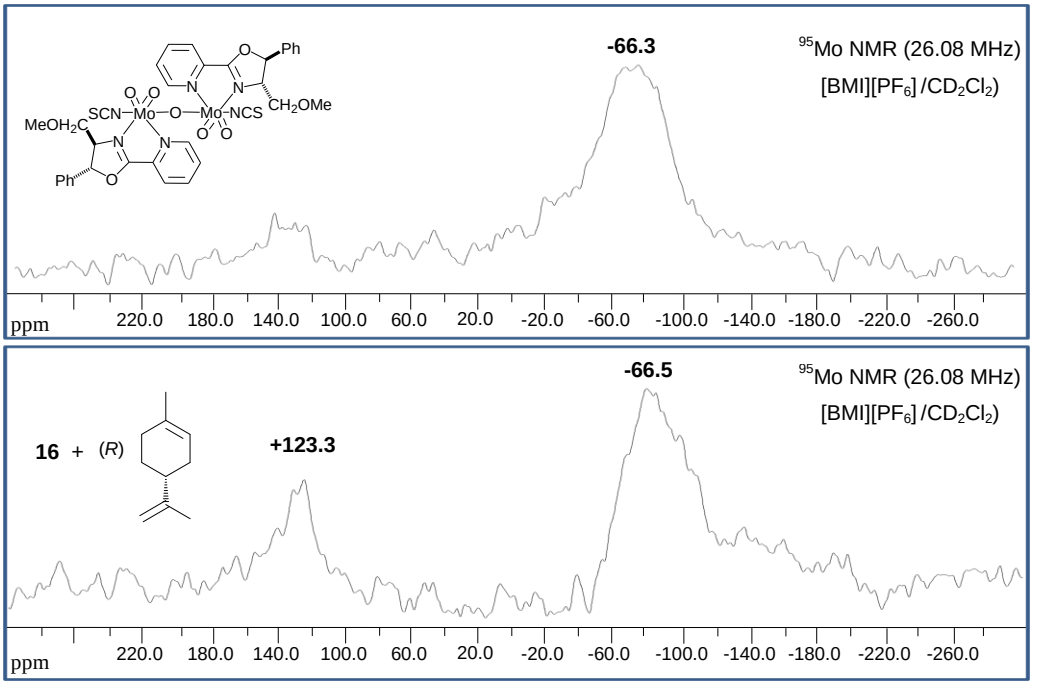

Figure 5.7. ^{95}Mo NMR spectra (26.08 MHz, 308 K) of complex **16** in [BMI][PF_6]/CD_2Cl_2 (top) and in the presence of (*R*)-limonene (down).

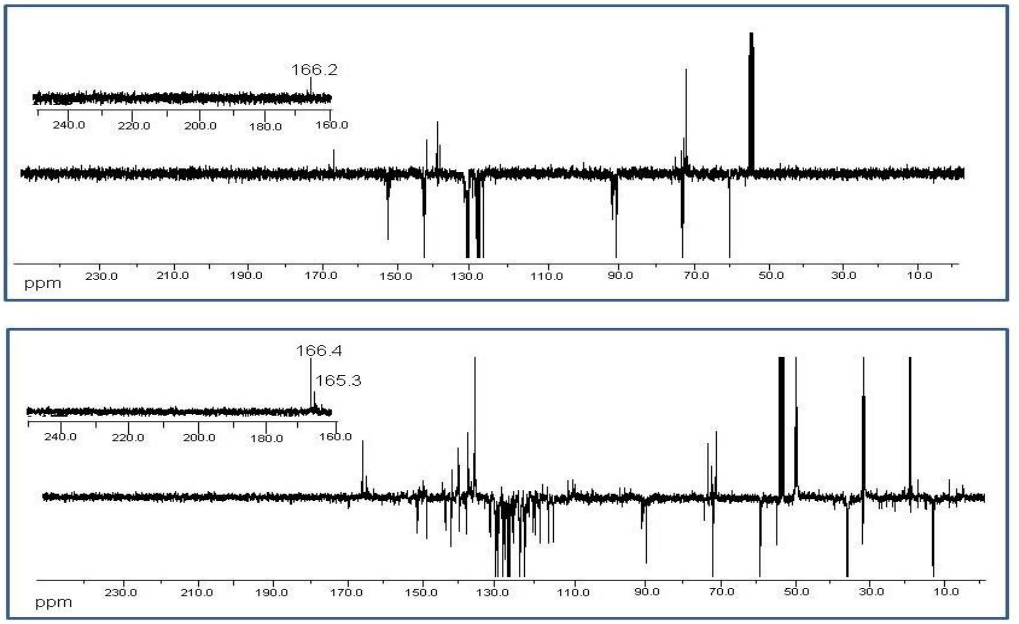

Figure 5.8. ^{13}C NMR spectra (75 MHz, 308 K) of complex **16** in CD_2Cl_2 (top) and [BMI][NTf_2]/CD_2Cl_2 (down). For each spectrum, inset represents the region between 250 and 160 ppm.

The lack of selectivity induced by complex **4** in pyrrolidinium-based ionic liquid can be due to a ligand de-coordination, in agreement with the large signal observed by ^{95}Mo NMR, both in the presence and in the absence of (*R*)-limonene (see Figure 5.9), as previously observed for dioxomolybdenum complexes containing hemi-labile ligands.[24]

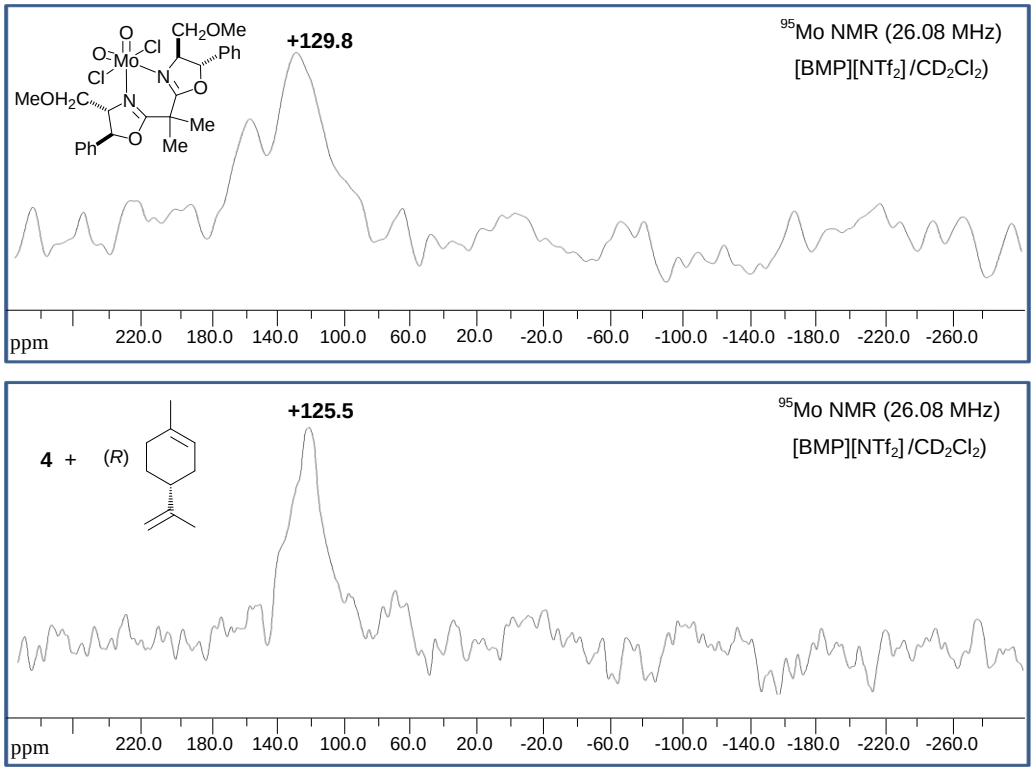

Figure 5.9. ^{95}Mo NMR spectra (26.08 MHz, 308 K) of complex **4** in [BMP][NTf_2]/CD_2Cl_2 (top) and in the presence of (*R*)-limonene (down)

Regarding to *trans*-β-methylstyrene epoxidation, the monometallic complexes **1** and **4** mainly led to the formation of the expected epoxide, being noticeably more active the complex **4** containing the bis(oxazoline) (entries 1 and 2, Table 5.5); less than 5% of benzaldehyde was observed in each case. Unfortunately, no asymmetric induction was observed. However, the bimetallic molybdenum system **16** was scarcely active, giving a mixture of benzaldehyde and benzylmethylketone instead of the corresponding epoxide (entry 3, Table 5.5). Starting with *trans*-β-methylstyrene epoxide in the presence of complex **16**, benzaldehyde and benzylmethylketone were

quantitatively obtained (Scheme 5.4); this result points to that the epoxide is formed but it quickly decomposes towards the formation of achiral by-products.

Table 5.5. *Trans*-β-methylstyrene epoxidation catalyzed by dioxomolybdenum complexes **1**, **4** and **16** in $[BMP][NTf_2]/CH_2Cl_2$.[a]

Entry	Catalyst	Solvent	Conv. (%)[b]	Epoxide yield (%)[b,c]
1	**1**	$[BMP][NTf_2]$	30	27 (3)
2	**4**	$[BMP][NTf_2]$	76	74 (2)
3	**6**	$[BMP][NTf_2]$	16	0 (10)[d]

[a] Results obtained from duplicated tests. Reaction conditions: 1 mmol *trans*-β-methylstyrene, 1.5 mmol TBHP in *n*-decane (*ca.* 5.5 M) and 0.025 mmol Mo in 1 mL of $[BMP][NTf_2]$ and 1.5 mL of CH_2Cl_2; 30 °C for 22h. [b] Determined by GC. [c] In brackets, benzaldehyde yield. [d] 6% of benzylmethylketone was also obtained.

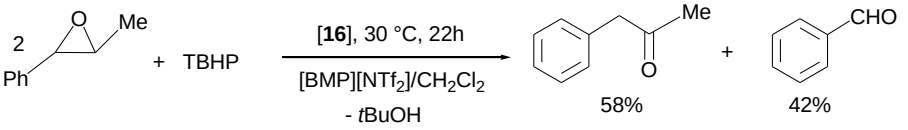

Scheme 5.4. Catalytic decomposition of *trans*-β-methylstyrene epoxide by complex 1**6** in $[BMP][NTf_2]/CH_2Cl_2$.

5.4. Palladium-catalyzed allylic substitutions.

Some preliminary palladium-catalyzed allylic substitution reactions were carried out in neat pyrrolidinium-based ionic liquid, using allylpalladium(II) chloride dimer $[Pd(\eta^3\text{-}C_3H_5)(\mu Cl)]_2$ in the presence of the appropriate ligand (**A** or **C**) as catalytic precursor (Scheme 5.5).

The substrate was common for all the reactions, *rac*-3-acetoxy-1,3-diphenyl-1-propene (**AS**-**1**, using the appropriated nucleophile (dimethylmalonate, **AS**-**2**; benzylamine **AS**-**4**; *p*-toluene sulfonic acid sodium salt **AS**-**6**; and diphenylphosphine, **AS**-**8**; for the alkylation, amination, sulfonylation and phosphination reaction, respectively). Results are summarized in Table 5.6.

The catalytic system Pd/**A** was not active in the reaction of allylic alkylation (entry 1, Table 5.6), in contrast to the high activities reported in the literature using related *N*,*N*-bidentate oxazolinyl-pyridine ligands in allylic alkylation reactions.[34] This

behavior can be explained by the robustness of the *N*,*N*',*O*-tridentate ligand leading to a saturated Pd species from a point of view of its coordination.

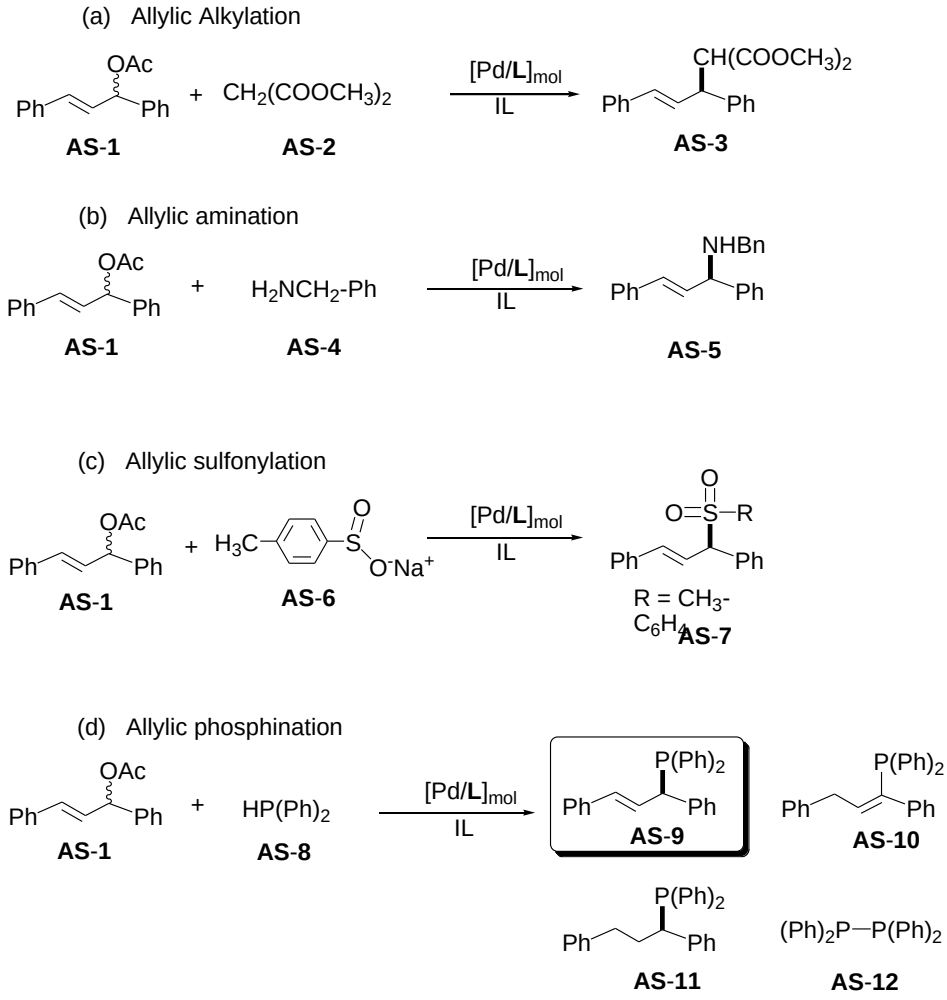

AS-1 = Substrate; **AS-2**, **AS-4**, **AS-6**, **AS-8** = Nucleophile

L = Ligand **A** or **C**

Scheme 5.5. Pd-catalyzed allylic substitution reactions tested in [BMP][NTf_2]: (a) allylic alkylation; (b) allylic amination; (c) Allylic sulfonylation (d) Allylic phosphination.

In order to avoid the formation of the Pd-O bond through the alkoxide arm of the ligand, different attempts to methylate the alcohol function in the oxazoline ligand **A** or its cyano precursor (**M-1**) were unsuccessful, since the desired product (**A-1** or **M-2,** Scheme 5.6) was obtained in a small amount (*ca.* 20%) together with the starting

material (*ca.* 15%) and some by-products, being the corresponding vinylpyridine **M-3** or **A-2** the major of them (*ca.* 40%).

Table 5.6. Pd-catalyzed allylic substitution reactions of *rac*-3-acetoxy-1,3-diphenyl-1-propene (**AS-1**) using different nucleophiles (**AS-2**, **AS-4**, **AS-6** and **AS-8**, see Scheme 5.5).

Entry	Ligand	NuH	S/Pd[a]	Solvent	Base[b]	T (ºC)	time (h)	Conv (%)[c]	ee (%)[d]
1	**A**	**AS-2**	100	CH_2Cl_2	BSA	25	24	0	-
2	**C**	**AS-2**	25	CH_2Cl_2	BSA	25	24	100	89 (*S*)
3	**C**	**AS-2**	50	[BMPyr][NTf_2]	BSA	25	24	100	88 (*S*)
4	**C**	**AS-2**	50	[BMPyr][NTf_2]	BSA	40	8	90	88 (*S*)
5[e]	**C**	**AS-2**	50	[BMPyr][NTf_2]	BSA	40	8	20	88 (*S*)
6	**C**	**AS-4**	50	[BMPyr][NTf_2]	-	40	24	0	
							2	20	
7	**C**	**AS-4**	50	[BMPyr][NTf_2]	-	100	15	35	0
							24	60	
8	**C**	**AS-6**	50	[BMPyr][NTf_2]	-	100	24	0	-
9	**C**	**AS-8**	20	[BMPyr][NTf_2]	-	40	48	15	9

[a] Result from duplicated reactions. Ratio substrate/Pd [b] BSA = *N*,*O*-bis (trimethylsilyl)acetamide. A pinch of KOAc was added. [c] Determined by ^{1}H NMR. [d] Determined by SFC. [e] Reusing of catalytic system in a second run.

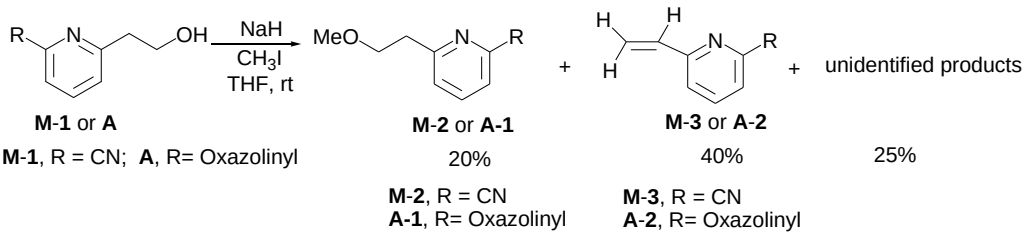

Scheme 5.6. Attempts to methylate the alcohol function in pyridine derivative ligands **M-1** and **A**.

On the contrary, the bis(oxazoline) **C** was active in the allylic alkylation reaction, but using a low substrate/palladium ratio (S/M = 25, it means 4 mol% of Pd) (entry 2 Table 5.6), analogously to what observed in the previous reported works using bis(oxazoline) ligands.[35] From a mechanistic point of view and due to the ionic nature of the resting state, polar solvents could favor the kinetics of the reaction. When allylic alkylation reactions were performed in the ionic liquid [BMP][NTf_2], less amount of catalyst was necessary comparing to the reaction in dichloromethane (entry 3 vs 1, Table 5.6); no differences in the enantiomeric induction were observed approximately 88% in all cases (entries 2-5, Table 5.6). When the catalytic system in

ionic liquid [BMP][NTf_2] was reused, loss of activity was observed (entry 4 vs 5, Table 5.6), probably due to the leaching or the poison of the active catalytic species during the extraction of the organic product.

The palladium catalytic system containing the oxazoline ligand **C** was also used in different allylic substitution reactions such as amination (entries 6 and 7, Table 5.6), sulfonylation (entry 8, Table 5.6) and phosphination (entry 9, Table 5.6) reactions. The catalytic system was inactive for the amination and sulfonylation reactions. For the allylic phosphination, very low conversion was obtained (*ca.* 15%) and the reaction was not chemoselective generating at least four products (**AS**-**9**-**AS**-**12**) Scheme 5.5). The enantiomeric excess corresponding to the phosphination product was very low (9%, entry 9 in, Table 5.6).

Only few experiments have been performed and it is necessary to search deeply to find better conditions, which could improve the activity and selectivity of these reactions. Respect to the reuse and recovery of the catalytic system, the vast number of ionic liquids maintains the hopes of being able to find one of them, which under suitable conditions, can allow the recycling without loss in activity and enantioselectivity. Recently Gómez and co-workers[36] reported palladium catalytic systems containing chiral diphosphite ligands, showing high activities and enantioselectivities in pyrrolidinium-based ionic liquid in allylic alkylation and amination reactions. The activity of this system even increases in relation to that obtained in dichloromethane for the amination (16% vs 75% conversion in CH_2Cl_2 and pyrrolidinium-based ionic liquid respectively). It is the first time that a palladium catalytic system could be recycled up to nine times without activity loss, preserving the enantioselectivity.

5.5. Conclusions

The catalytic applications of the new molybdenum complexes (**1**-**5**) have shown their efficiency in the epoxidation of cyclooctene, (*R*)-limonene and *trans*-β-methylstyrene, achieving high conversions and chemoselectivity, although no enantioselectivity was obtained.

Monometallic (**1**, **4**) and bimetallic (**16**) complexes bearing chiral oxazoline ligands have led to active and chemoselective catalytic systems in ionic liquids, in contrast to the catalytic behavior exhibited by $[MoO_2Cl_2(DME)]$ in the absence of ligand for the cyclooctene epoxidation which gave an important amount of the corresponding diol. In particular, complex **16** allowed the recycling of the catalytic system up to 5 times without activity loss.

In relation to the diastereoselectivity, catalyst **16**, in contrast to monometallic systems **1** and **4**, led to the exclusive formation of *trans*-1,2-(*R*)-limonene epoxide using the pyrrolidinium-based ionic liquid $[BMP][NTf_2]$ as solvent. However this diastereoselectivity induction was lost when imidazolium ionic liquid was used, due to the plausible formation of Mo-NHC carbene species by partial de-coordination of the oxazolinyl-pyridine ligand **G**, in agreement with the NMR observations.

Unfortunately, our systems were not enantioselective in the *trans*-β-methylstyrene epoxidation. Further studies are required concerning the catalyst design in order to induce enantioselectivity in the epoxidation reactions.

Good conversion and enantioselectivity was obtained in allylic alkylation using allylpalladium(II) chloride dimer $[Pd(\eta^3\text{-}C_3H_5)\text{-}(\mu\text{-}Cl)]_2$ in the presence of the bis(oxazoline) **C** in $[BMP][NTf_2]$. However, this catalytic system was not recyclable, probably due to leaching or the poison of the active catalytic species during the extraction of the organic product.

5.6. Acknowledgments

We gratefully acknowledge financial support from Fundação para a Ciência e a Tecnologia (FCT) of Portugal through project PTDC/QUI-QUI/098682/2008, CNRS, Université Paul Sabatier and Ministerio de Ciencia e Innovación (CTQ2010-15292). J. A. Brito thanks FCT for grant SFRH/BD/30917/2006. The National NMR Network (REDE/1517/RMN/2005) was supported by POCI 2010 and Fundação para a Ciência e a Tecnologia. We thank REDE71504/REM/2005.

5.7. References

1 (a) B. Cornils, W. A. Herrmann, Applied Homogeneous Catalysis with Organometallic Compounds, Eds. Wiley-VCH, Weihneim, 2nd edition, 2002, vol. 1, pp. 412-426; (b) Q.-H. Xia, H.-Q. Ge, C.-P. Ye, Z.-M. Liu, K.-X. Su, *Chem. Rev*., 2005, 105, 1603-1662; (c) F. E. Kühn, A. M. Santos, W. A. Herrmann, *Dalton Trans*., 2005, 2483-2491; (d) F. E. Kühn, J. Zhao, W. A. Herrmann, *Tetrahedron: Asymmetry*, 2005, **16**, 3469-3479.

2 J. M. Brégeault, *Dalton Trans*, 2003, 3289-3302.

3 (a) J. Kollar, Halcon, US Patents 3, 350, 422 and 3, 351, 635 1967; (b) M. N. Sheng, G. J. ZAjaczek, ARCO, GB Patent 1, 136, 923 1968.

4 D. J. Cole-Hamilton, R. P. Tooze, Catalyst, Separation, Recovery and Recycling, Ed., Springer, Dordrecht, 2006, vol. 30.

5 S. Zhang, X. Lu, Q. Zhou, X. Li, X. Zhang and S. Li in Ionic Liquids. Physicochemical properties, Elsevier, Amsterdam, 2009.

6 For a recent review see: H. Olivier-Bourbigou, L. Magna, D. Morvan, *Appl. Catal. A: General*, 2010, **373**, 1-56.

7 (a) J. Dupont, R. F. de Souza, P. A. Z. Suarez, *Chem. Rev*., 2002, **102**, 3367-3692; (b) P. Wasserscheid, T. Welton, Ionic liquids in synthesis, Wiley-VCH, Weinheim 2003; (c) C. Baudequin, J. Baudoux, J. Levillain, D. Cahard, A. Gaumon, J. Plaquevent, *Tetrahedron: Asymmetry*, 2003, **14**, 3081-3093; (d) P. J. Dyson, T. J. Geldbach, Metal Catalysed Reactions in Ionic Liquids, Springer, Dordrecht, 2005.

8 For selected reviews, see: (a) J. Durand, E. Teuma, M. Gómez, C. R. Chimie, 2007, 10, 152-177; (b) S. V. Malhorta, V. Kumar, V. S. Parmar, *Curr. Org. Synth*., 2007, **4**, 370-380; (c) K. Bica, P. Gaertner, *Eur. J. Org. Chem*., 2008, 3235-3250; M. H. G. Prechtl, J. D. Jackson, B. A. D. Brenno, J. Dupont, *Curr. Org. Chem*., 2009, **13**, 1259-1277.

9 Y. Chauvin, L. Mussmann, H. Olivier, *Angew. Chem. Int. Ed. Engl*., 1995, **34**, 2698-2700.

10 C. E. Song, E. J. Roh, *Chem. Commun*., 2000, 837-838.

11 C. E. Song, C. R. Oh, E. J. Roh, D. J. Choo, *Chem. Commun*., 2000, 1743-1744.

12 A. A. Valente, Z. Petrovski, L. C. Branco, C. A. M. Afonso, M. Pillinger, A. D. Lopes, C. C. Romão, C. D. Nunes, I. S. Gonçalves, *J. Mol. Catal. A: Chemical*, 2004, **218**, 5-11.

13 F. E. Kühn, J. Zhao, M. Abrantes, W. Sun, C. A. M. Afonso, L. C. Branco, I. S. Gonçalves, M. Pillinger, C. C. Romão, *Tetrahedron Lett*., 2005, **46**, 47-52.

14 D. Betz, A. Raith, M. Cokoya, F. E. Kühn, *ChemSusChem*, 2010, **3**, 559-562.

15 M. Abrantes, P. Neves, M. M. Antunes, S. Gago, F. A. Almeida Paz, A. E. Rodrígues, M. Pillinger, I. S. Gonçalves, C. M. Silva, A. A. Valente, *J. Mol. Catal. A: Chemical*, 2010, **320**, 19-26.

16 (a) M. Herbert, A. Galindo, F. Montilla, *Catal. Commun*., 2007, **8**, 987-990; (b) M. Herbert, E. Alvarez, D. J. Cole-Hamilton, F. Montilla, A. Galindo, *Chem. Commun*., 2010, **46**, 5933-5935.

17 S.-F. Cai, L.-S. Wang, C.-L. Fan, *Molecules*, 2009, **14**, 2935-2946.

18 C. Bibal, J-C. Daran, S. Deroover, R. Poli, *Polyhedron*, 2010, **29**, 639-647.

19 (a) S. Gago, S. S. Balula, S. Figuereido, A. D. Lopes, A. A. Valente, M. Pillinger, I. S. Gonçalves, *Appl. Catal. A: General*, 2010, **372**, 67-72; (b) P. Neves, C. C. L. Pereira, F. A. Almeida Paz, S. Gago, M. Pillinger, C. M. Silva, A. A. Valente, Romão, I. S. Gonçalves, *J. Organomet. Chem*., 2010, **695**, 2311-2319.

20 (a) W. R. Thiel, M. Jia, *Chem. Commun*., 2002, 2392-2393; (b) M. Jia, A. Steifert, M. Berger, H. Giegengack, S. Schulze, W. R. Thiel, *Chem. Mater*., 2004, **16**, 877-882; (c) M. Jia, A. Steifert, W. R. Thiel, *J. Catal.*, 2004, **221**, 319-324; (d) A. Castro, J. C. Alonso, P. Neves, A. A. Valente, P. Ferreira, *Eur. J. Inorg. Chem*., 2010, 602-607.

21 (a) K. R. Jain, F. E. Kühn, *Dalton Trans.*, 2008, 2221-2227; (b) K. A. Jain, W. A. Herrmann, F. E. Kühn, *Coord. Chem. Rev.*, 2008, **252**, 556-568.

22 P. Neves, S. Gago, C. C. L. Pereira, S. Figuereido, A. Lemos, A. D. Lopes, I. S. Gonçalves, M. Pillinger, C. M. Silva, A. A. Valente, *Catal. Lett*., 2009, **132**, 94-103.

23 M. Abrantes, F. A. Almeida Paz, A. A. Valente, C. C. L. Pereira, S. Gago, A. E. Rodrígues, J. Klinowski, M. Pillinger, I. S. Gonçalves, *J. Organomet. Chem*., 2009, **694**, 1828-1833.

24 M. Gómez, S. Jansat, G. Muller, G. Noguera, H. Teruel, V. Moliner, E. Cerrada, M. Hursthouse, *Eur. J. Inorg. Chem.*, 2001, 1071-1076.

25 (a) J. A. Brito, M. Gómez, G. Muller, H. Teruel, J. C. Clinet, E. Duñach, M. A. Maestro, *Eur. J. Inorg. Chem.*, 2004, 4278-4285; (b) J. A. Brito, H. Teruel, G. Muller, S. Massou, M. Gómez, *Inorg. Chim. Acta,* 2008, **361**, 2740-2746.

26 For reviews, see: (a) B. M. Trost, M. D. L. van Vranken, *Chem. Rev*., 1996, 96, 395-422; (b) M. Johannsen, K. A. Jorgensen, *Chem. Rev*., 1998, **98**, 1689-1708. (c) G. Helmchen, A. Pfaltz, *Acc. Chem. Res*., 2000, **33**, 336-345. (d) A. M. Masdeu-Bultó, M. Diéguez, E. Martín, M. Gómez, *Coord. Chem. Rev*., 2003, **242**, 159-201; (e) B. M. Trost, M. L. Crawley, *Chem. Rev*., 2003, **103**, 2921-2944. (f) E. E. Martín, M. Diéguez, *C. R. Chimie*, 2007, **10**, 188-205. (g) Z. Lu, S. Ma, *Angew. Chem. Int. Ed.*, 2008, **47**, 258-297.

27 (a) C Baudequin, J. Baudoux, J. Levillain, D. Cahard, A. Gaumont, J. Plaquevent, *Tetrahedron: Asymmetry*, 2003, **14**, 3081–3093; (b) C. de Bellefon, E. Pollet and P. Grenouillet, *J. Mol. Catal. A: Chemical*, 1999, **145**, 121-126; (c) Roger Sheldon, *Chem. Commun*., 2001, 2399–2407; (d) W. Chen, L. Xu, C. Chatterton, J. Xiao, *Chem. Commun*., 1999, 1247-1248; (e) L. Ross, W. Chen, L. Xu and L. Mao, *Organometallics*, 2001, **20**, 138-142.

28 S. Toma, B. Gotov, I. Kmentova and E. Solcaniova, *Green Chem*., 2000, **2**, 149-151.

29 (a) V.K. Aggarwal, L. Bell, M.P. Coogan, P. Jubault, *J; Chem. Soc. Perkin Trans.* 1998, **11**, 2037-2042; (b) K. Hallman, A. Frölander, T. Wondimagegn, M. Svensson, C. Moberg, *PNAS*, 2004, **101**, 5400-5404; (c) K. A. Nolin, R. W. Ahn, D. Toste, *J. Am. Chem. Soc*., 2005, **127**, 12462-12463.

30 G. Balavoine, J.C. Clinet, I. Lellouche, *Tetrahedron Lett.*, 1989, **30**, 5141-5144.

31 J. M. Mitchell, N. S. Finney, *J. Am. Chem. Soc.*, 2001, **132**, 862-869.

32 D. Betz, W. A. Herrmann, F. E. Kühn, *J. Organomet. Chem*., 2009, **694**, 3320-3324.

33 For related NHC-based dioxomolybdenum(VI) complexes, see: E. Mas-Marza, P. M. Reis, E. Peris, B. Royo, *J. Organomet. Chem*., 2006, **691**, 2708-2712.

34 (a) J. M. Canal, M. Gómez, F. Jiménez, M. Rocamora, G. Muller, E. Dunãch, D. Franco, A. Jiménez, F. H. Cano, *Organometallics,* 2000, **19**, 966-978; (b) K. Nordström, E. Macedo, C. Moberg, *J. Org. Chem*., 1997, **62**, 1604–1609; (c) 6. G.Chelucci, S. Medici, A. Saba, *Tetrahedron: Asymmetry*, 1997, **8**, 3183–3184.

35 (a) M. Gómez, S. Jansat, G. Muller, M. A. Maestro, J. M. Saavedra, M. Font-Bardía, X. Solans, *J. Chem. Soc., Dalton Trans*., 2001, 1432–1439; (b) M. A. Pericàs, C. Puigjaner, A. Riera, A. Vidal-Ferran, M. Gómez, F. Jiménez, G. Muller, M. Rocamora, *Chem. Eur. J*., 2002, **8**, 4164-4178.

36 I. Favier, A. Balanta Castillo, C. Godard, S. Castillón, C. Claver, M. Gómez, E. Teuma, Chem. Commun. 2011, DOI:10.1039/C1CC12157J.

Chapter 6 CONCLUSIONS AND PERSPECTIVES

6.1. Conclusions

New *cis*-dioxomolybdenum(VI) complexes containing optically pure chiral ligands (**A** = 2-(6-(4,5-dihydro-4-isopropyloxazol-2-yl)pyridin-2-yl)ethanol; **B** = N-(tetrahydrofuran-2-yl)picolinamide; **C** = 4,5-dihydro-2-(2-(4,5-dihydro-4-(methoxymethyl)-5-phenyloxazol-2-yl)propan-2-yl)-4-(methoxymethyl)-5-phenyloxazole, **D** = (2E)-2-(4,5-dihydro-4-isopropyloxazol-2-yl)-2-(4-isopropyloxazolidin-2-ylidene) acetonitrile) have been synthesized and fully characterized both in solution and solid state. Complexes **1** [$MoO_2Cl(\kappa^3$-*N*,*N*',*O*-**A**)], **3** [$MoO_2Cl_2(\kappa^2$-*N*,*O*-**B**)] and **4** [$MoO_2Cl_2(\kappa^2$-*N*,*N*-**C**)]) have been characterized by X ray diffraction, exhibiting a distorted octahedral coordination around the molybdenum atom with the oxo ligands in relative *cis* position. Complexes **1** and **4** represent the first structures described in the literature corresponding to a monometallic molybdenum species bearing a *N*,*N*',*O*-tridentated ligand and a bis(oxazoline), respectively. For complex **5** [$MoO_2Cl(\kappa^2$-*N*,*N*-**D**)], the proposed structure, taking into account the data derived from NMR and IR spectroscopy, elemental analysis and mass spectrometry, agrees with a trigonal bipyramid arrangement around the metal center.

Many of these *cis*-dioxomolybdenum complexes (**1**, **4** and **5**) are sensitive to moisture, except complex **3** which exhibits high stability under moisture and air conditions.

It has been evidenced the efficiency of the ^{95}Mo NMR as a tool to get information about the coordination chemistry of oxomolybdenum(VI) complexes in solution. A detailed study of oxomolybdenum(VI) compounds containing mono- and polydentated coordinated ligands showing different electron-donor properties, has permitted to establish a chemical shift scale depending on the ligand donor-electronic characteristics and consequently to look into the electronic density on the metal atom. In particular, this kind of study turns into a useful means to obtain structural information about catalytic intermediates, a key aspect for mechanistic studies.

The catalytic applications of the new molybdenum complexes **1**-**5** in organic solvents have showed their efficiency in the epoxidation of cyclooctene, (*R*)-limonene and *trans*-β-methylstyrene, achieving high conversions and chemoselectivity, but unfortunately no asymmetric induction could be obtained.

Monometallic (**1**, **4**) and bimetallic (**16**) complexes bearing chiral oxazoline-based ligands have led to active and chemoselective catalytic systems in ionic liquids; the catalytic system using complex **16** could be recycled up to 5 times without activity loss.

In relation to the diastereoselectivity, catalyst **16**, in contrast to the monometallic systems **1** and **4**, led to the exclusive formation of *trans*-1,2-(*R*)-limonene epoxide using the pyrrolidinium-based ionic liquid [BMP][NTf_2] as solvent. However this diastereoselectivity induction was lost when imidazolium ionic liquid was used, due to the plausible formation of Mo-NHC carbene species by partial de-coordination of the oxazolinyl-pyridine ligand **G**. Unfortunately, these systems were not enantioselective in the *trans*-β-methylstyrene epoxidation.

Some preliminary palladium-catalyzed allylic substitution reactions have been carried out in neat pyrrolidinium-based ionic liquid, using allylpalladium(II) chloride dimer $[Pd(\eta^3\text{-}C_3H_5)(\mu Cl)]_2$ in the presence of the appropriate ligand (**A** or **C**) as catalytic precursor. Moderate activity and good enantioselectivity were only obtained in the allylic alkylation of *rac*-3-acetoxy-1,3-diphenyl-1-propene using Pd/**C** catalytic system in [BMP][NTf_2]. Nevertheless, this catalytic system was not recyclable, probably due to leaching or the poison of the active catalytic species during the extraction of the organic product.

6.2. Perspectives

The asymmetric induction for Mo-catalyzed epoxidation reactions remains a challenge for the oxidation of prochiral substrates. In the present work, the lack of asymmetric induction is related to the lability of the chiral spectator under catalytic

conditions. Moreover, involvement of radicals in the epoxidation reaction proved by spin trap experiments can also disfavored the enantioselective process. More studies are required concerning the catalyst design to find an appropriated system in which the molybdenum species work in perfect harmony with the ligand and the oxidant. In addition, the polarity of the solvent can play a negative role in the asymmetric induction, due to the concomitant formation of *t*BuOH, that could be stimulating the de-coordination of the chiral ligand by competition for a coordination place around the metal and in consequence generating the lost of enantioselectivity. Therefore, an interesting point to undertake is the search of alternative oxidizing agents for the epoxidation reactions.

In relation to the Pd-catalyzed allylic substitutions, the preliminary study carried out in this Thesis evidenced that the catalytic systems containing bis(oxazoline) ligands are relatively low active; oxazolinyl-pyridine ligands could improve the activity, analogously to the behavior observed in organic solvents.

Chapter 7

Annexes

Table 7.1. Atomic coordinates ($x10^4$) and equivalent isotropic displacement parameters ($A^2 \times 10^3$) for complex **1**. U(eq) is defined as one third of the trace of the orthogonalized Uij tensor for complex **1**

	x	y	z	U(eq)
Mo(1)	9152(1)	5808(1)	8481(1)	26(1)
Cl(1)	9712(1)	5720(1)	9713(1)	40(1)
O(3)	9293(2)	7602(2)	8492(1)	42(1)
N(1)	6720(2)	5721(3)	8871(1)	24(1)
N(2)	8573(3)	3429(2)	8775(1)	30(1)
O(2)	8402(2)	5403(2)	7723(1)	45(1)
O(1)	11224(2)	5105(2)	8351(1)	37(1)
O(4)	4707(2)	4511(2)	9309(1)	36(1)
C(8)	6164(3)	4528(3)	9054(1)	27(1)
C(4)	9036(4)	963(3)	8908(2)	49(1)
C(7)	7078(3)	3217(3)	9004(1)	30(1)
C(6)	6523(4)	1910(3)	9202(2)	41(1)
C(5)	7532(4)	767(3)	9136(2)	50(1)
C(3)	9571(4)	2320(3)	8732(2)	39(1)
C(9)	4173(3)	5997(3)	9327(1)	32(1)
C(10)	5525(3)	6837(3)	8997(1)	25(1)
C(2)	11270(4)	2561(3)	8541(2)	50(1)
C(1)	11547(4)	3761(4)	8057(2)	53(1)
C(11)	5077(3)	7664(3)	8369(1)	32(1)
C(13)	3766(3)	8740(3)	8527(2)	43(1)
C(12)	4582(4)	6706(4)	7791(1)	45(1)

Table 7.2. Bond lengths [Å] and angles [deg] for complex **1**.

Mo(1)-O(2)	1.6965(19)	C(11)-C(12)	1.532(4)
Mo(1)-O(3)	1.700(2)	C(11)-C(13)	1.532(4)
Mo(1)-O(1)	1.8800(19)	C(11)-H(11)	1.0000
Mo(1)-N(1)	2.188(2)	C(13)-H(13A)	0.9800
Mo(1)-N(2)	2.374(2)	C(13)-H(13B)	0.9800
Mo(1)-Cl(1)	2.5264(9)	C(13)-H(13C)	0.9800
N(1)-C(8)	1.274(3)	C(12)-H(12A)	0.9800
N(1)-C(10)	1.477(3)	C(12)-H(12B)	0.9800
N(2)-C(3)	1.343(4)	C(12)-H(12C)	0.9800
N(2)-C(7)	1.353(4)	O(2)-Mo(1)-O(3)	105.20(11)
O(1)-C(1)	1.426(4)	O(2)-Mo(1)-O(1)	97.92(10)
O(4)-C(8)	1.326(3)	O(3)-Mo(1)-O(1)	106.84(9)
O(4)-C(9)	1.474(3)	O(2)-Mo(1)-N(1)	88.22(9)
C(8)-C(7)	1.461(4)	O(3)-Mo(1)-N(1)	95.60(9)
C(4)-C(5)	1.355(5)	O(1)-Mo(1)-N(1)	154.12(9)
C(4)-C(3)	1.404(4)	O(2)-Mo(1)-N(2)	86.27(10)
C(4)-H(4)	0.9500	O(3)-Mo(1)-N(2)	162.81(9)
C(7)-C(6)	1.378(4)	O(1)-Mo(1)-N(2)	83.67(8)
C(6)-C(5)	1.378(4)	N(1)-Mo(1)-N(2)	71.61(9)
C(6)-H(6)	0.9500	O(2)-Mo(1)-Cl(1)	161.13(8)
C(5)-H(5)	0.9500	O(3)-Mo(1)-Cl(1)	90.40(8)
C(3)-C(2)	1.494(4)	O(1)-Mo(1)-Cl(1)	87.35(6)
C(9)-C(10)	1.537(4)	N(1)-Mo(1)-Cl(1)	79.61(5)
C(9)-H(9A)	0.9900	N(2)-Mo(1)-Cl(1)	76.27(6)
C(9)-H(9B)	0.9900	C(8)-N(1)-C(10)	109.4(2)
C(10)-C(11)	1.533(4)	C(8)-N(1)-Mo(1)	118.60(18)
C(10)-H(10)	1.0000	C(10)-N(1)-Mo(1)	131.92(17)
C(2)-C(1)	1.513(5)	C(3)-N(2)-C(7)	119.0(3)
C(2)-H(2A)	0.9900	C(3)-N(2)-Mo(1)	126.5(2)
C(2)-H(2B)	0.9900	C(7)-N(2)-Mo(1)	114.53(19)
C(1)-H(1A)	0.9900	C(1)-O(1)-Mo(1)	123.25(19)
C(1)-H(1B)	0.9900	C(8)-O(4)-C(9)	106.2(2)

N(1)-C(8)-O(4)	117.4(2)	C(1)-C(2)-H(2A)	108.5
N(1)-C(8)-C(7)	122.5(2)	C(3)-C(2)-H(2B)	108.5
O(4)-C(8)-C(7)	120.0(2)	C(1)-C(2)-H(2B)	108.5
C(5)-C(4)-C(3)	120.5(3)	H(2A)-C(2)-H(2B)	107.5
C(5)-C(4)-H(4)	119.7	O(1)-C(1)-C(2)	111.7(3)
C(3)-C(4)-H(4)	119.7	O(1)-C(1)-H(1A)	109.3
N(2)-C(7)-C(6)	123.0(3)	C(2)-C(1)-H(1A)	109.3
N(2)-C(7)-C(8)	112.6(2)	O(1)-C(1)-H(1B)	109.3
C(6)-C(7)-C(8)	124.3(3)	C(2)-C(1)-H(1B)	109.3
C(7)-C(6)-C(5)	117.8(3)	H(1A)-C(1)-H(1B)	107.9
C(7)-C(6)-H(6)	121.1	C(12)-C(11)-C(13)	110.8(2)
C(5)-C(6)-H(6)	121.1	C(12)-C(11)-C(10)	113.1(2)
C(4)-C(5)-C(6)	119.9(3)	C(13)-C(11)-C(10)	110.1(2)
C(4)-C(5)-H(5)	120.1	C(12)-C(11)-H(11)	107.5
C(6)-C(5)-H(5)	120.1	C(13)-C(11)-H(11)	107.5
N(2)-C(3)-C(4)	119.7(3)	C(10)-C(11)-H(11)	107.5
N(2)-C(3)-C(2)	119.5(3)	C(11)-C(13)-H(13A)	109.5
C(4)-C(3)-C(2)	120.6(3)	C(11)-C(13)-H(13B)	109.5
O(4)-C(9)-C(10)	104.9(2)	H(13A)-C(13)-H(13B)	109.5
O(4)-C(9)-H(9A)	110.8	C(11)-C(13)-H(13C)	109.5
C(10)-C(9)-H(9A)	110.8	H(13A)-C(13)-H(13C)	109.5
O(4)-C(9)-H(9B)	110.8	H(13B)-C(13)-H(13C)	109.5
C(10)-C(9)-H(9B)	110.8	C(11)-C(12)-H(12A)	109.5
H(9A)-C(9)-H(9B)	108.9	C(11)-C(12)-H(12B)	109.5
N(1)-C(10)-C(11)	112.9(2)	H(12A)-C(12)-H(12B)	109.5
N(1)-C(10)-C(9)	101.9(2)	C(11)-C(12)-H(12C)	109.5
C(11)-C(10)-C(9)	116.1(2)	H(12A)-C(12)-H(12C)	109.5
N(1)-C(10)-H(10)	108.5	H(12B)-C(12)-H(12C)	109.5
C(11)-C(10)-H(10)	108.5		
C(9)-C(10)-H(10)	108.5		
C(3)-C(2)-C(1)	115.3(3)		
C(3)-C(2)-H(2A)	108.5		

Symmetry transformations used to generate equivalent atoms:

Table 7.3. Anisotropic displacement parameters ($Å^2$ x 10^3) for complex **1**. The anisotropic displacement factor exponent takes the form: $-2\pi^2 [h^2 a^{*2} U^{11} + \ldots + 2 h k a^* b^* U^{12}]$

	U^{11}	U^{22}	U^{33}	U^{23}	U^{13}	U^{12}
Mo(1)	24(1)	27(1)	28(1)	-2(1)	1(1)	-5(1)
Cl(1)	44(1)	44(1)	31(1)	-11(1)	-10(1)	0(1)
O(3)	37(1)	29(1)	60(1)	6(1)	3(1)	-7(1)
N(1)	22(1)	23(1)	29(1)	2(1)	-2(1)	-1(1)
N(2)	32(1)	25(1)	32(1)	-9(1)	-3(1)	-3(1)
O(2)	39(1)	68(2)	29(1)	-3(1)	1(1)	-11(1)
O(1)	29(1)	35(1)	48(1)	-16(1)	6(1)	-3(1)
O(4)	28(1)	33(1)	46(1)	6(1)	7(1)	-4(1)
C(8)	26(2)	29(2)	26(1)	0(1)	0(1)	-7(1)
C(4)	55(2)	26(2)	66(2)	-12(2)	-11(2)	5(2)
C(7)	32(2)	25(1)	33(1)	-1(1)	-4(1)	-6(1)
C(6)	42(2)	30(2)	51(2)	3(2)	-3(2)	-7(1)
C(5)	58(2)	23(2)	69(2)	3(2)	-11(2)	-7(2)
C(3)	44(2)	29(2)	44(2)	-14(1)	-6(1)	2(1)
C(9)	28(1)	32(2)	37(1)	5(1)	5(1)	4(2)
C(10)	22(2)	28(1)	26(1)	0(1)	-1(1)	-2(1)
C(2)	43(2)	33(2)	75(2)	-22(2)	9(2)	4(1)
C(1)	43(2)	50(2)	66(2)	-34(2)	18(2)	-4(2)
C(11)	32(1)	35(2)	30(1)	7(1)	-3(1)	-3(1)
C(13)	41(2)	44(2)	45(2)	8(2)	-8(1)	8(1)
C(12)	43(2)	63(2)	30(1)	-1(2)	-6(1)	0(2)

Table 7.4. Atomic coordinates ($x10^4$) and equivalent isotropic displacement parameters ($Å^2 x\ 10^3$) for complex **3**. U(eq) is defined as one third of the trace of the orthogonalized Uij tensor.

	x	y	z	U(eq)
Mo(1)	4481(1)	4246(1)	6776(1)	26(1)
Cl(1)	3776(1)	5488(1)	6192(1)	36(1)
Cl(2)	5868(1)	3220(1)	7938(1)	40(1)
O(1)	4673(3)	4024(1)	5059(2)	39(1)
O(2)	2600(3)	3969(1)	6923(3)	44(1)
O(3)	5064(3)	4729(1)	8967(2)	31(1)
O(4)	5886(3)	6466(1)	13184(2)	36(1)
N(1)	7138(3)	4715(1)	7266(2)	24(1)
N(2)	6364(3)	5575(2)	10487(3)	37(1)
C(1)	8199(3)	4637(2)	6379(3)	29(1)
C(2)	9704(4)	4986(2)	6647(3)	34(1)
C(3)	10108(4)	5417(2)	7874(4)	40(1)
C(4)	9030(4)	5497(2)	8818(3)	36(1)
C(5)	7562(3)	5129(2)	8473(3)	25(1)
C(6)	6264(3)	5134(2)	9356(3)	27(1)
C(7)	5023(4)	5626(2)	11287(4)	43(1)
C(8)	4838(4)	6407(2)	11777(3)	40(1)
C(9)	6451(4)	5766(2)	13716(4)	43(1)
C(10)	5404(5)	5230(2)	12730(4)	52(1)
Mo(2)	-468(1)	3588(1)	1598(1)	28(1)
Cl(3)	-1134(1)	2336(1)	1129(1)	36(1)
Cl(4)	882(1)	4621(1)	2747(1)	56(1)
O(5)	-215(3)	3776(1)	-113(2)	41(1)
O(6)	-2362(3)	3878(1)	1665(3)	45(1)
O(7)	99(2)	3168(1)	3848(2)	32(1)
N(3)	2192(3)	3123(1)	2138(2)	25(1)
C(11)	3229(4)	3174(2)	1246(3)	31(1)
C(12)	4739(4)	2833(2)	1553(3)	35(1)
C(13)	5164(4)	2432(2)	2820(4)	38(1)
C(14)	4106(4)	2405(2)	3792(3)	32(1)

C(15)	2632(3)	2757(1)	3404(3)	25(1)
C(16)	1375(3)	2802(2)	4327(3)	27(1)
N(4)	1592(3)	2487(1)	5612(2)	26(1)
C(17)	348(18)	2581(8)	6531(13)	25(3)
C(18)	1250(20)	2453(7)	8105(16)	27(2)
O(8)	1149(11)	1688(6)	8324(13)	35(2)
C(19)	-499(12)	1517(6)	7629(16)	42(2)
C(20)	-911(18)	1961(8)	6261(18)	42(3)
C(17')	489(11)	2581(4)	6617(10)	29(2)
C(18')	1149(15)	2263(5)	8106(9)	36(2)
O(8')	796(10)	1497(4)	7964(6)	40(1)
C(19')	-595(7)	1389(3)	6829(11)	44(2)
C(20')	-1070(9)	2127(4)	6133(9)	31(1)

Table 7.5. Bond lengths [Å] and angles [deg] for complex **3**.

Mo(1)-O(1)	1.690(2)	C(13)-C(14)	1.393(4)
Mo(1)-O(2)	1.693(2)	C(14)-C(15)	1.380(4)
Mo(1)-O(3)	2.1871(19)	C(15)-C(16)	1.495(3)
Mo(1)-N(1)	2.350(2)	C(16)-N(4)	1.309(3)
Mo(1)-Cl(2)	2.3629(8)	N(4)-C(17')	1.456(8)
Mo(1)-Cl(1)	2.3991(8)	N(4)-C(17)	1.491(10)
O(3)-C(6)	1.248(3)	C(17)-C(18)	1.524(12)
O(4)-C(8)	1.424(4)	C(17)-C(20)	1.542(13)
O(4)-C(9)	1.429(4)	C(18)-O(8)	1.429(11)
N(1)-C(1)	1.343(3)	O(8)-C(19)	1.438(10)
N(1)-C(5)	1.344(3)	C(19)-C(20)	1.493(13)
N(2)-C(6)	1.319(3)	C(17')-C(18')	1.503(9)
N(2)-C(7)	1.477(3)	C(17')-C(20')	1.543(8)
C(1)-C(2)	1.395(4)	C(18')-O(8')	1.444(8)
C(2)-C(3)	1.376(5)	O(8')-C(19')	1.419(8)
C(3)-C(4)	1.394(4)	C(19')-C(20')	1.523(8)
C(4)-C(5)	1.387(4)	O(1)-Mo(1)-O(2)	106.04(12)
C(5)-C(6)	1.495(3)	O(1)-Mo(1)-O(3)	159.11(10)
C(7)-C(10)	1.504(5)	O(2)-Mo(1)-O(3)	94.64(10)
C(7)-C(8)	1.528(5)	O(1)-Mo(1)-N(1)	90.03(10)
C(9)-C(10)	1.504(5)	O(2)-Mo(1)-N(1)	163.90(10)
Mo(2)-O(5)	1.685(2)	O(3)-Mo(1)-N(1)	69.37(7)
Mo(2)-O(6)	1.692(2)	O(1)-Mo(1)-Cl(2)	96.06(8)
Mo(2)-O(7)	2.1925(19)	O(2)-Mo(1)-Cl(2)	95.88(9)
Mo(2)-N(3)	2.351(2)	O(3)-Mo(1)-Cl(2)	84.47(6)
Mo(2)-Cl(4)	2.3575(10)	N(1)-Mo(1)-Cl(2)	81.11(6)
Mo(2)-Cl(3)	2.3934(8)	O(1)-Mo(1)-Cl(1)	94.77(8)
O(7)-C(16)	1.268(3)	O(2)-Mo(1)-Cl(1)	96.63(9)
N(3)-C(11)	1.325(3)	O(3)-Mo(1)-Cl(1)	79.68(6)
N(3)-C(15)	1.343(3)	N(1)-Mo(1)-Cl(1)	82.73(6)
C(11)-C(12)	1.392(5)	Cl(2)-Mo(1)-Cl(1)	160.51(3)
C(12)-C(13)	1.376(5)	C(6)-O(3)-Mo(1)	121.81(16)

C(8)-O(4)-C(9)	110.4(3)	O(7)-Mo(2)-Cl(3)	80.24(6)
C(1)-N(1)-C(5)	118.7(2)	N(3)-Mo(2)-Cl(3)	82.16(6)
C(1)-N(1)-Mo(1)	124.50(19)	Cl(4)-Mo(2)-Cl(3)	159.08(4)
C(5)-N(1)-Mo(1)	116.65(16)	C(16)-O(7)-Mo(2)	121.70(16)
C(6)-N(2)-C(7)	120.8(2)	C(11)-N(3)-C(15)	119.3(2)
N(1)-C(1)-C(2)	122.2(3)	C(11)-N(3)-Mo(2)	124.00(19)
C(3)-C(2)-C(1)	118.3(2)	C(15)-N(3)-Mo(2)	116.67(16)
C(2)-C(3)-C(4)	120.2(3)	N(3)-C(11)-C(12)	121.9(3)
C(5)-C(4)-C(3)	117.8(3)	C(13)-C(12)-C(11)	118.9(3)
N(1)-C(5)-C(4)	122.8(2)	C(12)-C(13)-C(14)	119.2(3)
N(1)-C(5)-C(6)	111.5(2)	C(15)-C(14)-C(13)	118.2(3)
C(4)-C(5)-C(6)	125.8(2)	N(3)-C(15)-C(14)	122.4(2)
O(3)-C(6)-N(2)	121.1(2)	N(3)-C(15)-C(16)	112.2(2)
O(3)-C(6)-C(5)	118.3(2)	C(14)-C(15)-C(16)	125.4(2)
N(2)-C(6)-C(5)	120.6(2)	O(7)-C(16)-N(4)	120.4(2)
N(2)-C(7)-C(10)	112.1(3)	O(7)-C(16)-C(15)	118.3(2)
N(2)-C(7)-C(8)	110.2(3)	N(4)-C(16)-C(15)	121.3(3)
C(10)-C(7)-C(8)	101.9(3)	C(16)-N(4)-C(17')	123.1(4)
O(4)-C(8)-C(7)	105.4(3)	C(16)-N(4)-C(17)	119.4(6)
O(4)-C(9)-C(10)	105.7(3)	C(17')-N(4)-C(17)	4.8(9)
C(9)-C(10)-C(7)	102.5(2)	N(4)-C(17)-C(18)	105.2(12)
O(5)-Mo(2)-O(6)	105.83(12)	N(4)-C(17)-C(20)	111.1(11)
O(5)-Mo(2)-O(7)	158.57(10)	C(18)-C(17)-C(20)	103.4(9)
O(6)-Mo(2)-O(7)	95.56(10)	O(8)-C(18)-C(17)	104.9(10)
O(5)-Mo(2)-N(3)	88.72(10)	C(18)-O(8)-C(19)	103.5(9)
O(6)-Mo(2)-N(3)	165.41(10)	O(8)-C(19)-C(20)	107.2(8)
O(7)-Mo(2)-N(3)	69.93(7)	C(19)-C(20)-C(17)	103.7(9)
O(5)-Mo(2)-Cl(4)	96.94(9)	N(4)-C(17')-C(18')	112.5(8)
O(6)-Mo(2)-Cl(4)	95.57(9)	N(4)-C(17')-C(20')	111.2(6)
O(7)-Mo(2)-Cl(4)	82.06(7)	C(18')-C(17')-C(20')	100.8(6)
N(3)-Mo(2)-Cl(4)	81.36(6)	O(8')-C(18')-C(17')	105.5(6)
O(5)-Mo(2)-Cl(3)	95.48(9)	C(19')-O(8')-C(18')	109.1(5)
O(6)-Mo(2)-Cl(3)	97.15(9)	O(8')-C(19')-C(20')	107.2(5)

C(19')-C(20')-C(17')	103.2(5)	

Symmetry transformations used to generate equivalent atoms:

Table 7.6. Anisotropic displacement parameters ($Å^2 x\ 10^3$) for complex **3**. The anisotropic displacement factor exponent takes the form: $-2\pi^2[h^2a^*2U^{11} + ... + 2\ h\ k\ a^*\ b^*\ U^{12}]$

	U^{11}	U^{22}	U^{33}	U^{23}	U^{13}	U^{12}
Mo(1)	26(1)	22(1)	31(1)	-6(1)	6(1)	-5(1)
Cl(1)	32(1)	27(1)	52(1)	1(1)	12(1)	2(1)
Cl(2)	51(1)	27(1)	41(1)	5(1)	8(1)	0(1)
O(1)	48(1)	38(1)	28(1)	-9(1)	3(1)	0(1)
O(2)	31(1)	33(1)	68(2)	-8(1)	12(1)	-10(1)
O(3)	33(1)	32(1)	33(1)	-8(1)	15(1)	-10(1)
O(4)	48(1)	30(1)	28(1)	-5(1)	5(1)	-7(1)
N(1)	24(1)	24(1)	26(1)	1(1)	8(1)	2(1)
N(2)	34(1)	43(2)	39(1)	-19(1)	17(1)	-14(1)
C(1)	28(1)	30(1)	29(1)	-2(1)	8(1)	6(1)
C(2)	27(1)	40(2)	40(2)	2(1)	14(1)	4(1)
C(3)	26(2)	46(2)	49(2)	-7(2)	12(1)	-10(1)
C(4)	31(2)	38(2)	42(2)	-12(1)	12(1)	-10(1)
C(5)	26(1)	23(1)	29(1)	-3(1)	10(1)	-1(1)
C(6)	26(1)	28(1)	28(1)	-7(1)	10(1)	-7(1)
C(7)	36(2)	52(2)	45(2)	-25(1)	20(1)	-15(1)
C(8)	37(2)	48(2)	34(1)	-9(1)	7(1)	8(1)
C(9)	46(2)	42(2)	44(2)	13(1)	18(1)	3(1)
C(10)	69(2)	32(2)	67(2)	-9(2)	45(2)	-11(2)
Mo(2)	27(1)	23(1)	33(1)	5(1)	4(1)	7(1)
Cl(3)	32(1)	29(1)	49(1)	-3(1)	12(1)	-1(1)
Cl(4)	65(1)	27(1)	70(1)	-6(1)	-1(1)	-3(1)
O(5)	42(1)	42(1)	38(1)	14(1)	5(1)	6(1)
O(6)	35(1)	40(1)	58(1)	2(1)	9(1)	17(1)
O(7)	29(1)	36(1)	30(1)	8(1)	8(1)	13(1)
N(3)	23(1)	24(1)	28(1)	4(1)	3(1)	0(1)
C(11)	29(1)	35(2)	30(1)	6(1)	6(1)	-3(1)
C(12)	24(1)	50(2)	33(1)	1(1)	9(1)	-4(1)
C(13)	24(1)	50(2)	41(2)	4(1)	11(1)	7(1)

C(14)	29(1)	38(2)	31(1)	7(1)	7(1)	6(1)
C(15)	25(1)	23(1)	26(1)	1(1)	6(1)	1(1)
C(16)	31(1)	22(1)	29(1)	-1(1)	9(1)	1(1)
N(4)	28(1)	25(1)	27(1)	2(1)	9(1)	6(1)
C(17)	32(6)	34(7)	12(4)	4(4)	15(4)	4(5)
C(18)	33(5)	19(5)	30(4)	1(3)	8(3)	6(4)
O(8)	32(3)	27(4)	47(4)	10(3)	14(3)	-2(3)
C(19)	40(4)	33(3)	54(5)	4(3)	14(3)	-11(3)
C(20)	38(4)	40(5)	49(5)	-3(4)	11(3)	-9(4)
C(17')	28(3)	15(3)	45(5)	-3(3)	10(3)	1(2)
C(18')	51(4)	35(5)	24(2)	-4(3)	15(2)	3(3)
O(8')	53(4)	30(3)	37(2)	9(2)	13(2)	10(2)
C(19')	40(3)	30(3)	65(5)	3(2)	18(3)	-3(2)
C(20')	29(2)	23(3)	41(3)	7(2)	12(2)	4(2)

Table 7.7. Hydrogen coordinates ($x10^4$) and isotropic displacement parameters ($Å^2 x\ 10^3$) for complex **3**.

	x	y	z	U(eq)
H(2A)	7340(40)	5790(18)	10820(30)	29(8)
H(1)	7916	4334	5540	34
H(2)	10432	4927	5999	41
H(3)	11125	5662	8079	48
H(4)	9292	5793	9669	43
H(7)	3983	5445	10667	52
H(8A)	5165	6753	11078	48
H(8B)	3698	6507	11841	48
H(9A)	6337	5702	14746	51
H(9B)	7609	5702	13668	51
H(10A)	4401	5118	13089	62
H(10B)	6000	4773	12650	62
H(11)	2933	3451	372	38
H(12)	5464	2876	898	42
H(13)	6167	2176	3031	45
H(14)	4393	2151	4696	39
H(4A)	2420(40)	2291(19)	5860(40)	32(9)
H(17)	-177	3070	6399	30
H(18A)	2402	2608	8235	33
H(18B)	735	2723	8804	33
H(19A)	-1245	1635	8292	50
H(19B)	-602	994	7388	50
H(20A)	-2032	2154	6117	51
H(20B)	-805	1671	5390	51
H(17')	216	3106	6700	35
H(18C)	2336	2346	8397	43
H(18D)	614	2485	8852	43
H(19C)	-1499	1186	7236	53
H(19D)	-343	1047	6087	53
H(20C)	-1990	2340	6503	37
H(20D)	-1373	2089	5050	37

Table 7.8. Atomic coordinates ($x10^4$) and equivalent isotropic displacement parameters ($A^2 \times 10^3$) for complex **4**. U(eq) is defined as one third of the trace of the orthogonalized Uij tensor.

	x	y	z	U(eq)
C(2)	1051(2)	4275(2)	6807(2)	26(1)
C(7)	4259(3)	5179(2)	5725(2)	23(1)
C(8)	5738(3)	5377(2)	5104(2)	26(1)
C(9)	4540(3)	5319(2)	4438(2)	26(1)
C(11)	2151(4)	1598(3)	6819(3)	70(1)
C(14)	76(3)	4935(2)	6808(2)	25(1)
C(15)	-570(3)	4840(2)	7385(2)	32(1)
C(17)	-1800(3)	6103(2)	6758(2)	32(1)
C(18)	-1144(3)	6208(2)	6187(2)	36(1)
C(19)	-214(3)	5628(2)	6199(2)	34(1)
C(20)	6560(2)	4602(2)	5076(2)	29(1)
C(21)	6925(3)	3963(2)	5717(2)	40(1)
C(25)	6966(3)	4528(3)	4353(2)	43(1)
C(36)	-1327(4)	11559(3)	8047(3)	63(1)
C(38)	4167(4)	5823(2)	11448(2)	47(1)
C(48)	6212(4)	8025(3)	7570(2)	49(1)
N(2)	3714(2)	5060(2)	4937(1)	23(1)
O(2)	2242(2)	4511(2)	3314(1)	34(1)
O(4)	5401(2)	5404(1)	5901(1)	30(1)
O(11)	-1157(2)	10883(2)	8692(2)	46(1)
Cl(1)	1124(1)	5752(1)	4361(1)	36(1)
Cl(2)	3298(1)	3029(1)	4624(1)	34(1)
Mo(1)	2001(1)	4295(1)	4274(1)	24(1)
C(1)	1014(3)	3833(2)	5942(2)	25(1)
C(3)	2623(3)	4700(2)	6354(2)	23(1)
C(4)	3768(3)	5220(2)	6477(2)	25(1)
C(5)	3519(3)	6251(2)	6595(2)	37(1)
C(6)	4655(3)	4855(2)	7286(2)	35(1)
C(10)	1102(3)	2802(2)	5989(2)	31(1)
C(12)	4171(3)	6241(2)	4018(2)	32(1)

C(13)	4900(3)	7399(2)	3291(2)	41(1)
C(16)	-1510(3)	5418(2)	7366(2)	34(1)
C(22)	7672(3)	3247(3)	5615(3)	57(1)
C(23)	8050(3)	3183(3)	4895(3)	55(1)
C(24)	7709(4)	3819(3)	4272(3)	56(1)
C(26)	-122(3)	9604(2)	9393(2)	29(1)
C(27)	-1169(3)	8943(2)	9141(2)	28(1)
C(28)	511(3)	8259(2)	9065(2)	24(1)
C(29)	1153(3)	7486(2)	8788(2)	25(1)
C(30)	880(3)	7540(3)	7805(2)	45(1)
C(31)	739(3)	6562(2)	9076(2)	41(1)
C(32)	2467(3)	7521(2)	9168(2)	24(1)
C(33)	4292(3)	6999(2)	9258(2)	25(1)
C(34)	4294(3)	7680(2)	9974(2)	24(1)
C(35)	-172(3)	10339(2)	8722(2)	35(1)
C(37)	4582(3)	7206(2)	10836(2)	32(1)
C(39)	-1682(3)	8678(2)	9857(2)	28(1)
C(40)	-1586(3)	7816(2)	10215(2)	40(1)
C(41)	-2065(3)	7634(3)	10880(2)	44(1)
C(42)	-2648(3)	8307(3)	11201(2)	39(1)
C(43)	-2741(3)	9172(2)	10847(2)	40(1)
C(44)	-2270(3)	9366(3)	10179(2)	36(1)
C(45)	4914(3)	7340(2)	8627(2)	25(1)
C(46)	5977(3)	6951(2)	8617(2)	30(1)
C(47)	6616(3)	7296(3)	8096(2)	41(1)
C(49)	5130(4)	8416(3)	7569(2)	49(1)
C(50)	4492(3)	8079(2)	8093(2)	40(1)
N(1)	2035(2)	4255(2)	5705(1)	22(1)
N(3)	902(2)	9008(2)	9437(2)	24(1)
N(4)	3084(2)	8055(2)	9741(1)	22(1)
O(1)	749(2)	3676(2)	4062(1)	37(1)
O(3)	2198(2)	4745(1)	7029(1)	27(1)
O(5)	2102(2)	2562(1)	6659(2)	38(1)

O(6)	5009(2)	6475(2)	3578(1)	39(1)
O(7)	2097(2)	10489(2)	10382(2)	42(1)
O(8)	4184(2)	9634(2)	10651(2)	47(1)
O(9)	-659(2)	8150(1)	8818(1)	30(1)
O(10)	3039(2)	6869(1)	8856(1)	28(1)
O(12)	3780(2)	6477(2)	10792(1)	40(1)
Cl(3)	2288(1)	8673(1)	11304(1)	49(1)
Cl(4)	2846(1)	9923(1)	8803(1)	44(1)
Mo(2)	2733(1)	9496(1)	10191(1)	28(1)

Table 7.9. Bond lengths [A] and angles [deg] for complex **4**.

C(2)-O(3)	1.473(3)	C(25)-C(24)	1.384(5)
C(2)-C(14)	1.500(4)	C(25)-H(25)	0.9500
C(2)-C(1)	1.541(4)	C(36)-O(11)	1.416(5)
C(2)-H(2)	1.0000	C(36)-H(36A)	0.9800
C(7)-N(2)	1.287(3)	C(36)-H(36B)	0.9800
C(7)-O(4)	1.342(3)	C(36)-H(36C)	0.9800
C(7)-C(4)	1.492(4)	C(38)-O(12)	1.414(4)
C(8)-O(4)	1.459(4)	C(38)-H(38A)	0.9800
C(8)-C(20)	1.497(4)	C(38)-H(38B)	0.9800
C(8)-C(9)	1.538(4)	C(38)-H(38C)	0.9800
C(8)-H(8)	1.0000	C(48)-C(47)	1.368(5)
C(9)-N(2)	1.478(4)	C(48)-C(49)	1.398(6)
C(9)-C(12)	1.517(4)	C(48)-H(48)	0.9500
C(9)-H(9)	1.0000	N(2)-Mo(1)	2.309(2)
C(11)-O(5)	1.426(4)	O(2)-Mo(1)	1.695(2)
C(11)-H(11A)	0.9800	O(11)-C(35)	1.398(4)
C(11)-H(11B)	0.9800	Cl(1)-Mo(1)	2.3827(8)
C(11)-H(11C)	0.9800	Cl(2)-Mo(1)	2.3683(8)
C(14)-C(15)	1.368(4)	Mo(1)-O(1)	1.686(2)
C(14)-C(19)	1.394(4)	Mo(1)-N(1)	2.326(2)
C(15)-C(16)	1.387(5)	C(1)-N(1)	1.494(4)
C(15)-H(15)	0.9500	C(1)-C(10)	1.505(4)
C(17)-C(18)	1.371(5)	C(1)-H(1)	1.0000
C(17)-C(16)	1.383(5)	C(3)-N(1)	1.276(3)
C(17)-H(17)	0.9500	C(3)-O(3)	1.330(3)
C(18)-C(19)	1.381(5)	C(3)-C(4)	1.515(4)
C(18)-H(18)	0.9500	C(4)-C(6)	1.543(4)
C(19)-H(19)	0.9500	C(4)-C(5)	1.552(4)
C(20)-C(21)	1.378(4)	C(5)-H(5A)	0.9800
C(20)-C(25)	1.392(4)	C(5)-H(5B)	0.9800
C(21)-C(22)	1.405(5)	C(5)-H(5C)	0.9800
C(21)-H(21)	0.9500	C(6)-H(6A)	0.9800

C(6)-H(6B)	0.9800	C(30)-H(30C)	0.9800
C(6)-H(6C)	0.9800	C(31)-H(31A)	0.9800
C(10)-O(5)	1.422(4)	C(31)-H(31B)	0.9800
C(10)-H(10A)	0.9900	C(31)-H(31C)	0.9800
C(10)-H(10B)	0.9900	C(32)-N(4)	1.283(4)
C(12)-O(6)	1.412(4)	C(32)-O(10)	1.342(3)
C(12)-H(12A)	0.9900	C(33)-O(10)	1.461(3)
C(12)-H(12B)	0.9900	C(33)-C(45)	1.502(4)
C(13)-O(6)	1.420(4)	C(33)-C(34)	1.533(4)
C(13)-H(13A)	0.9800	C(33)-H(33)	1.0000
C(13)-H(13B)	0.9800	C(34)-N(4)	1.481(4)
C(13)-H(13C)	0.9800	C(34)-C(37)	1.521(4)
C(16)-H(16)	0.9500	C(34)-H(34)	1.0000
C(22)-C(23)	1.367(6)	C(35)-H(35A)	0.9900
C(22)-H(22)	0.9500	C(35)-H(35B)	0.9900
C(23)-C(24)	1.355(6)	C(37)-O(12)	1.412(4)
C(23)-H(23)	0.9500	C(37)-H(37A)	0.9900
C(24)-H(24)	0.9500	C(37)-H(37B)	0.9900
C(26)-N(3)	1.476(4)	C(39)-C(40)	1.377(5)
C(26)-C(35)	1.522(4)	C(39)-C(44)	1.400(5)
C(26)-C(27)	1.534(4)	C(40)-C(41)	1.378(5)
C(26)-H(26)	1.0000	C(40)-H(40)	0.9500
C(27)-O(9)	1.464(3)	C(41)-C(42)	1.379(5)
C(27)-C(39)	1.504(5)	C(41)-H(41)	0.9500
C(27)-H(27)	1.0000	C(42)-C(43)	1.379(5)
C(28)-N(3)	1.273(4)	C(42)-H(42)	0.9500
C(28)-O(9)	1.341(3)	C(43)-C(44)	1.379(5)
C(28)-C(29)	1.493(4)	C(43)-H(43)	0.9500
C(29)-C(32)	1.510(4)	C(44)-H(44)	0.9500
C(29)-C(31)	1.548(4)	C(45)-C(46)	1.381(4)
C(29)-C(30)	1.552(4)	C(45)-C(50)	1.391(4)
C(30)-H(30A)	0.9800	C(46)-C(47)	1.376(5)
C(30)-H(30B)	0.9800	C(46)-H(46)	0.9500

C(47)-H(47)	0.9500	H(11A)-C(11)-H(11B)	109.5
C(49)-C(50)	1.373(5)	O(5)-C(11)-H(11C)	109.5
C(49)-H(49)	0.9500	H(11A)-C(11)-H(11C)	109.5
C(50)-H(50)	0.9500	H(11B)-C(11)-H(11C)	109.5
N(3)-Mo(2)	2.295(2)	C(15)-C(14)-C(19)	119.2(3)
N(4)-Mo(2)	2.298(2)	C(15)-C(14)-C(2)	120.4(3)
O(7)-Mo(2)	1.696(2)	C(19)-C(14)-C(2)	120.3(3)
O(8)-Mo(2)	1.688(2)	C(14)-C(15)-C(16)	120.9(3)
Cl(3)-Mo(2)	2.3505(10)	C(14)-C(15)-H(15)	119.5
Cl(4)-Mo(2)	2.3875(9)	C(16)-C(15)-H(15)	119.5
O(3)-C(2)-C(14)	111.0(2)	C(18)-C(17)-C(16)	119.4(3)
O(3)-C(2)-C(1)	102.6(2)	C(18)-C(17)-H(17)	120.3
C(14)-C(2)-C(1)	115.9(2)	C(16)-C(17)-H(17)	120.3
O(3)-C(2)-H(2)	109.0	C(17)-C(18)-C(19)	121.0(3)
C(14)-C(2)-H(2)	109.0	C(17)-C(18)-H(18)	119.5
C(1)-C(2)-H(2)	109.0	C(19)-C(18)-H(18)	119.5
N(2)-C(7)-O(4)	116.8(3)	C(18)-C(19)-C(14)	119.7(3)
N(2)-C(7)-C(4)	128.8(3)	C(18)-C(19)-H(19)	120.2
O(4)-C(7)-C(4)	113.9(2)	C(14)-C(19)-H(19)	120.2
O(4)-C(8)-C(20)	112.5(2)	C(21)-C(20)-C(25)	118.8(3)
O(4)-C(8)-C(9)	102.3(2)	C(21)-C(20)-C(8)	124.0(3)
C(20)-C(8)-C(9)	114.7(2)	C(25)-C(20)-C(8)	117.3(3)
O(4)-C(8)-H(8)	109.0	C(20)-C(21)-C(22)	119.4(4)
C(20)-C(8)-H(8)	109.0	C(20)-C(21)-H(21)	120.3
C(9)-C(8)-H(8)	109.0	C(22)-C(21)-H(21)	120.3
N(2)-C(9)-C(12)	108.8(3)	C(24)-C(25)-C(20)	120.7(4)
N(2)-C(9)-C(8)	104.0(2)	C(24)-C(25)-H(25)	119.6
C(12)-C(9)-C(8)	111.7(2)	C(20)-C(25)-H(25)	119.6
N(2)-C(9)-H(9)	110.7	O(11)-C(36)-H(36A)	109.5
C(12)-C(9)-H(9)	110.7	O(11)-C(36)-H(36B)	109.5
C(8)-C(9)-H(9)	110.7	H(36A)-C(36)-H(36B)	109.5
O(5)-C(11)-H(11A)	109.5	O(11)-C(36)-H(36C)	109.5
O(5)-C(11)-H(11B)	109.5	H(36A)-C(36)-H(36C)	109.5

H(36B)-C(36)-H(36C)	109.5	N(1)-C(1)-H(1)	109.4
O(12)-C(38)-H(38A)	109.5	C(10)-C(1)-H(1)	109.4
O(12)-C(38)-H(38B)	109.5	C(2)-C(1)-H(1)	109.4
H(38A)-C(38)-H(38B)	109.5	N(1)-C(3)-O(3)	118.0(3)
O(12)-C(38)-H(38C)	109.5	N(1)-C(3)-C(4)	129.1(3)
H(38A)-C(38)-H(38C)	109.5	O(3)-C(3)-C(4)	112.8(2)
H(38B)-C(38)-H(38C)	109.5	C(7)-C(4)-C(3)	113.7(2)
C(47)-C(48)-C(49)	118.8(3)	C(7)-C(4)-C(6)	111.4(3)
C(47)-C(48)-H(48)	120.6	C(3)-C(4)-C(6)	108.5(2)
C(49)-C(48)-H(48)	120.6	C(7)-C(4)-C(5)	105.6(2)
C(7)-N(2)-C(9)	106.8(2)	C(3)-C(4)-C(5)	107.9(3)
C(7)-N(2)-Mo(1)	132.4(2)	C(6)-C(4)-C(5)	109.6(2)
C(9)-N(2)-Mo(1)	119.37(17)	C(4)-C(5)-H(5A)	109.5
C(7)-O(4)-C(8)	107.6(2)	C(4)-C(5)-H(5B)	109.5
C(35)-O(11)-C(36)	111.7(3)	H(5A)-C(5)-H(5B)	109.5
O(1)-Mo(1)-O(2)	105.35(11)	C(4)-C(5)-H(5C)	109.5
O(1)-Mo(1)-N(2)	164.61(10)	H(5A)-C(5)-H(5C)	109.5
O(2)-Mo(1)-N(2)	89.98(9)	H(5B)-C(5)-H(5C)	109.5
O(1)-Mo(1)-N(1)	88.34(9)	C(4)-C(6)-H(6A)	109.5
O(2)-Mo(1)-N(1)	166.09(9)	C(4)-C(6)-H(6B)	109.5
N(2)-Mo(1)-N(1)	76.41(8)	H(6A)-C(6)-H(6B)	109.5
O(1)-Mo(1)-Cl(2)	96.19(8)	C(4)-C(6)-H(6C)	109.5
O(2)-Mo(1)-Cl(2)	96.29(7)	H(6A)-C(6)-H(6C)	109.5
N(2)-Mo(1)-Cl(2)	80.43(6)	H(6B)-C(6)-H(6C)	109.5
N(1)-Mo(1)-Cl(2)	84.40(6)	O(5)-C(10)-C(1)	108.5(2)
O(1)-Mo(1)-Cl(1)	96.75(8)	O(5)-C(10)-H(10A)	110.0
O(2)-Mo(1)-Cl(1)	94.18(8)	C(1)-C(10)-H(10A)	110.0
N(2)-Mo(1)-Cl(1)	83.26(6)	O(5)-C(10)-H(10B)	110.0
N(1)-Mo(1)-Cl(1)	81.56(6)	C(1)-C(10)-H(10B)	110.0
Cl(2)-Mo(1)-Cl(1)	160.57(3)	H(10A)-C(10)-H(10B)	108.4
N(1)-C(1)-C(10)	112.0(2)	O(6)-C(12)-C(9)	106.7(3)
N(1)-C(1)-C(2)	103.8(2)	O(6)-C(12)-H(12A)	110.4
C(10)-C(1)-C(2)	112.7(2)	C(9)-C(12)-H(12A)	110.4

O(6)-C(12)-H(12B)	110.4	N(3)-C(28)-O(9)	117.2(3)
C(9)-C(12)-H(12B)	110.4	N(3)-C(28)-C(29)	129.9(3)
H(12A)-C(12)-H(12B)	108.6	O(9)-C(28)-C(29)	112.7(2)
O(6)-C(13)-H(13A)	109.5	C(28)-C(29)-C(32)	113.6(2)
O(6)-C(13)-H(13B)	109.5	C(28)-C(29)-C(31)	109.6(3)
H(13A)-C(13)-H(13B)	109.5	C(32)-C(29)-C(31)	106.2(2)
O(6)-C(13)-H(13C)	109.5	C(28)-C(29)-C(30)	107.0(2)
H(13A)-C(13)-H(13C)	109.5	C(32)-C(29)-C(30)	109.2(3)
H(13B)-C(13)-H(13C)	109.5	C(31)-C(29)-C(30)	111.3(3)
C(17)-C(16)-C(15)	119.8(3)	C(29)-C(30)-H(30A)	109.5
C(17)-C(16)-H(16)	120.1	C(29)-C(30)-H(30B)	109.5
C(15)-C(16)-H(16)	120.1	H(30A)-C(30)-H(30B)	109.5
C(23)-C(22)-C(21)	120.8(4)	C(29)-C(30)-H(30C)	109.5
C(23)-C(22)-H(22)	119.6	H(30A)-C(30)-H(30C)	109.5
C(21)-C(22)-H(22)	119.6	H(30B)-C(30)-H(30C)	109.5
C(24)-C(23)-C(22)	119.8(4)	C(29)-C(31)-H(31A)	109.5
C(24)-C(23)-H(23)	120.1	C(29)-C(31)-H(31B)	109.5
C(22)-C(23)-H(23)	120.1	H(31A)-C(31)-H(31B)	109.5
C(23)-C(24)-C(25)	120.5(4)	C(29)-C(31)-H(31C)	109.5
C(23)-C(24)-H(24)	119.8	H(31A)-C(31)-H(31C)	109.5
C(25)-C(24)-H(24)	119.8	H(31B)-C(31)-H(31C)	109.5
N(3)-C(26)-C(35)	108.8(3)	N(4)-C(32)-O(10)	117.5(3)
N(3)-C(26)-C(27)	103.6(2)	N(4)-C(32)-C(29)	129.8(3)
C(35)-C(26)-C(27)	112.1(2)	O(10)-C(32)-C(29)	112.8(2)
N(3)-C(26)-H(26)	110.7	O(10)-C(33)-C(45)	111.0(2)
C(35)-C(26)-H(26)	110.7	O(10)-C(33)-C(34)	102.7(2)
C(27)-C(26)-H(26)	110.7	C(45)-C(33)-C(34)	114.1(2)
O(9)-C(27)-C(39)	111.6(2)	O(10)-C(33)-H(33)	109.6
O(9)-C(27)-C(26)	102.3(2)	C(45)-C(33)-H(33)	109.6
C(39)-C(27)-C(26)	114.6(2)	C(34)-C(33)-H(33)	109.6
O(9)-C(27)-H(27)	109.4	N(4)-C(34)-C(37)	111.4(2)
C(39)-C(27)-H(27)	109.4	N(4)-C(34)-C(33)	103.8(2)
C(26)-C(27)-H(27)	109.4	C(37)-C(34)-C(33)	111.4(2)

N(4)-C(34)-H(34)	110.0	C(46)-C(45)-C(50)	119.0(3)
C(37)-C(34)-H(34)	110.0	C(46)-C(45)-C(33)	119.1(3)
C(33)-C(34)-H(34)	110.0	C(50)-C(45)-C(33)	121.8(3)
O(11)-C(35)-C(26)	107.1(3)	C(47)-C(46)-C(45)	120.5(3)
O(11)-C(35)-H(35A)	110.3	C(47)-C(46)-H(46)	119.7
C(26)-C(35)-H(35A)	110.3	C(45)-C(46)-H(46)	119.7
O(11)-C(35)-H(35B)	110.3	C(48)-C(47)-C(46)	121.0(4)
C(26)-C(35)-H(35B)	110.3	C(48)-C(47)-H(47)	119.5
H(35A)-C(35)-H(35B)	108.5	C(46)-C(47)-H(47)	119.5
O(12)-C(37)-C(34)	108.3(2)	C(50)-C(49)-C(48)	120.6(3)
O(12)-C(37)-H(37A)	110.0	C(50)-C(49)-H(49)	119.7
C(34)-C(37)-H(37A)	110.0	C(48)-C(49)-H(49)	119.7
O(12)-C(37)-H(37B)	110.0	C(49)-C(50)-C(45)	120.1(3)
C(34)-C(37)-H(37B)	110.0	C(49)-C(50)-H(50)	119.9
H(37A)-C(37)-H(37B)	108.4	C(45)-C(50)-H(50)	119.9
C(40)-C(39)-C(44)	119.1(3)	C(3)-N(1)-C(1)	106.9(2)
C(40)-C(39)-C(27)	124.0(3)	C(3)-N(1)-Mo(1)	132.8(2)
C(44)-C(39)-C(27)	116.9(3)	C(1)-N(1)-Mo(1)	118.21(15)
C(39)-C(40)-C(41)	120.4(3)	C(28)-N(3)-C(26)	107.1(2)
C(39)-C(40)-H(40)	119.8	C(28)-N(3)-Mo(2)	133.7(2)
C(41)-C(40)-H(40)	119.8	C(26)-N(3)-Mo(2)	119.05(17)
C(40)-C(41)-C(42)	121.0(3)	C(32)-N(4)-C(34)	106.5(2)
C(40)-C(41)-H(41)	119.5	C(32)-N(4)-Mo(2)	132.2(2)
C(42)-C(41)-H(41)	119.5	C(34)-N(4)-Mo(2)	119.95(16)
C(43)-C(42)-C(41)	118.8(3)	C(3)-O(3)-C(2)	107.4(2)
C(43)-C(42)-H(42)	120.6	C(10)-O(5)-C(11)	111.6(3)
C(41)-C(42)-H(42)	120.6	C(12)-O(6)-C(13)	112.5(3)
C(42)-C(43)-C(44)	121.0(3)	C(28)-O(9)-C(27)	106.8(2)
C(42)-C(43)-H(43)	119.5	C(32)-O(10)-C(33)	106.9(2)
C(44)-C(43)-H(43)	119.5	C(37)-O(12)-C(38)	113.1(2)
C(43)-C(44)-C(39)	119.7(4)	O(8)-Mo(2)-O(7)	105.29(11)
C(43)-C(44)-H(44)	120.1	O(8)-Mo(2)-N(3)	166.64(10)
C(39)-C(44)-H(44)	120.1		

O(7)-Mo(2)-N(3)	87.89(9)	
O(8)-Mo(2)-N(4)	90.09(10)	
O(7)-Mo(2)-N(4)	164.61(10)	
N(3)-Mo(2)-N(4)	76.72(8)	
O(8)-Mo(2)-Cl(3)	97.38(10)	
O(7)-Mo(2)-Cl(3)	95.25(9)	
N(3)-Mo(2)-Cl(3)	83.26(7)	
N(4)-Mo(2)-Cl(3)	82.99(6)	
O(8)-Mo(2)-Cl(4)	94.69(10)	
O(7)-Mo(2)-Cl(4)	95.30(9)	
N(3)-Mo(2)-Cl(4)	81.72(7)	
N(4)-Mo(2)-Cl(4)	82.73(6)	
Cl(3)-Mo(2)-Cl(4)	161.28(3)	

Symmetry transformations used to generate equivalent atoms:

Table 7.10. Anisotropic displacement parameters ($Å^2$ x 10^3) for complex **4**. The anisotropic displacement factor exponent takes the form: $-2\pi^2 [h^2 a^{*2} U^{11} + ... + 2 h k a^* b^* U^{12}]$

	U^{11}	U^{22}	U^{33}	U^{23}	U^{13}	U^{12}
C(2)	25(2)	26(2)	27(1)	0(1)	8(1)	0(1)
C(7)	21(2)	20(2)	27(2)	-1(1)	3(1)	0(1)
C(8)	23(2)	26(2)	29(2)	2(1)	6(1)	-5(1)
C(9)	26(2)	27(2)	25(2)	-2(1)	7(1)	1(1)
C(11)	73(3)	30(2)	98(4)	10(2)	5(3)	9(2)
C(14)	25(2)	26(2)	24(1)	-3(1)	5(1)	-3(1)
C(15)	32(2)	32(2)	33(2)	4(1)	11(1)	-1(1)
C(17)	29(2)	35(2)	33(2)	-9(1)	10(2)	4(1)
C(18)	43(2)	33(2)	32(2)	2(1)	9(2)	7(2)
C(19)	41(2)	33(2)	35(2)	3(1)	20(2)	3(2)
C(20)	18(2)	26(2)	40(2)	-2(1)	2(1)	-3(1)
C(21)	30(2)	37(2)	52(2)	7(2)	8(2)	-2(1)
C(25)	33(2)	50(3)	46(2)	-2(2)	12(2)	5(2)
C(36)	63(3)	45(2)	67(3)	7(2)	-8(2)	19(2)
C(38)	57(3)	40(2)	42(2)	11(2)	6(2)	-3(2)
C(48)	56(3)	63(3)	37(2)	-14(2)	30(2)	-29(2)
N(2)	23(1)	23(1)	24(1)	-2(1)	5(1)	1(1)
O(2)	35(1)	39(1)	27(1)	-1(1)	6(1)	6(1)
O(4)	22(1)	40(1)	27(1)	-4(1)	3(1)	-5(1)
O(11)	40(2)	37(1)	61(2)	3(1)	9(1)	16(1)
Cl(1)	37(1)	34(1)	35(1)	2(1)	9(1)	12(1)
Cl(2)	38(1)	27(1)	36(1)	-4(1)	6(1)	5(1)
Mo(1)	23(1)	26(1)	20(1)	-4(1)	2(1)	-1(1)
C(1)	23(2)	27(2)	26(2)	0(1)	9(1)	1(1)
C(3)	23(2)	22(2)	24(1)	1(1)	5(1)	2(1)
C(4)	23(2)	28(2)	21(1)	-5(1)	1(1)	-2(1)
C(5)	41(2)	29(2)	41(2)	-11(1)	11(2)	0(2)
C(6)	25(2)	50(2)	24(2)	-1(1)	-2(1)	-1(1)
C(10)	27(2)	29(2)	37(2)	-3(1)	7(1)	-7(1)
C(12)	30(2)	36(2)	31(2)	4(1)	8(1)	0(1)

C(13)	44(2)	43(2)	38(2)	8(2)	11(2)	-5(2)
C(16)	33(2)	40(2)	33(2)	-2(1)	18(2)	1(1)
C(22)	34(2)	37(2)	89(3)	11(2)	0(2)	1(2)
C(23)	32(2)	44(2)	79(3)	-20(2)	-4(2)	5(2)
C(24)	40(2)	69(3)	59(3)	-22(2)	12(2)	8(2)
C(26)	25(2)	26(2)	35(2)	-5(1)	7(1)	-1(1)
C(27)	23(2)	26(2)	33(2)	-5(1)	6(1)	4(1)
C(28)	23(2)	26(2)	24(1)	1(1)	7(1)	-2(1)
C(29)	22(2)	25(2)	26(2)	-5(1)	4(1)	-1(1)
C(30)	37(2)	63(2)	31(2)	-13(2)	2(2)	7(2)
C(31)	28(2)	25(2)	68(2)	-7(2)	14(2)	-8(1)
C(32)	28(2)	23(2)	23(2)	2(1)	10(1)	1(1)
C(33)	24(2)	23(1)	29(2)	2(1)	10(1)	5(1)
C(34)	21(2)	24(2)	28(2)	-1(1)	7(1)	-1(1)
C(35)	32(2)	25(2)	48(2)	1(1)	11(2)	2(1)
C(37)	28(2)	37(2)	28(2)	2(1)	5(1)	0(1)
C(39)	19(2)	29(2)	33(2)	-9(1)	2(1)	-4(1)
C(40)	39(2)	30(2)	52(2)	1(2)	18(2)	3(2)
C(41)	44(2)	40(2)	51(2)	2(2)	15(2)	-5(2)
C(42)	30(2)	54(2)	33(2)	-7(2)	7(2)	-12(2)
C(43)	37(2)	43(2)	43(2)	-11(2)	15(2)	3(2)
C(44)	35(2)	36(2)	38(2)	-4(2)	11(1)	4(2)
C(45)	27(2)	25(2)	25(2)	-2(1)	9(1)	1(1)
C(46)	25(2)	35(2)	31(2)	-5(1)	8(1)	5(1)
C(47)	30(2)	60(2)	37(2)	-11(2)	13(2)	-3(2)
C(49)	67(3)	43(2)	43(2)	10(2)	23(2)	-2(2)
C(50)	46(2)	36(2)	42(2)	8(2)	19(2)	10(2)
N(1)	20(1)	21(1)	22(1)	-4(1)	3(1)	-1(1)
N(3)	21(1)	20(1)	30(1)	-2(1)	6(1)	-2(1)
N(4)	21(1)	21(1)	24(1)	-2(1)	5(1)	1(1)
O(1)	32(1)	42(1)	32(1)	-8(1)	1(1)	-9(1)
O(3)	25(1)	34(1)	22(1)	-5(1)	7(1)	-2(1)
O(5)	33(1)	28(1)	51(2)	5(1)	7(1)	4(1)

O(6)	38(1)	43(1)	39(1)	11(1)	16(1)	2(1)
O(7)	32(1)	30(1)	61(2)	-20(1)	9(1)	-4(1)
O(8)	27(1)	45(1)	59(2)	-24(1)	-4(1)	-2(1)
O(9)	19(1)	31(1)	40(1)	-12(1)	9(1)	-5(1)
O(10)	25(1)	27(1)	33(1)	-9(1)	11(1)	0(1)
O(12)	31(1)	48(1)	36(1)	16(1)	1(1)	-8(1)
Cl(3)	65(1)	54(1)	33(1)	-2(1)	22(1)	10(1)
Cl(4)	45(1)	34(1)	59(1)	11(1)	26(1)	2(1)
Mo(2)	23(1)	25(1)	36(1)	-11(1)	4(1)	-3(1)

ITQB-UNL | Av. da República, 2780-157 Oeiras, Portugal
Tel (+351) 214 469 100 | Fax (+351) 214 411 277

www.itqb.unl.pt